FINITE ELEMENT MODELING OF A PIER-ON-BANK BRIDGE SCOUR

by

Vidya Subhash Chavan

A dissertation submitted to the faculty of
The University of North Carolina at Charlotte
in partial fulfillment of the requirements
for the degree of Doctor of Philosophy in
Infrastructure and Environmental Systems

Charlotte

2021

Approved by:

_____
Dr. Shen-En Chen

_____
Dr. Wenwu Tang

_____
Dr. John Diemer

_____
Dr. Nicole Braxtan

_____
Dr. Craig Allan

ABSTRACT

VIDYA SUBHASH CHAVAN. Finite element modeling of a pier-on-bank bridge scour (Under the direction of DR. SHEN-EN CHEN)

Scour is a critical condition change for a bridge hydraulic system, especially during storms and subsequent flooding. Caused by swiftly moving water, scours remove sand and soil, creating holes surrounding a bridge pier compromising the integrity of the bridge structure. Flooding and scour are the number one causes of bridge failures in the United States and are responsible for almost 60% of bridge failures. The danger of bridge scour failures lies in the fact that they can occur without warning. Moreover, depending upon the formation of the soil stratum surrounding the bridge foundation, scour can attain maximum depth within days, months, and even years. Thus, frequent and accurate monitoring of existing scour conditions is vital for long-term bridge management. Early detection of the capacity loss of bridge foundations resulting from extreme scour conditions would benefit DOTs in minimizing expenditures and preventing severe losses from bridge failures. Thus, DOTS are always looking for fast and effective bridge monitoring techniques and accurate, comprehensive analysis methods to aid in investigating bridge scour susceptibility. This dissertation addressed a unique scour problem addressing bridges with piers-on-bank. Many research studies have been carried out to examine the effect of extreme scour conditions on bridge piers located in the water. However, only limited studies were focused on the investigation of scour effects on piers-on-bank bridges. The objective of this study was to understand the potential scour effects

on the pier-on-bank bridge foundations. The investigative approach involved use of terrestrial LiDAR scanning to quantify local scour area around bridge piers. Finite element (FE) modeling technique is then applied to simulate the scouring effect on the bridge pier. In this study, a case study bridge with piers-on-bank was first selected, the Phillips Road bridge at the University of North Carolina at Charlotte campus spans over the Toby Creek. The bridge has multiple piers on both banks of the creek and the piers have experienced scour problems. LiDAR scans of the bridge help quantify the dimensions of the scours resulting in simulated square scour holes. To understand the impacts of current scour conditions on the case study bridge, comprehensive three-dimensional finite element models of the bridge piers were developed using ABAQUS. Non-linear finite element analysis was carried out on the bridge pier models. The Element Removal (ER) technique was used to simulate the mass losses resulting from the scour. To study the performance of bridge piles under critical scour conditions, different scour of the case study bridge were analyzed. Both single and two-pier models were developed to determine the effect of localized scour holes around multiple piers and the potential impact of widened scour area (combined scour) between the adjacent piers. The two-pier model was analyzed for the different load case scenarios subjected to combined actions of axial load, lateral load, and moments. The analytical results show that local scours around a single pier can significantly affect the lateral behavior of the bridge piers and resulted in considerable increase in pile displacement and the bending moments along the pile. Comparison of the local and combined scour between the two-piles shows that the combined scour exponentially increases the pile head displacement. However, the

effect of combined scour on the bending moment response is not significantly different from the results of the local scour effect alone. This research work demonstrated clearly that scour problems can be significant even for piers-on-bank structures and should be addressed in the design. The nonlinear FEM analysis with ER technique can be used for analyzing scour problems. However, the current study only focuses on the soil-pile interaction problem and a more in-depth analysis considering soil-pile-flow interactions should be conducted.

ACKNOWLEDGMENTS

This Ph.D. journey has been fascinating for me both professionally as well as personally. Firstly, I would like to extend my sincere thanks to my advisor Dr. Shen-En Chen. His valuable guidance and encouragement helped me to sail through this journey successfully. I'm very thankful to him for being so patient with me and continuously helping me achieve this goal.

I'm very thankful to Dr. Wenwu Tang for giving me an opportunity to work on the exciting Deephyd project. I'm incredibly grateful to all my committee members –Dr. Tang, Dr. John Diemer, Dr. Nicole Braxtan, and Dr. Craig Allan for their insightful comments and guidance.

I want to acknowledge the funding support from the North Carolina Department of Transportation (NCDOT) and the support of the NCDOT steering and implementation committee: Messrs. John W. Kirby, Matthew Lauffer, Tom Langan, Gary Thompson, Paul Jordan, Mark Swartz, Mark Ward, Derek Bradner, Brian Radakovic and Kevin Fischer.

I would like to thank Mr. Peter Franz from UNCC facility management for data availability. I'm very thankful to all my team members from the Deephyd project- Navanit Sri Shanmugam, Tianyang Chen, Tarini Shukla, and Zachery Slocum.

A very special thanks to Dr. Srinivas Pulugurtha for showing me this excellent path of pursuing Ph.D. I'm sincerely grateful to you – Dr. Jy Wu, Dr. David Young, Dr. Janos Gergely, Dr. Brett Tempest and Dr. Matthew Whelan.

My final acknowledgement is to my family. I'm forever grateful to my parents - Aai and Pappa. My sisters had an immense contribution in shaping my life. Both my sisters- Arati and Anjali, had sacrificed a lot and are always there for me. I'm also thankful to my in-laws for their love and support.

And, finally, to the most important people of my life – my husband, my pillar of strength – Pramod and our two little ones Neel and Nihira. Your unconditional love and patience made this journey even more beautiful. Thank you forever and beyond.

DEDICATION

To my parents, in-laws, sisters and loving and wonderful husband - Pramod and our blessing – Neel and icing- Nihira.

TABLE OF CONTENTS

LIST OF TABLES

LIST OF FIGURES

LIST OF ABBREVIATIONS

AASHTO	The American Association of State Highway and Transportation Officials
NBI	National Bridge Inventory
FEA	Finite Element Analysis
FHWA	Federal Highway Administration
LiDAR	Light Detection and Ranging
ER	Element Removal

1 INTRODUCTION

Scour, caused by swiftly moving water, removes soil from the riverbed and embankments, creating holes surrounding a bridge foundation. Erosion of the foundation material caused by scour affects the integrity of bridge structure eventually leading to early damage or collapse. Flooding and scour are the number one cause of bridge failures in the United States and are responsible for almost 60% of the bridge failures. About 83% of the structures listed in the National Bridge Inventory (NBI) cross some sort of waterway and are exposed to the threats of flooding and scour. According to Flint et al. (2017), 70% of bridges-over-waterway are NOT designed to withstand scour, and 21,000 bridges are currently designated as "scour critical", and bridge failures are due to scour, often during floods and peak flow events which are becoming more frequent possibly due to climate change. Another study conducted by Cook et al. (2004) has estimated an annual hydraulic collapse frequency of approximately 1/5,000. Rapid climate change, frequent hurricane seasons and resulting catastrophic floods will make the bridge scour problem worse in the future. It is estimated that the average cost for flood damage repair of highway bridges is at $50 million per year (Ayres associates, 2016).

To minimize bridge failures resulting from scour, and to take timely action, the Federal Highway Administration's national scour-evaluation program mandated that bridges over water must be inspected every two years. Based on the existing scour conditions of substructure and superstructure elements, the bridges that are listed as scour critical, should be considered for immediate action to repair, rehabilitate, or replace.

Scour is a complex phenomenon involving soil-water-structure interactions. The requirements of the number of parameters involved in scour analysis, make it challenging to model and predict. Many research studies have been conducted to understand the scour mechanism and its impact on bridge strength and stability (Achmus et al. 2010, Alipour et al. 2013). However, most of the work on scour vulnerability assessment of bridges focused on the bridge piers located in water. Hence, there is a significant gap in the literature for pier-on bank bridge scour studies.

While hundreds of bridges are deteriorated by the erosive actions of flowing water, there are many bridges with piers-on-bank. Piers-on-bank bridges are common for auto crossings over small streams with sites not suitable for culverts. Local scour holes developed around piers-on-bank bridges are as critical as the piers/bridge foundations in water especially when the waterway is constricted and inadequate to handle flooding during torrential rain. The scour problem for piers-on-bank is not investigated because it is always assumed that the waterway basin is sufficiently deep to accommodate the design flow of the stream water. Scour holes developed on the riverbanks do not receive the recharge sediment supply from the upstream flowing water and can remain exposed for a long time if no remedial actions are taken. Moreover, contracted river flow and continuously changing river boundaries erode the riverbanks creating deep erosion cuts which may further encourage scouring or erosion for piers-on-bank foundations. This problem is frequently seen on riverbanks without vegetation or riprap protections.

Local scour around the bridge piers has gained significant attention as this is the critical scour component contributing to total scour depth when compared to general

scour and contraction scour. However, in the case of bridge piers located on the bank – consideration of local scour holes is not enough, owing to the proximity of these holes to deep embankments cuts which are often associated with changes of water course. This study focuses on the effects of critical scour conditions on the pier-on-bank pile foundations.

1.1 Problem Statement and Purpose

This dissertation examined scour problems related to a piers-on-bank bridges resulting from frequent flooding and/or constricted waterways. As discussed in the above section, scour around the bridge piers on riverbanks is as important as in-water bridge piers. To understand the scour effects, this study evaluates the effects of existing scour conditions on pier-on-bank bridge foundations using a nonlinear finite element analysis method. Moreover, to understand the behavior of pile foundations under critical scour conditions, this study examined local scour up to design scour depth around a single pier and the effect of extended scour between the two adjacent piers.

1.2 Research Objectives

This study focused on the unique issue of scour problems of pier-on-bank bridge foundations. The goals of this study are to demonstrate the use of terrestrial LiDAR for bridge scour monitoring of piers-on-bank bridges and the analysis of the effect of severe scour conditions on the bridge pile foundation. Towards the second goal, a finite element method is used for the soil-pile analysis.

The specific objectives of current study are:

1. To determine the existing scour conditions of a case study bridge.

2. To evaluate the effect of local scour on lateral behavior of single pile under combined actions of loading.
3. To investigate the effect of compounded/combined scour between the two in-line piers under the influence of different load scenarios.

1.3 Research Methodology

The methodology for the above research work is summarized in Figure 1-1. A case study bridge was first identified. The case study bridge has piers-on-bank and has experienced a significant scour problem. The bridge scour was first monitored using a ground based terrestrial LiDAR scan, from which the scouring scenario was established. The bridge scour was then characterized as a square scour hole surrounding the pier and analyzed using FEM analysis.

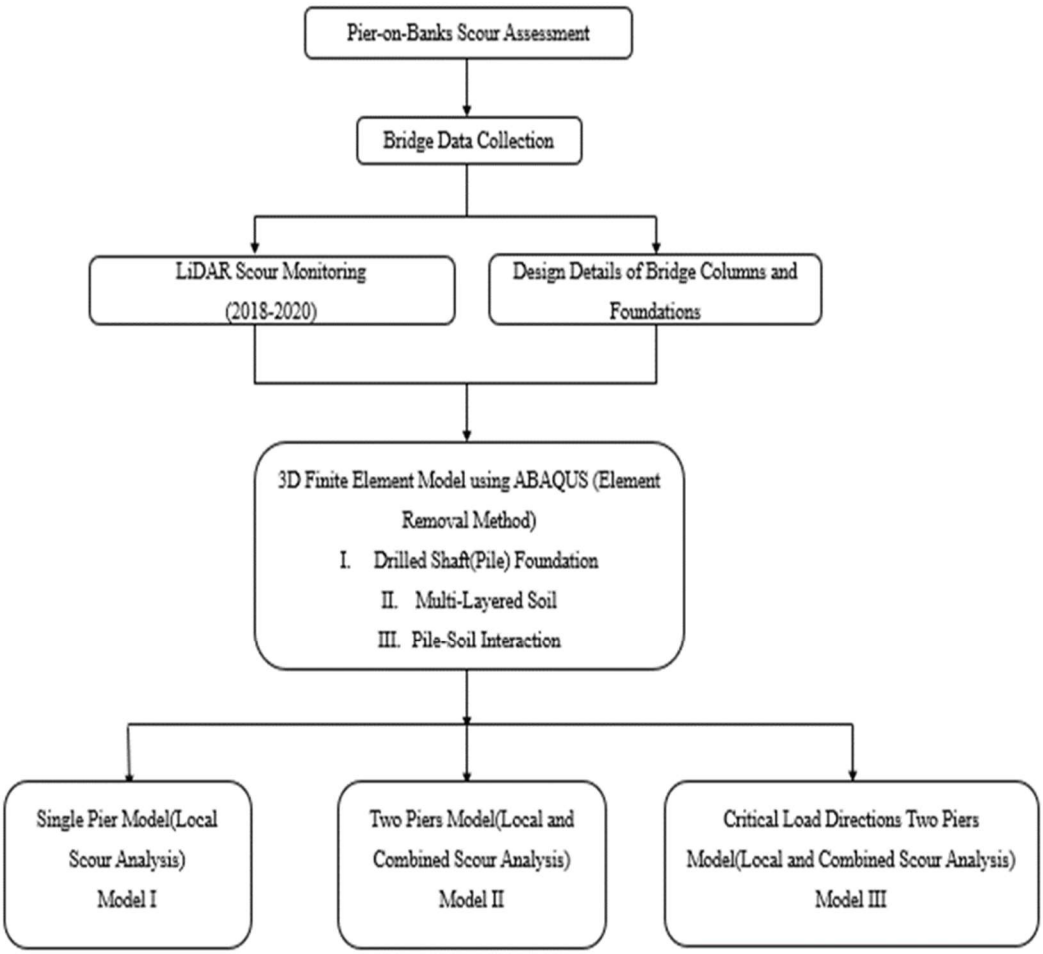

Figure 1-1. Workflow of research methodology for LiDAR based bridge pier scour assessment

1.4 Scope of the Work

The Phillips Road Bridge at the University of North Carolina at Charlotte campus was selected as the case study bridge for this research work. Phillips Road Bridge over Toby Creek (35°18'28.2"N 80°44'16.6"W) has its intermediate bents on banks. The bridge has visible scouring problems due to frequent flooding of the Toby Creek. Specifically, the bridge is located at a meandering point and, the expanded river flood plain below the Phillips road bridge resulted in scour of the left bank and soil deposition on the right bank. As a result, the scour phenomenon described in current study only existed on the left bank.

Design details of the bridge pile foundations and the geotechnical details of the soil stratum were taken from the original design documents used for the construction of bridge. The design analysis results were used as validation of the current study.

1.5 Dissertation Outline

Following this Introduction, Chapter 2 presents a literature review of basic scour mechanisms and the types of scour, a review of scour effects on the lateral behavior of the bridges, and the most commonly used analysis methods of laterally loaded piles. Chapter 3 presents a discussion of peer-reviewed journal papers submitted to the ASCE journal. This dissertation discusses the nonlinear finite element modelling of local scour of bridge piers using the element removal (ER) technique. Chapter 4 presents a research article submitted to the CivilEng journal. This article summarizes the analysis results of the effects of local and combined (global) scours between two in-line piers on bank.

Chapter 5 presents the conclusions based on this research work. Chapter 6 discusses the scope for future studies. The dissertation appendix includes additional results of the two analysis models not covered in the journal submissions comprising Chapter 3 and Chapter 4.

2 LITERATURE REVIEW

2.1 Introduction

This chapter summarizes the literature review conducted to understand the scour problem and its effect on bridge pier foundations. The literature review is presented in three parts. The first part introduces bridge scour definition, mechanism of scour hole generation, and different types of scours. The second part discusses possible modes of bridge failure under scoured conditions. The third part discusses commonly used analysis methods of laterally loaded piles.

2.2 Bridge Scour Definition and Types of Scours

Bridge scour is the removal of sediments such as sand and rocks and/or from around bridge abutments or piers (Figure 2-1). Scour, caused by swiftly moving water, can scoop out scour holes, compromising the integrity of a structure. Scour occurs in three main forms, namely, general scour, contraction scour, and local scour. General scour occurs naturally in river channels and includes the aggradation and degradation of the riverbed. Sometimes described as long-term scour, general scour can result from lowering of the stream bed due to deficit or fluctuating sediment supply from upstream. Figure 2.1 shows a generalized scour scenario and including a single pier-on-bank. Contraction scour is the result of contracted/obstructed flow from construction of structures such as bridge piers and abutments and can be of uniform or non-uniform depth across the stream cross-section. Local scour caused by acceleration of flow and resulting vortices, removes soil and/or from around and below the bridge piers,

abutments, and embankments. In addition to these types of scours, lateral migration of streams/meandering streams can erode riverbanks, abutments, and the approach roadway and results in scour.

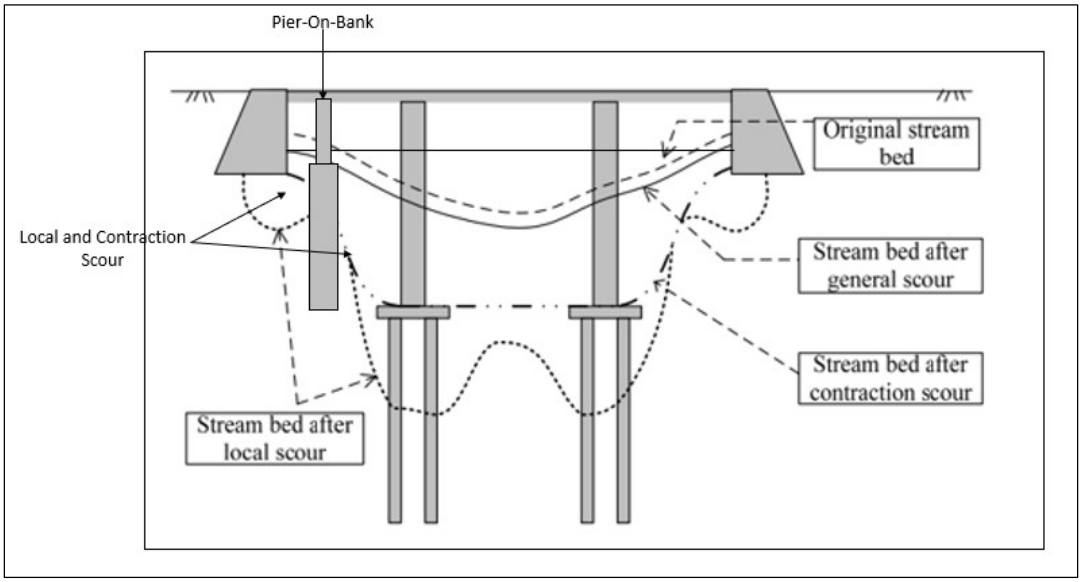

Figure 2-1.Scour types occurring at a bridge site (Modified after Lin et al.2010)

2.3 Local and Global (Combined) Scour Mechanism

Obstruction caused by piers and abutments to the rapidly moving water results in the formation of vortices at the base of piers. A horseshoe vortex resulting from pileup of water on upstream side and acceleration of flow at the nose of pier removes bed material around the pier base and scoops out a hole surrounding a pier. Wake vortices occurring on the downstream of the pier also removes soil around the pier. The horseshoe vortex and the acceleration of the flow near the piles result in high bed shear stress, creating local scour around the bridge pier. High velocity channel flow during high flood levels can be partially obstructed by a bridge pier, and the flow pattern of a channel around the pier significantly altered causing the formation of local scour holes. These local scour holes expand in width (Global or Combined Scour), and results in complete loss of soil between the two piers and the creation of global or combined scour. With increases in the flood stage, this scour hole gets deeper and further washes out the soil around the adjacent piles.

2.4 Scouring and it's Effect on Bridge Stability

Scouring affects the bridge stability in many ways. It alters static and dynamic characteristics of bridges and may lead to excessive deflections and increased maximum stresses induced in structural members. In general, there are four possible modes of bridge failure under scouring conditions viz, vertical failure, lateral failure, torsional failure, and bridge deck failure.

2.4.1 Vertical Failure

In the case of shallow foundations, scouring undermines the foundation and results in inadequate soil support in the form of the reduction of vertical bearing capacity of the soil (Figure 2-2). The bed removal under and around the foundation causes increased stresses and consequently reduces the stiffness of the remaining soil (Figure 2-3). It ultimately changes the frequency of vibration, which depends on the stiffness the system.

In the case of pile foundations, removal of soil around the pile reduces the skin resistance along the pile and reduces the vertical bearing capacity (Figure 2-4). For end bearing piles, the piles lose their vertical bearing capacity when scour undermines the bearing layer (e.g., hard layer or bedrock) that the pile tips rest on (Figure 2-5).

2.4.2 Lateral Failure

Lateral failure consists of pushover failures of piers, structural hinging of piles, kick-out failures of foundations, and excessive lateral movement of piers or foundations. Pushover failure occurs when transverse flood and debris add to bridge piers and exerts increased lateral load until the bridge pier fails. The greater scour depth increases the likelihood of pushover failure of the bridge (Figure.2-6).

Structural hinging occurs when transverse force increases the maximum bending moments in structural elements. Also, the piles with limited embedment into a pile cap

fails due to inadequate bending moment resistance (Figure 2-7). Finally, wash out of the piles from the location of pile tips results in kick-out failure of foundations (Figure 2-8).

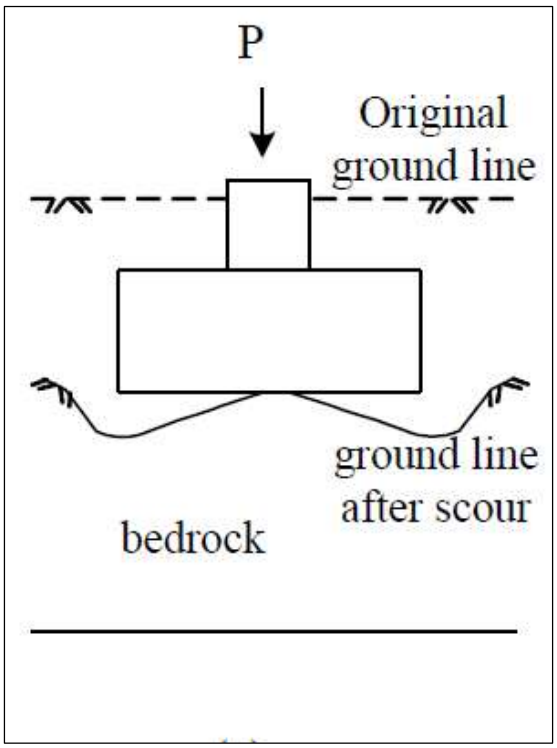

Figure 2-2.Undermining of footing base (After Lin et al.2010)

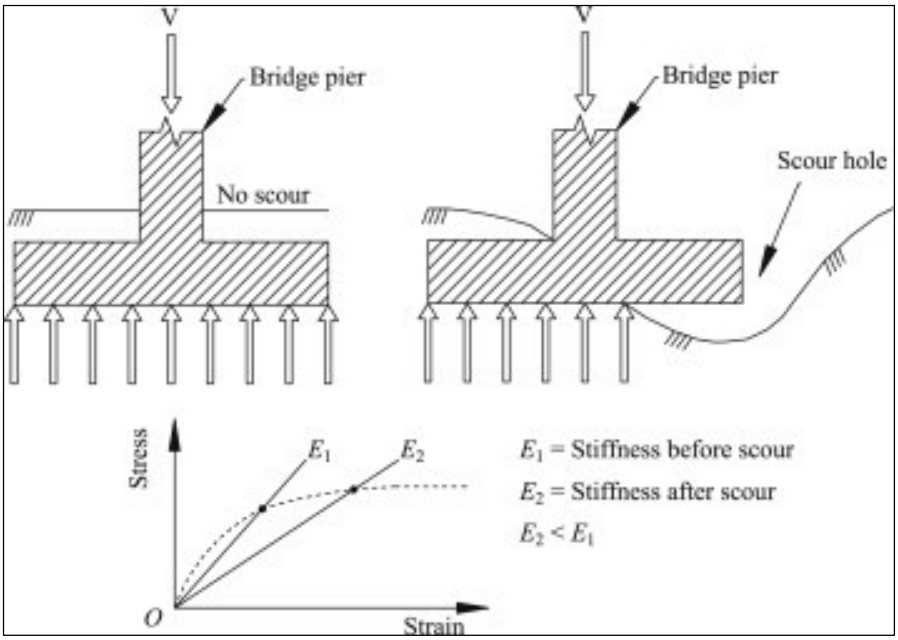

Figure 2-3. Reduction in stiffness caused by scour (After Prendergast et al.2014)

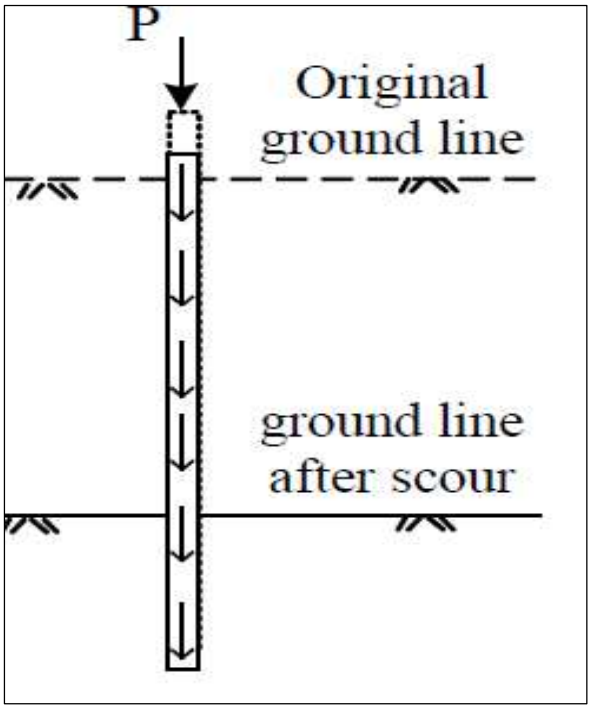

Figure 2-4. Penetration of friction pile (After Lin et al.2010)

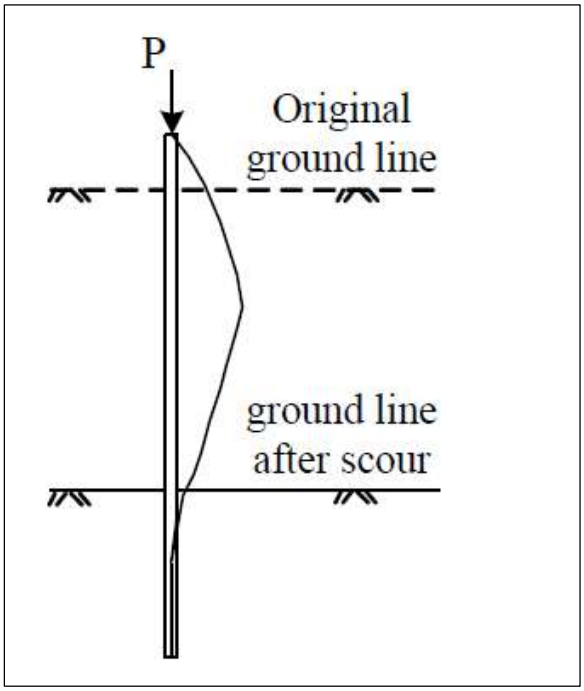

Figure 2-5.Buckling of piles (After Lin et al.2010)

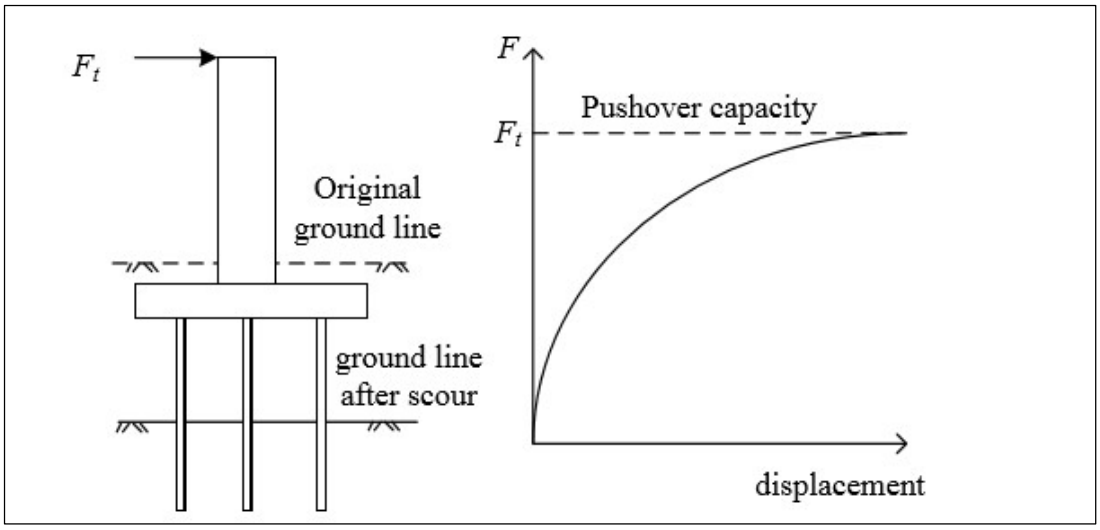

Figure 2-6.Pushover failure (After Lin et al.2010)

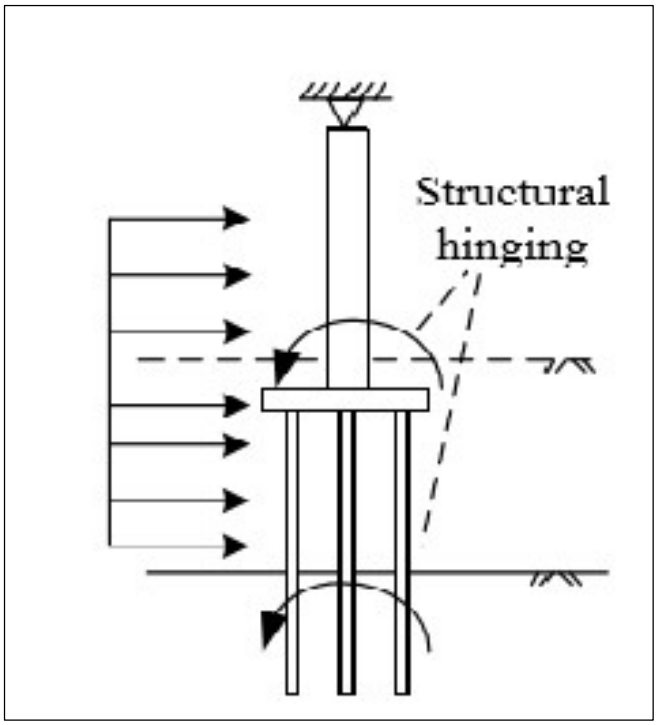

Figure 2-7.Structural hinging (After Lin et al.2010)

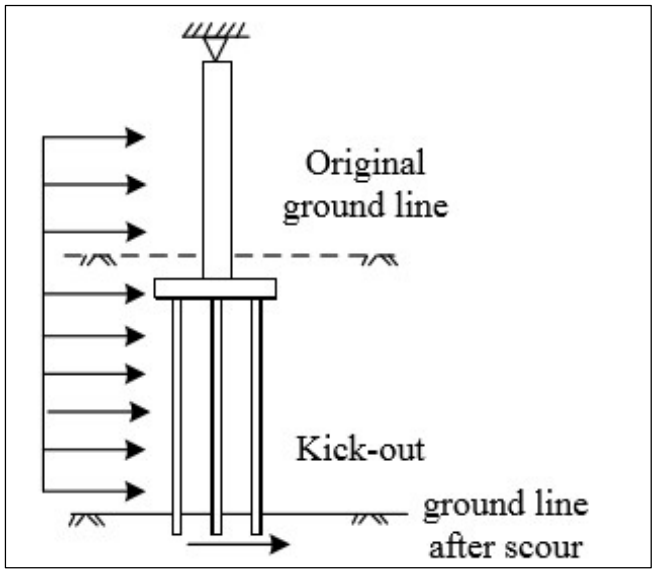

Figure 2-8. Kick out of foundations (After Lin et al.2010)

2.5 Modelling Techniques

The modelling of scour presents unique challenges and will be addressed separately in Chapters 3 and 4. Table 2-1 summarized the issues related to the modelling techniques.

Category	Authors	Methods	Details
Analysis Methods	Lin et al. 2014; Klinga and Alipour 2015	p-y method of	Analysis of laterally loaded piles
	Kim and Jeong (2011), Mardfekri et al. (2013), Strömblad (2014), Salim (2017), Youssouf et al. (2019),	Finite Element Method	Behavior of laterally loaded piles
	Senturk and Pul (2017)	Finite Element Method	Pushover analysis of bridge piers
	Khodair et al. (2014)	Finite Difference (FD) method	To study the effect of pile-soil interaction under axial and lateral loads
General Pile-Soil Modelling Methods	Govindasamy et al. 2010	Observational Method	Observational method based on measured scour data and observed or estimated flow parameters for estimating future scour depth
	Kishore at al. (2009)	laboratory tests	Effects of scour on laterally loaded piles
	Beg (2010)	Experimental studies	Local scour around two piers placed in the transverse direction to the flow
Scour Specific Modelling Methods	Lin et al. (2010)	LPile	Scour effects on buckling capacity of a bridge pier
	McConnell and Cann (2010))	FE Method	Scour effects on the pushover behavior of a bridge
	Lin et al. (2012)	Integrated analysis	Performance of pile-

		technique	supported bridges under scoured conditions.
	Prendergast et al. (2013)	Laboratory and field testing	Changes in natural vibrational frequencies of a bridge.
	Alipour et al. (2013)	p-y,t-z,q-z method	Probability of bridge failures under multi-hazard scenarios of scouring and earthquakes.
	Klinga et al. (2015)	p-y,t-z,q-z method	Buckling analyses, longitudinal and transverse pushover analyses, and modal analyses of scoured bridges.
	Khandel and Soliman (2021)	Deep learning based integrated neural network	Assessment of different flood hazard intensities to simulate structural behavior of a bridge foundation under scour condition.

Specifically, the methods are differentiated to generate pile-soil modelling and scour specific modelling techniques for piles.

3 LIDAR DETECTION AND MODELLING EFFECTS OF LOCAL SCOUR ON BRIDGE PIERS

Abstract

Scour, caused by swiftly moving water, can remove alluvial sediment and soil, creating holes surrounding a bridge component and compromising the integrity of the bridge structure. To quantify local scour on bridge piers, terrestrial LiDAR scanning, which generates high-resolution point cloud data for the scour, can be used to quantify the scoured area. In this paper, the Phillips Road Bridge over Toby Creek (35°18'28.2"N 80°44'16.6"W, Charlotte, NC, USA), a pier-on-bank bridge with critical/significant local scour holes and deep riverbank erosion cuts was selected as case study bridge. To investigate the scour effect on the bridge with pier-on-bank performance, the scoured area around a single pier was first scanned with LiDAR and modeled using nonlinear finite element (FE) analysis, where the local scour is modeled as mass losses using the Element Removal (ER) technique. The FE results are compared to the design loading scenario and the results substantiated that the local scouring can cause large deflection and increased bending moment on the bridge pier.

Keywords: Local Scour, LiDAR Scan, Bridge Piers, Finite Element

Introduction

Scour is a critical condition change for a bridge hydraulic system, especially during storms and resulting high water conditions. Scour, caused by swiftly moving water, can remove alluvial sediment and soil, creating holes surrounding a bridge component and compromising the integrity of a structure (Warren 2011). Scour associated with bridge piers usually starts out as local scour(s) and is often associated with acceleration of flow and resulting turbulent vortices. Local scour typically starts as a scour hole surrounding the bridge pier (Lin et al. 2019). If not addressed, local scours can worsen and result in enlarged mass losses surrounding the bridge supports. The danger of bridge scour failures lies in the fact that they can occur without prior warning. Thus, there is a need for an effective monitoring strategy to identify scour problems surrounding a bridge structure. Figure 3-1 shows the mechanisms of local scour surrounding a single bridge pier, where the soil/sediment mass may be removed due to high water velocities and increased turbulence, (which are functions of the hydrodynamic characteristics of the river flow) and the competence of the geomaterial surrounding the bridge pier to resist the scouring process (Melville and Coleman 2000).

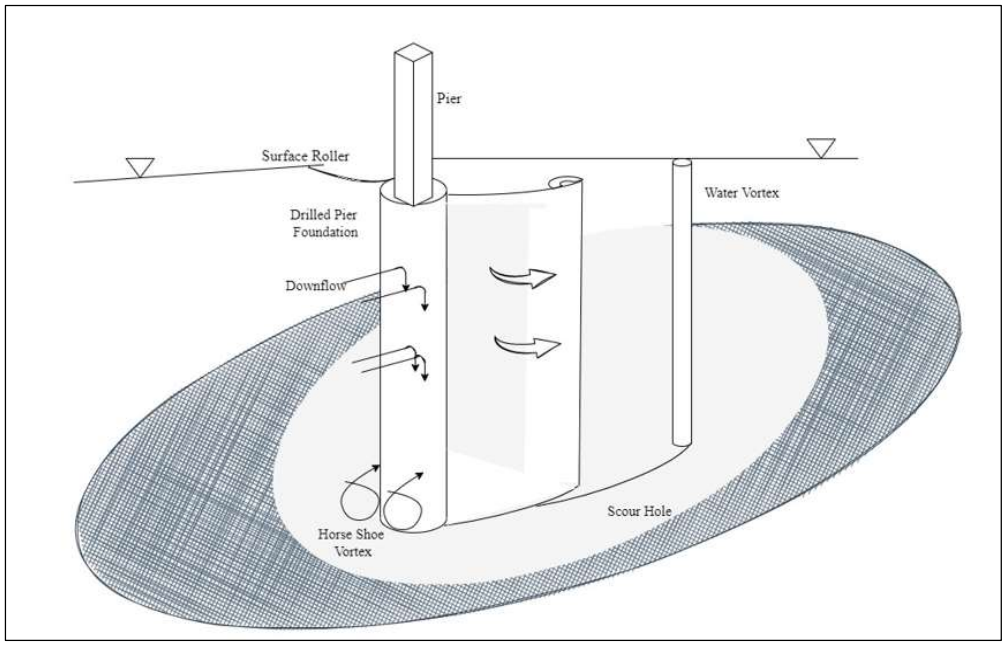

Figure 3-1 Distortions and scour at a circular pier

To minimize the risk of bridge failure, Departments of Transportation (DOTs) are interested in comprehensive and accurate methods to assess existing bridge conditions so that immediate actions may be taken and help develop remediation plans to minimize risks to safety and finances. However, current efforts to quantify scour effects on bridges during bridge inspections are limited. According to the National Bridge Inspection Standard (NBIS), bridges over 6 m in length must be inspected and rated every other year. Based on the Standard, NBI item 60 for substructure condition is rated on a scale of 0 to 9 where 0 is a failed state beyond corrective action and 9 means excellent condition (FHWA 1995). Furthermore, NBI Item 113 for scour-critical bridges is rated from 0 being scour critical to 9 where the bridge foundation is well above floodwater elevations. Thus, current bridge scour assessment is insufficient to capture the true state of scour and the potential dangers to the bridge.

The only scour quantifier used in Item 113 is scour depth and not the real extent of the scour. Extensive research has been conducted to assess the scour conditions based on maximum observed scour depth in the past, including prediction of future scour depth based on laboratory experiments and theoretical methods. For example, Bridge Scour Assessment method (BSA-1) has been widely used as an observational method based on measured scour data and observed or estimated flow parameters for estimating future scour depth instead of site-specific erosion testing (Govindasamy et al. 2010). Kishore at al. (2009) performed laboratory tests to study the effects of scour on laterally loaded piles. Yang et al. (2021) considered fluid-soil interaction in scour stability evaluation of bridge piers under different scour depths and flow velocity conditions. Beg (2010)

conducted extensive experimental studies of local scour around two piers placed in the transverse direction to the flow. Many studies have shown that the effect of scour hole dimensions on a pile's lateral response is more critical than other responses and scour depth alone is not sufficient to quantify scour damage level (Breusers et al. 1977). However, most of the studies conducted were based on either calculated scour depth or merely considered scour depth.

To study the effects of extreme scour conditions to the performances of bridge foundation and bridge superstructure, scour effects on buckling capacity of a bridge pier have been studied by Avent and Alawady (2005) and Lin et al. (2010). McConnell and Cann (2010) investigated scour effects on the pushover behavior of a bridge. Lin et al. (2012) proposed an integrated analysis technique to study the performance of pile-supported bridges under scoured conditions.

Changes in natural vibrational frequencies of a bridge due to scour have been studied by Alipour et al. (2013) considered multi-hazard scenarios of scouring and earthquakes to determine the probability of failure of bridges. Klinga et al. (2015) conducted buckling analyses, longitudinal and transverse pushover analyses, and modal analyses of scoured bridge structures. Khandel and Soliman (2021) developed a deep learning based integrated neural network for the assessment of different flood hazard intensities to simulate the structural behavior of a bridge foundation under scour condition.

The scouring effect is critically dependent on the soil types and several studies have been focused on either cohesive and non-cohesive unconsolidated geologic

materials. Lin et al. (2014) considered stress history effects of sand erosion on the laterally loaded piles. Liang et al. (2015) studied the effects of extreme scour on the buckling of bridge piles considering the stress history of soft clay. Ben et al. (2019) demonstrated the effect of stress history in evaluating scour effects on lateral behavior of monopiles in soft clay.

Other than field investigations, numerical methods (Lin et al. 2014; Klinga and Alipour 2015) have been used to investigate the changes in structural responses, including shear stresses, bending moments, pile head displacement, and rotation before and after scouring. Lin et al. (2019) developed a closed-form solution for the estimation of vertical effective stress and pile lateral capacities considering scour hole depth, width and slope angle. Majumdar and Chakraborty (2021) used lower bound finite element limit analysis to assess the scour impact on a under-reamed piles in clay. Their study demonstrated significant reduction in bearing and uplift capacities of under-reamed piles while considering the stress history of clay.

This paper reports on a study involving a unique scour problem for piers-on-bank bridge structures. Bridges with piers-on-bank are common for relatively small streams with high bridge approaches. The piers-on-bank Phillips Road bridge (Figure 3-2a and 3-2b) on the UNC Charlotte campus is a three-span continuous prestressed concrete girder bridge with a deck that is 50.5 m in length that spans over Toby Creek. The two-lane bridge was completed and opened in March 2016. Two sets of bridge piers supporting the bridge were built on the two banks of Toby Creek. A review of the literature revealed very few studies of scour problems for bridges with piers-on-bank, as they usually do not

have scour problems. However, in the case of the Phillips Road bridge, the constrained channel size, an increasingly impervious urbanizing catchment in combination with episodic torrential rains have resulted in significant turbulent overflow from river flooding that caused the formation of local scouring surrounding the north side bridge piers.

Figure 3-3 shows one of the bridge piers where two scour mechanisms are occurring concurrently: One involves the localized scour hole formation around the bridge pier and the other involves lateral bank erosion (contraction scour) along the entire bank face.

(**a**) (**b**)

Figure 3-2.Figure 3-2. Location and view of Phillips Road bridge: (a) aerial image of the bridge site; (b) downstream view of the bridge structure (Photo credit: S.E. Chen).

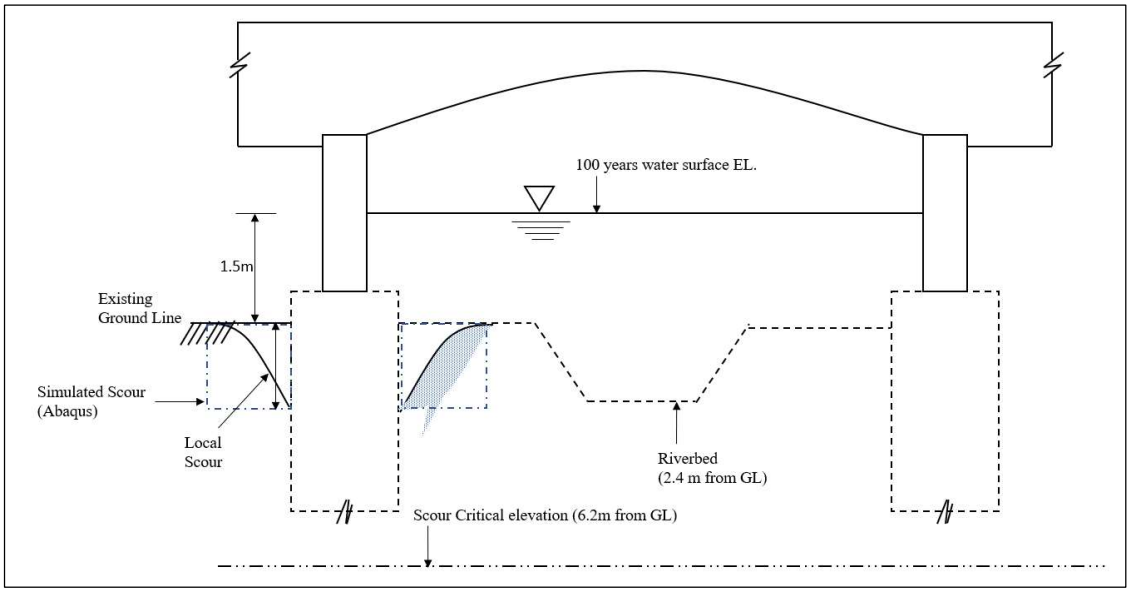

(a)

(b)

Figure 3-3.Phillips Road bridge scour development: a) Schematics of the local scour formation and simulation and b) local scouring (arrows) around bridge piers and channel erosion after a torrential rain (Photo credit: S.E. Chen).

To determine the dimensions of the local scour problem, terrestrial LiDAR scans of the bridge piers have been conducted periodically to determine the extent and evolution of the scours. Terrestrial LiDAR has been used for bridge monitoring, including bridge deflection under static loading (Liu et al. 2010), detection of bridge defects (Liu et al. 2011), and bridge clearance measurements (Liu et al. 2012) and more recently for scour quantification (Suro et al. 2019). Terrestrial LiDAR scans can provide high-resolution point cloud data of a bridge hydraulic structure, which can then be used to quantify material losses surrounding a scoured bridge pier. In addition, rapid and repeated laser scans can generate periodic quantification of scours and help define the process of erosion and determine the rate of removal of a streambed or bank material surrounding the bridge foundation.

To study the effects of the scour to the bridge pier, this paper reports on a study of a single bridge pier undergoing active scouring using the finite element method. The scouring extent was first determined using LiDAR scans, which was then idealized as a square scour hole surrounding the bridge pier. A nonlinear Finite Element (FE) method using element removal (ER) technique was then used to simulate the scouring effect. The ER technique quantifies the scour as soil mass losses, which can have an impacts to the bridge pier deflection and moment distribution. The loading scenario is determined from the original bridge design reports and is applied and compared with the FE results.

In this paper, the three-dimensional FE method is used first to develop a base model to simulate the substrate-pile interaction of the drilled pier subjected to combined loading. This model is then verified and developed further to simulate and study different scour scenarios for the case study bridge.

Numerical Method/Scour Modeling

A review of bridge scour analysis methods shows that the most widely used technique is the p-y method of analysis of laterally loaded piles (Lin et al. 2014; Klinga and Alipour 2015), which uses p-y curves developed from full-scale test results. The method assumes a beam on a Winkler-foundation model and uses p-y, t-z, and q-z curves to characterize the pile's lateral, axial, and end bearing responses. Using the p-y method, the geologic substrate is typically considered as a series of nonlinear springs spaced at regular intervals along the pile length. The p-y curves used in commercial software are mostly derived from field experiments conducted on various soil conditions, although user-defined p-y curves can also be used to model the soil responses. However, the lateral soil resistance based on the p-y method cannot consider interactions between individual soil elements. Moreover, the shearing forces at the interface between the pile and surrounding substrate are also neglected - as is the case of the solutions proposed by Poulos (1971). Also, as the p-y method cannot consider scour-hole dimensions/extent of scour hole, the scour width effects are approximated based on the estimation of effective soil stress around the pile (Lin, 2012).

The FE method is an effective tool to study the soil-pile interaction involving the scouring problem. The FE method provides the capability of considering continuity of the soil mass, appropriate nonlinear material models for both the pile and geologic substrate, defining different boundary conditions and nonlinear interaction effects necessary to model the soil-pile contact problems. Kim and Jeong (2011), Mardfekri et al. (2013), Strömblad (2014), Salim (2017), Youssouf et al. (2019), have employed three-dimensional FE methods to study the effect of soil-pile interaction on laterally loaded piles. Senturk and Pul (2017) performed three-dimensional finite element push-over analyses of bridge piers considering the nonlinear behavior of reinforced concrete and soil under quasi-static loading. Khodair et al. (2014) compared the results obtained from the Finite Difference (FD) method and FE method to study the effect of pile-soil interaction under axial and lateral loads. Finally, Peiris et al. (2014) studied pile behavior under seismic excitations using the FE method.

Phillips Road bridge Study

The study site

The Phillips Road bridge (Figure 3-2a, 3-2b) has a clear roadway width of 9.8 m and supports two traffic lanes of 4.9 m width each. The overall width of the bridge deck is 15.5 m. The cast-in-situ concrete slab (514.4 mm uniform thickness) is supported by seven prestressed concrete girders on top of the three bridge spans. The intermediate bents are supported on drilled pier foundations, while the end bent abutments are founded on pile-supported strip footing.

Phillips Road bridge spans over the Toby Creek which is a headwater tributary that rises in the Newell community of Charlotte, North Carolina, and drains approximately 13.3 km^2 and discharges to the Mallard Creek, a tributary of the Yadkin-PeeDee River system. Toby Creek has an estimated average discharge of 0.17 m^3/s and a mean flow velocity of 0.274 m/s (EPA 2021). The total stream length is 6.68 km. The width of the creek at the bridge at low flow stage is approximately 3.0 m and has a maximum bank full depth of 2.1 m. The constricted river cross section underneath the bridge in combination with high flow velocities during episodic runoff events, has resulted in significant bank erosion and has induced localized scour at the piers on both streambanks (Figure 3-3).

Phillips Road bridge piers and embankments have undergone many cycles of floods in the recent past. As a result, lidar scans taken over a period of two years have revealed local scour of approximately 1.1 m and 1.5 m diameters near bridge piers on both sides of the river channel. Although the depth of local scour holes observed is not more than 1.5 m, on the opposite sides of the piers (channel side) lateral erosion up to 3-3.4 m has been observed. The observed loss of embankment soil or riverbank is non-uniform along the two pier bents and could be broadly categorized as contraction scour. Thus, the piers on the north-west side of the case study bridge demonstrated a combination of local and contraction scour. This combined scour problem is worsened due to the accumulation of large quantities of debris in the river channel, which would likely serve to further increase the scour volume in future runoff events.

Scour assessment using LiDAR scans

To quantify the extent of the scoured area, a FARO Focus S 350 LiDAR was used. FARO LiDAR uses a mono-dyne laser with a wavelength of 1,550 nm. Vegetation and other obstacles covering the target must be removed before the scan. Due to the geometric shape of a scour, a full scan of the scour cannot be made from a single scan. Hence, the LiDAR must be shot from multiple angles while keeping in mind the scanning angles and the height of the laser head. Then, they should be merged or 'stitched' together to get a complete picture. This LiDAR device has a maximum scanning range of 350 m consisting of millions of cloud points. So, the scan was segmented to capture just the region of interest, which is the scour. Figure 3-4 shows the point cloud of the scour surrounding the selected pier of the Phillips Road bridge from a single scan. As seen in Figure 3-4c, the entire scour area cannot be observed due to obstacles. However, the maximum depth and the diameter can be obtained from this scan. The point cloud data is then used to quantify (surface area and volume) of the scour by defining a reference plane. Figure. 3-4a shows a sample reference plane drawn to quantify the scour. Detailed description of the mass loss quantification method from LiDAR scans can be found in Liu et al. (2011).

Three-dimensional finite element modelling

To study the effect of scouring on important structural design parameters, a three-dimensional, non-linear finite element analysis of a single drilled pier foundation was developed using the FEA software Abaqus™ by Dassault systems®.

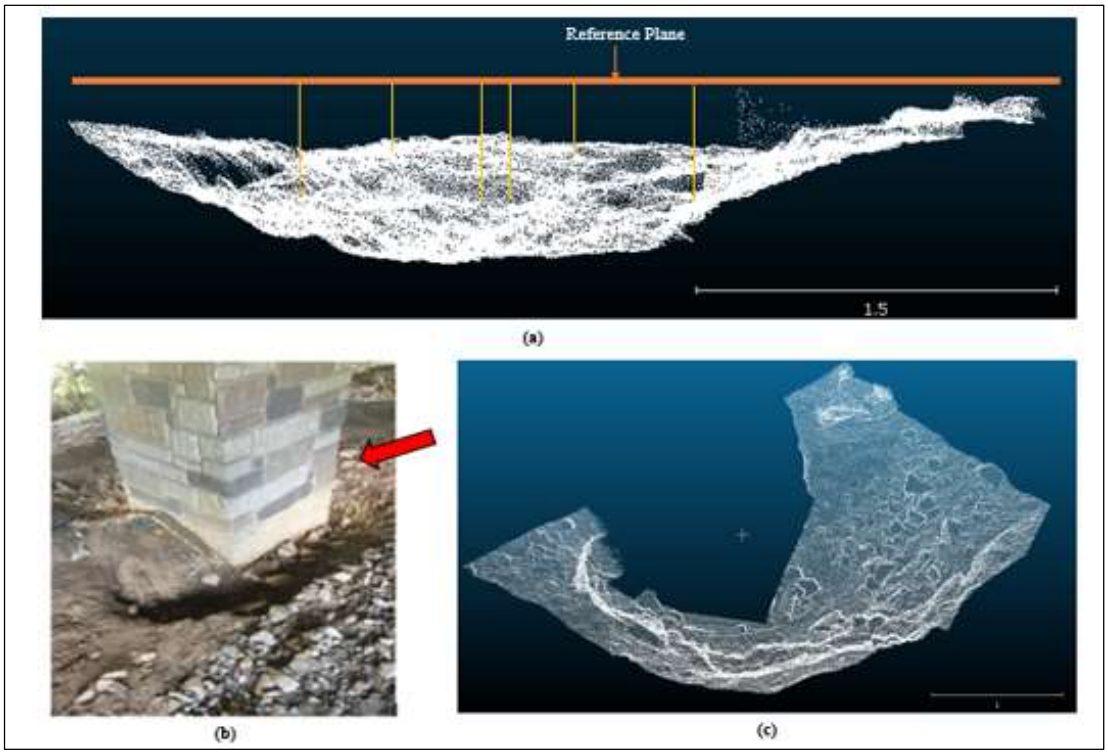

Figure 3-4. Scour scan using LiDAR (**a**) LiDAR scan of scour point cloud (not a river cross-section) – 1.5m; (**b**) image of scour hole; (**c**) scour hole point clouds looking from the direction of arrow in (b); (photo credit: S.E. Chen)

The bridge pier of the study site is supported on a 1.68 m diameter, 12.95 m long drilled shaft or drilled pile foundation. The pile protruded 15.0 cm above the ground level and was driven through four-layered heterogenous cohesive-frictional (c-ø soil) as shown in Figure 3-5. However, the soil is modeled 2.13 m below the tip of the pile in Abaqus™. As suggested by a few other studies including Chen and Poulos (1993); Karthigeyan et al. (2007); Strömblad (2014). the soil domain is extended to an extent of 10 times the pile (10D) diameter from the centerline to avoid the artificial boundary effect on pile-soil behavior. Thus, the overall dimension of the model assembly in Abaqus™ is 34.34 m × 34.34 m × 12.95 m.

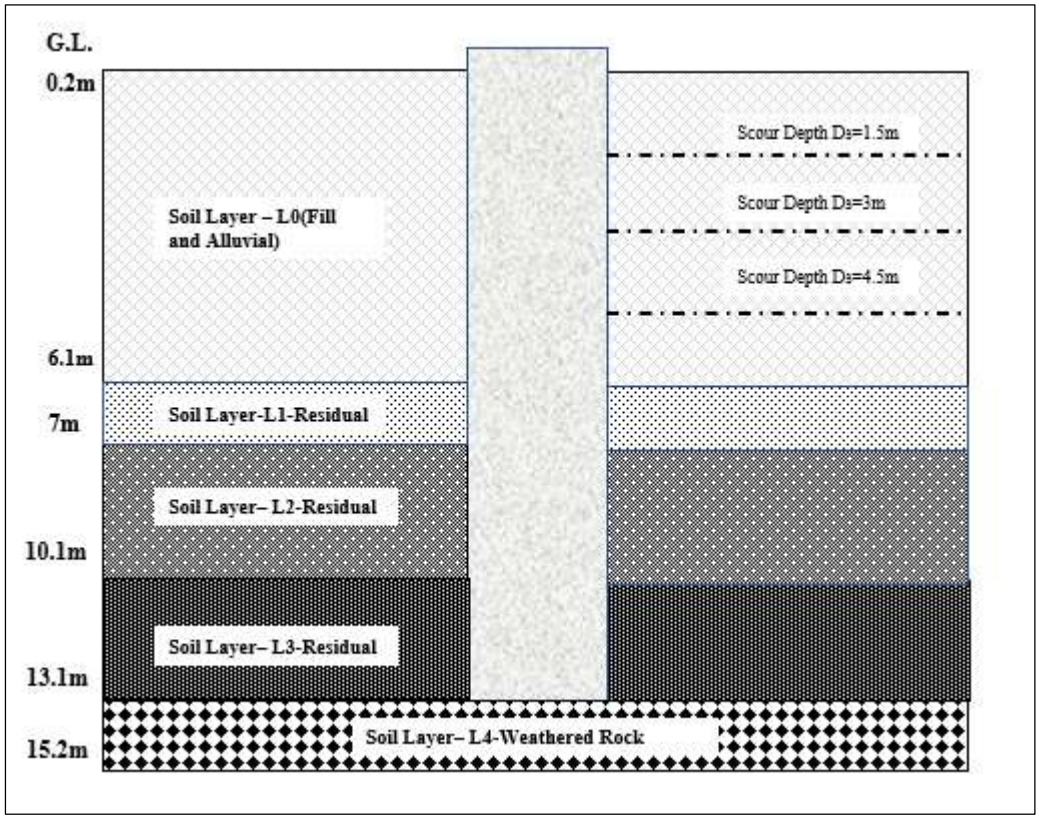

Figure 3-5. Schematic of soil profile and scour depths for the Phillips Road bridge pier

The concrete used for pile construction was an AASHTO (2012) class A concrete with characteristic strength (f'_c) of 31 MPa, Young's modulus (E_c) of $2.7x10^4$ MPa, and a poisson's ratio of 0.2. Main reinforcement of the pile comprised of structural steel with yield strength (f_y) of 413 MPa, modulus of elasticity (E_s) of 20 x 10^4 MPa, and poisson's ration (μ_s) of 0.2.

Furthermore, #4 plain or deformed bars were used as lateral ties. The pile reinforcement was made of twenty-seven vertical #10 rebar with a clear cover of 127 mm, and hoop reinforcement of #4 rebar with a pitch of 127 mm. In this study, the piles were modeled using linear elastic material properties of concrete and steel as stated above.

The soil profile of the Phillips Road bridge site is shown in Figure 3-5. To describe the complex nature of soil and large deformation arising from stiffness reduction due to scouring, soil substrate was modelled as elastic-plastic nonlinear model. There are different material models available in Abaqus™ that can be used to model the pile-soil interaction. However, in this paper, the most commonly used Mohr-Coulomb plasticity model (Khodair and Abdel-Mohti 2014; Mardfekri et al. 2013) was used to depict the nonlinear behavior of soil. The Mohr-Coulomb yield criteria assumes that a yield function is governed by the maximum shear stress that depends on the normal stress. Mohr-Coulomb criteria states that,

$$\tau = c - \sigma \tan\varphi \quad (1)$$

where, τ = shear stress, C = cohesion intercept of the soil, σ = normal stress (negative in compression) and ϕ = angle of internal friction. Soil elastic properties and plasticity parameters required to define the Mohr-Coulomb model for numerical simulation are listed in Table 3-1. The soil properties used in this study were the in-situ soil properties obtained from the site investigation (geotechnical) report of the study site.

Table 3-1.Properties of different soil layers at study site (Phillips Road bridge, UNC Charlotte)

	Elastic Properties			**Mohr-Coulomb Plasticity Parameters**			
Soil	**Unit weight (γs) (kN/m^3)**	**Young's modulus (E) (kPa)**	**Poisson's ratio (υ)**	**Cohesion intercept (c) (kPa)**	**Friction angle (Ø°)**	**Dilation angle (ψ°)**	**Absolute Plastic Strain (ε50)**
L0-c-phi	8.258	47880	0.25	1000	26	0.01	0.1
L1-c-phi	9.043	28728	0.3	800	26	0.01	0.01
L2-c-phi	9.828	76608	0.32	4000	36	0.01	0.005
L3-c-phi	12.183	95760	0.35	72000	40	0.01	0.00005
L4-c-phi	12.183	95760	0.35	72000	40	0.01	0.00005

Both pile and soil were modeled as 3D, deformable, solid elements, whereas the longitudinal and transverse reinforcements of the pile were modeled as wire elements (Khodair and Abdel-Mohti 2014). The reinforcement was embedded in a 'host region' concrete using 'embedded region' interaction property in Abaqus™. Two distinct types of elements were selected for modelling the pile and the soil. Conventional three-dimensional brick elements C3D8 were used to model the soil elements to account for the continuum nature of the soil. The rebar was modeled as a two-node linear 3D truss element T3D2. To minimize the computational time required for analysis, it is typical to model soil close to the pile into a finer mesh and coarser mesh for soil more remote from the pile. In this paper, in order to precisely capture the effect of scouring on pile behavior, the soil to be scoured was defined into a very fine mesh with a pre-defined boundary of a square, while relatively coarser mesh was used for soil more towards the boundaries as shown in Figure 3-6. Abaqus™ model of this study comprised a total of 83,345 linear hexahedral elements (C3D8) and 2,310-line elements of T3D2 element types.

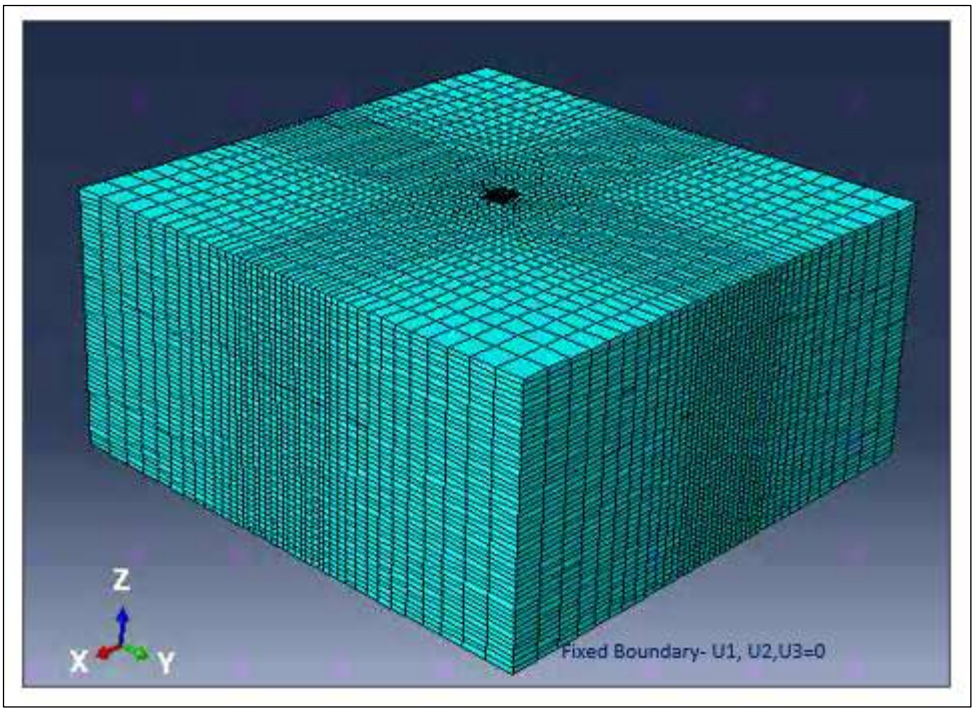

Figure 3-6. Three-dimensional finite element mesh and boundary condition

Pile-soil interaction

The load transfer mechanism of laterally loaded piles depends mainly upon the interaction between the pile and soil. In Abaqus™, the pile-soil interaction was modeled using a small-sliding, surface-to-surface master/slave contact pair formulation (Abaqus 2013). The pile, being stiffer than the surrounding soil, was selected as a master surface while the soil was selected as a slave surface. The interaction between these two surfaces was defined in terms of normal and tangential behaviors. For depicting the normal behavior between pile and soil, the 'hard contact' penalty constraint enforcement method was selected. Contact surfaces were allowed to separate after contact with no change in default contact. In the tangential direction, a penalty friction algorithm (Xing et al. 2019)

along with no limit shear stress parameters were used. A friction coefficient of 0.3 was used to define the friction between the pile and soil contact surfaces. All other settings were kept as default for the analysis. Interaction properties used in the development of Abaqus FE model are tabulated in Table 3-2.

Table 3-2 Interaction properties used in FE Model

	Properties/parameters used in FE model	
Interaction	Mechanical contact	Surface-to-surface
	Sliding formation	Small sliding
	Discretization method	Surface-to-surface
	Model change(Scour simulation)	Geometry
Interaction property	**Tangential behavior**	-
	Friction formulation	Penalty
	Friction coefficient	0.3
	Shear stress	No limit
	Normal behavior	
	Pressure-overclosure	Hard contact
	Constraint enforcement	Penalty
	Seperation after contact	Allowed
	Tie contact	surface to surface

The analysis was carried out in the following steps:

1) Initial → Geostatic → Load Drilled Pier (for no-scour pier)

2) Initial →Geostatic → Model Change (by Element Removal) → Load Drilled Pier (for scoured pier)

The geostatic step (Ben et al. 2019) was used to simulate in-situ stress conditions in the bridge pier model before applying the design loads on the pier top. A user-specified predefined stress field was created by defining the effective vertical stress, σ', for each soil layer.

$$\sigma' = \gamma sat.\, h \quad (2)$$

where γsat is the saturated unit weight of soil and h is the depth to soil layer of interest.

The lateral earth pressure coefficient, k0, was then defined to calculate the horizontal stress distribution of the soil. Stresses were calculated for the "geostatic" step, which was in equilibrium with the external loading (gravity load in this case) and boundary conditions and produced zero to negligible deformations.

$$k0 = 1 - \sin\phi \quad (3)$$

where, ϕ = Coefficient of friction for the soil.

Loading and boundary conditions

The design vertical load of 2,748.86 kN, the design lateral load of 66.72 kN, and the design moment of 149.13 kN-m were calculated as per the AASHTO LRFD method and were applied at the top of the pier through a reference point identified at the top of

the pier's cross-section. The degrees of freedom of the elements at the top of the pier were restrained using a kinematic constraint to limit the motion of the coupling nodes to the reference node.

The bottom of the pile was fixed to simulate the embedment of the pile into underlying rock at its tip. Lateral boundaries of the soil surface were restrained against translation in all directions. Figure 3-6 shows a 3D view of the finite element mesh of the model sans the bridge pier. To simulate scour in the model, soil elements are removed using “Element Removal”. We will first discuss the verification of the non-scoured FEM model with the original bridge design.

Verification of modeling results

Results of the three-dimensional FEM model were verified by comparing the computed bending moment, and lateral displacement values with those obtained from L-Pile software used for the pile design of the Phillips Road bridge. The local scouring was previously not considered in the bridge design and was not considered in the geotechnical investigation. About 6.1 m of the soil below ground level is an artificial fill installed after the construction of the foundation and thus it was not accounted for in the lateral soil resistance calculation of the pier. Accordingly, for verification of the results/comparing the results of Abaqus FE model with L-Pile results, a finite element model is developed without considering the top 6.1 m of soil (as shown in Figure 3-7). The plot of normalized bending moment values vs depth from the geotechnical report and the FE models are shown in Figure 3-8. Both curves show peak moment at 8 m depth. Comparing the results of the two methods, the p-y method used in the L-Pile program

overestimates the bending moment capacity (average=37.1%). This difference can be attributed to the fundamental/inherent difference between the assumptions made in the two numerical techniques – Specifically, L-Pile simplified the geometric effects of the soil into spring elements whereas the 3D FE modeling is a more realistic simulation of reality.

Pile-head deflection obtained using the two methods is 2.57 mm and 2.95 mm for the L-Pile (used in the geotechnical report) and the FE models, respectively. As the two methods are in good agreement with each other, it can be safely concluded that the assumptions made, and data used to develop the FE model are accurate enough to use the model for investigating scour effects. Table 3-5 compares the maximum bending moments from L-Pile and FE model results and shows a percentage difference of 43%.

Scour Hole Dimensions

Figure 3-4c shows the local scour hole of 1.5 m diameter formed around bridge pier. Additionally, as seen in Figure 3-3b, riverbank erosions (deep cuts) of about 3-3.5 m depth were developed in close proximity to the local scour holes. Considering the intensity of heavy floods in Charlotte, this study has assumed/projected a significant widening of local scour holes in the future. As the piers on the northwest side of the case study bridge demonstrated a combination of local and contraction scour, the combined scour problem is worsened due to the accumulation of large quantities of debris in the river channel, which would likely further increase the scour volume in the future.

Thus, this study has assumed three different scour hole dimensions for analysis purposes, as shown in Table 3-3. Despite the uneven and non-symmetric geometry of in-situ scour holes, this study has used square-shaped scour holes.

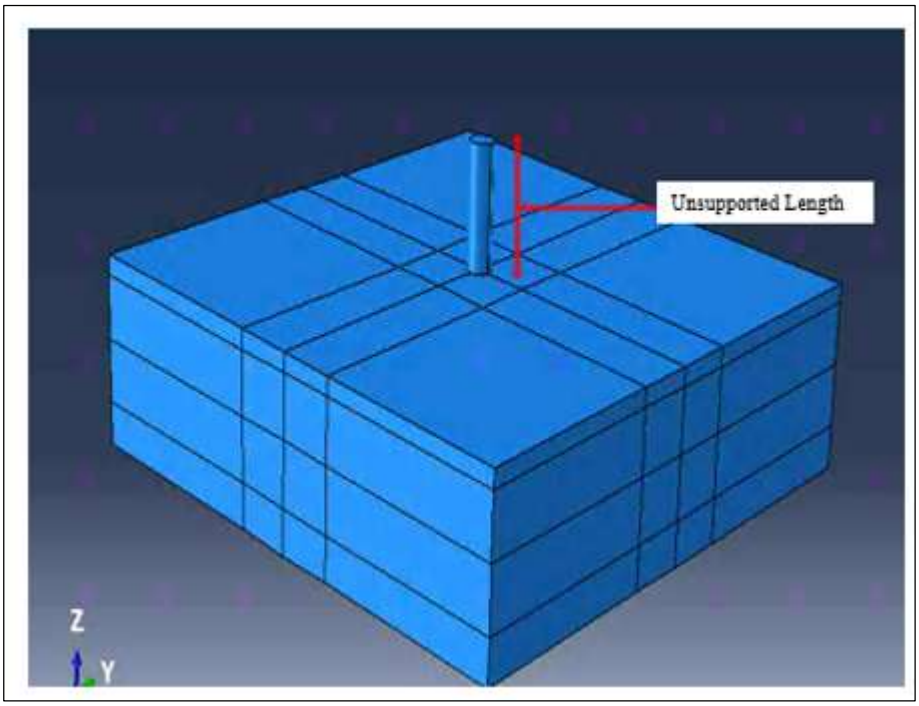

Figure 3-7. Isometric view of the FEM without topsoil layer(fill)

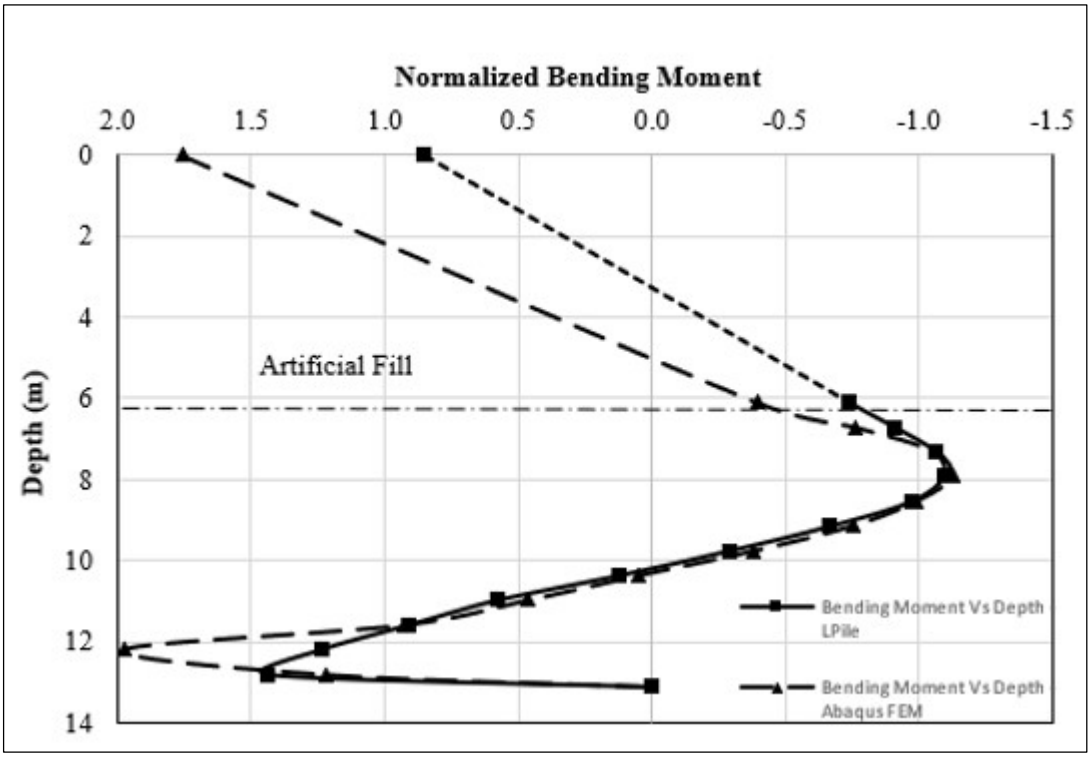

Figure 3-8. Validation of bending moments - Lpile and Abaqus FEM

Table 3-3. Scour cases

Analysis Cases	Scour Hole Dimensions (L X B X D)
Case 0: No Scour	-
Case 1: Scour Depth 1.5 m	1.5 m X 1.5 m X 1.5 m
Case 2: Scour Depth 3 m	3 m X 3 m X 3 m
Case 3: Scour Depth 4.5 m	4.5 m X 4.5 m X 4.5 m

Scour Simulation

To simulate the scour/erosion of soil surrounding the pier, the region/mesh of a scour hole geometry was removed by defining a distinct analysis step in Abaqus™. 'Model Change' interaction in Abaqus™ was used to delete and deactivate the effect of scoured region on the remaining model. This technique is identified as "Element Removal" (ER) and is established as part of the scientific workflow in Abaqus™. As the scoured region described herein is only a result of soil mass loss, scour holes were created by deleting the mesh elements as per the pre-defined square scour hole dimensions. Strömblad (2014) modeled scour using a circular shape, which is easier to model for a single drilled shaft. However, the square shape hole would allow better modeling of multiple holes or combined scour conditions. Hence, square scour holes were used in the current study.

Alternatively, the scour problem could be solved by specifying user defined variables, such as stress state of failure, to automatically remove the elements.

After the ER step, there will not be any more interaction between the pile and the scoured region. Forces exerted by the elements/region of the scoured region were ramped down to zero during the ER step; consequently, the effect of the removed scour hole on the rest of the model was completely absent at the end of the ER step (Abaqus, 2013). Abaqus performed no further element/stiffness calculations for the removed elements.

For a first-order simulation, the LiDAR detected scour for the bridge pier is depicted as a rectangular hole surrounding the pier. As per the design scour depth mentioned in the geotechnical report, 6.1 m of the soil below ground level (Soil Layer

L0) is susceptible to scour. This level was also in agreement with the scour depths of 1.4m to 3.7m recorded for the last two years using a terrestrial LiDAR survey. For the case studies considered in this paper, three different scour depths of 1.5 m, 3 m, and 4.5 m (Table 3-3, Figure 3-9) were examined to investigate the effect of varying scour levels on bridge pile foundations.

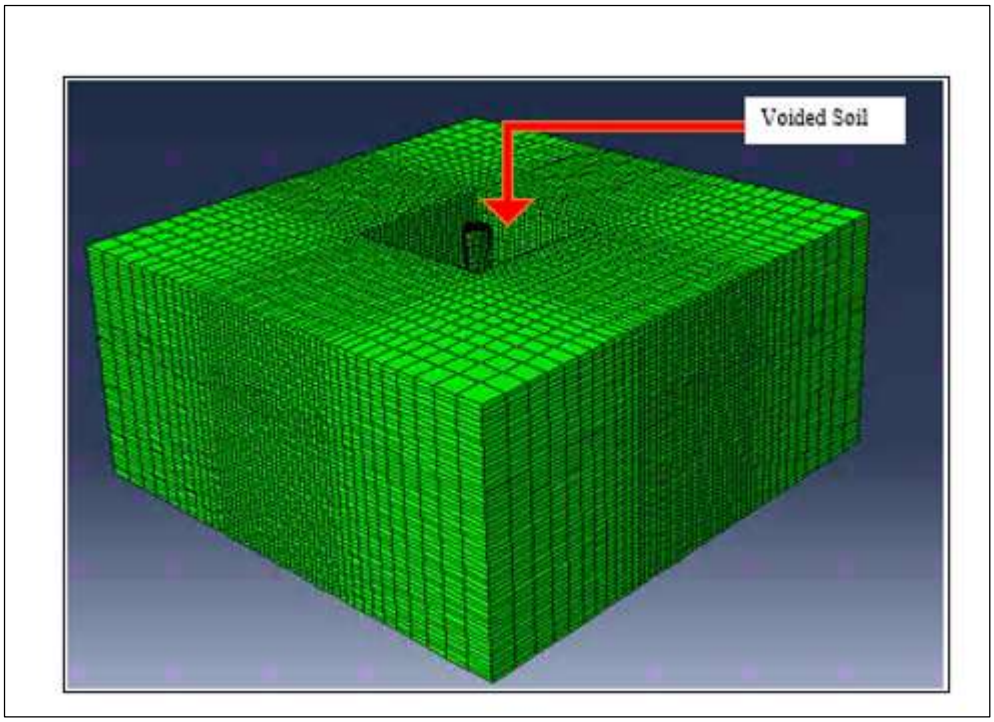

Figure 3-9. Three-dimensional Abaqus model showing scour case 1 (voided area indicates scour hole)

Results and Discussions

Lateral displacement vs depth responses

Figure 10 shows the graph of pile deflection computed for three different scour depths viz. 0 m (no scour), 1.5 m, 3 m and 4.5 m. The figure demonstrates that the scoured cases resulted in significant deflected pier tops with the same design loads. Pile head deflection resuls are summarized in Table 3-4. Although the lateral deflection is within the specified limit of maximum allowed pile displacement (ASHTO 2012; Ghasemi et al. 2016), the significantly increased deflection values with the increase in scour cause concerns about potential early instability of the bridge piers. Furthermore, this increase in pile deflection is a result of the increased unsupported length of the pier due to scour, hence, it is important to recognize the local scour effect on the bridge piers.

Table 3-4. Pile-head deflection (mm) using FEM

No Scour	With Scour Case 1 (1.5 m)	With Scour Case 2 (3 m)	With Scour Case 1 (4.5 m)
0.356	0.635	1.118	1.882

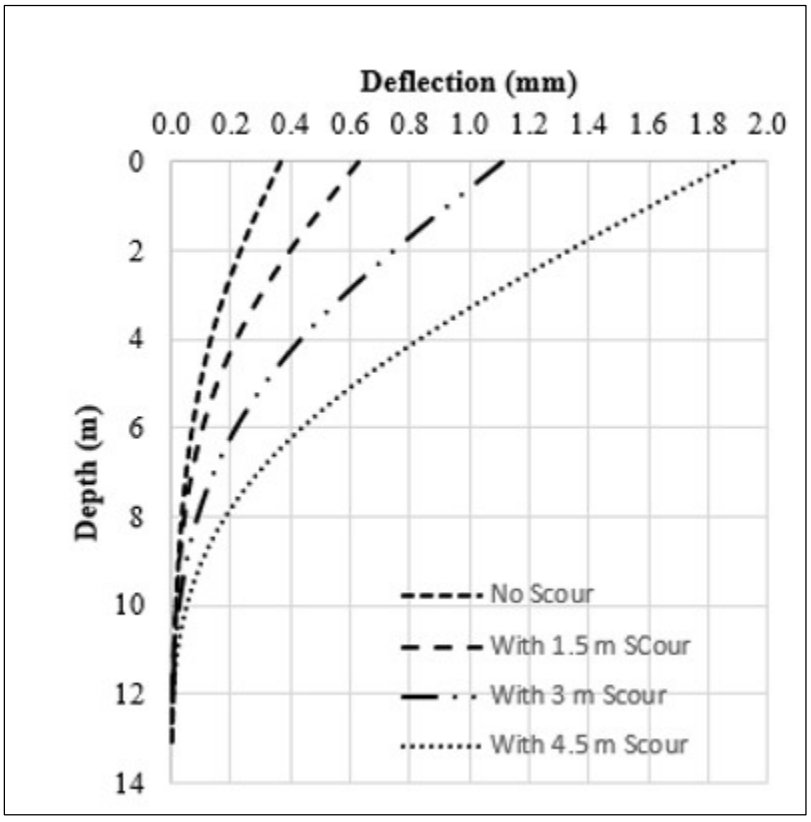

Figure 3-10.Lateral displacement vs depth for no scour and scour cases 1-3

Profiles of the bending moment

Figure 3-11 shows the computed bending moment curves along the pile depth for no scour case and three different scour cases described in Table 3-3. For scour case 1, the maximum bending moment has increased significantly from 45.06 kN-m to 98.64 kN-m for the first 1.5 m of scour depth. The bending moment is further increased by about 62.41 % (from 1.5 m to 3 m scour) and 53.55% (3 m to 4.5 m scour depths). The results are summarized in Table 3-5. Although these bending moments are well within the ultimate bending moment capacities of the pile, a rapid increase in the moment values demonstrated the effect of local scours on the lateral behavior of the pile foundation. For the no scour case, the maximum bending moment occurred at 3 m below the ground level, and at 3.7 m, 4.3 m, and 5.5 m depth, for scour cases 1 to 3, respectively. This shows the increase in the unsupported length of the pile due to scour resulted in increased values of maximum moment. With increase in scour depth, the lateral resistance of soil, and soil stiffness reduced significantly and resulted in the increased lateral loading on the bridge foundation.

Table 3-5. Model validation data

	Validation Model (kN-m)		**Scour Simulation Model (kN-m)**			
Depth(m)	LPile	FEM (without top 6.1 m soil, Fig. 3-7)	No Scour	Scour Depth(m)		
				1.5	3	4.5
6.7	600.777	339.241	18.256	56.963	122.961	238.734
			% increase with respect to no scour case	+212%	+573%	+1,207%

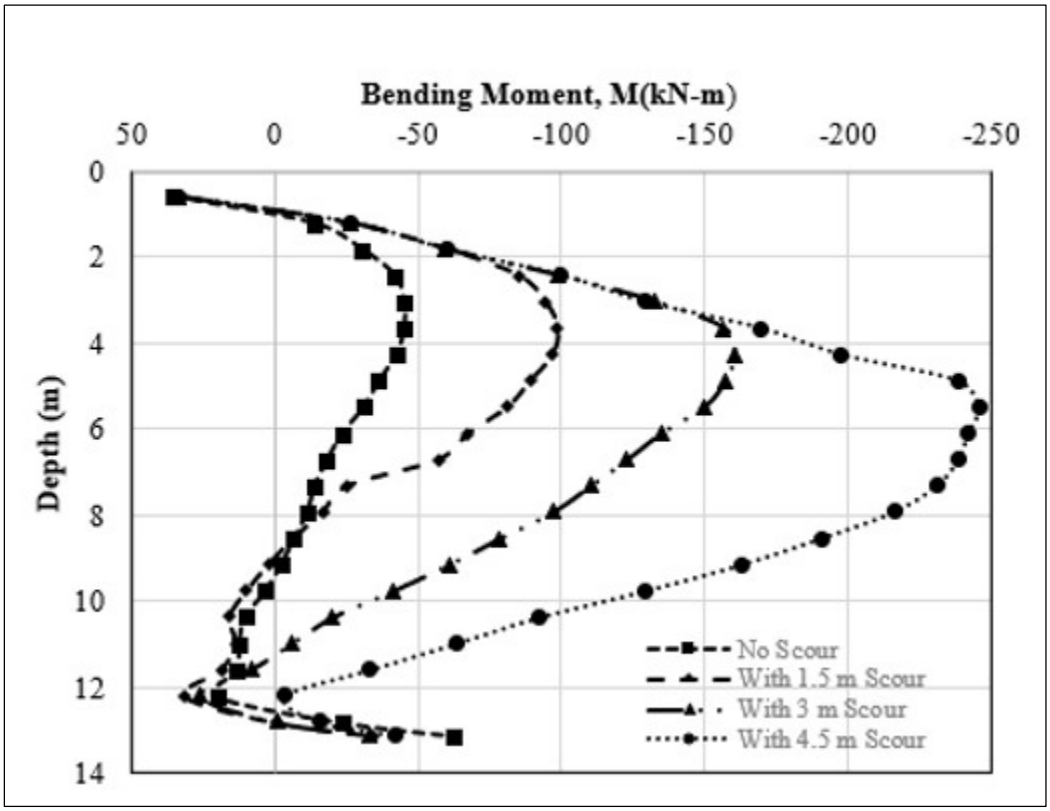

Figure 3-11.Bending moment profiles for no scour and scour cases 1-3

Conclusion

The Phillips Road bridge above the Toby Creek has its piers on the creek banks (piers-on-bank) and all the piers have experienced local scour problems resulting from the constricted creek cross section underneath the bridge and the excessive and turbulent flow during several storm flooding events. Due to significant landscape slopes and incised stream channels, significant number of bridges in central and eastern North Carolina are bridges with piers-on-bank posing unique local scour problems. To investigate the local scour problem for piers on bank for the Phillips Road bridge, LiDAR scans have been performed on the piers and showed that the local scour has diameters around 1.1 m and 1.5 m for the bridge piers on the east side of the river channel. The observed loss of embankment soil or riverbank is non-uniform along the two banks and could be broadly categorized as contraction scour. The piers on the northwest side of the case study bridge demonstrated a combination of local and contraction scour, which can further worsen the conditions of the hydraulic system for the bridge due to the accumulation of large quantities of debris in the river channel, which would likely further increase the scour volume in the future.

The scour volume from the LiDAR scans have been used to establish a square scour hole and are applied in the numerical investigation using three-dimensional, nonlinear finite element analysis to study the scouring effect on the structural performance of a bridge pier. Based on the results of simulation, the following conclusions are drawn:

1. Terrestrial LiDAR scans can be used effectively for frequent and periodic investigations of scour extent. Moreover, the collected site-specific data can be used to establish a possible bridge damage/bridge failure scenario such as estimating the true extents of the scour beyond estimated scour depth.
2. Based on the results of the 3D non-linear finite element analysis, it can be concluded that the local scour significantly increased the maximum bending moment values in piles, which can increase the possibility of pile failure.
3. Due to the increase in unsupported length, the lateral deflection of the pile increased considerably with an increase in the scour extent.
4. Local scour alone can alter noticeably the structural load carrying capacity of the pile. In the current study, the effect resulted in 212% increase in the bending moment (see Table 3-5) for the existing scour at the Phillips Road bridge. This effect would be even worse if local scour is coupled with general scour and/or contraction scour. Thus, bridge foundations need to be frequently inspected and analyzed for the existing scour conditions to take any preventive measures to avoid future damage to the bridge structure.

Finally, scouring between the adjacent piers can significantly reduce the supporting soil mass surrounding the piers on the creek bank and accelerate the deteriorating conditions of the hydraulic structures for the Phillips Road Bridge and like structures. Hence, future studies will investigate the effects of multiple pier scouring effects due to interconnection of local scours at each bridge pier.

References

AASHTO, L. (2012). AASHTO LRFD Bridge Design Specifications. American Association of State Highway and Transportation Officials, Washington, DC.

Abaqus. (2013). Abaqus version 6.13 documentation.

Alipour, A., Shafei, B. and Shinozuka, M. (2013). "Reliability-Based Calibration of Load and Resistance Factors for Design of RC Bridges Under Multiple Extreme Events: Scour and Earthquake." Journal of Bridge Engineering, 18(5), 362-371.

Apsilidis, N., Diplas, P., Dancey, C. L., Vlachos, P. P. and Raben, S. G. (2010). "Local Scour at Bridge Piers: The Role of Reynolds Number on Horseshoe Vortex Dynamics." In Scour and Erosion (pp. 86-94).

Avent, R. R. and Alawady, M. (2005). "Bridge Scour and Substructure Deterioration: Case Study." Journal of Bridge Engineering, 10(3), 247-254.

Beg, M. (2010). "Characteristics of Developing Scour Holes Around Two Piers Placed in Transverse Arrangement." In Scour and Erosion (pp. 76-85).

Ben H., Lai, Y., Wang, L., Hong, Y. and Zhu, R. (2019). "Scour Effects on The Lateral Behavior of A Large-Diameter Monopile in Soft Clay: Role of Stress History." Journal of Marine Science and Engineering, 7(6), 170.

Breusers, H.N.C., Nicollet, G. and Shen, H.W. (1977) "Local Scour around Cylindrical Piers," Journal of Hydraulic Research, 15(3), 211-252.

Chen, L., and Poulos, H. G. (1993). "Analysis of Pile-Soil Interaction under Lateral Loading Using Infinite and Finite Elements." Computers and Geotechnics, 15(4), 189-220.

EPA (2021), Toby Creek Watershed Report, US EPA Geoviewer. US EPA. Retrieved 7 July 2021, Watershed Report | Office of Water | US EPA.

FHWA (1995), Recording and Coding Guide for the Structure Inventory and Appraisal of the Nation's Bridges, Report No. FHWA-PD-96-001, Federal Highway Administration, US Department of Transportation, Washington, DC.

Ghasemi, S.H. and Nowak, A.S. (2016) "Reliability Analysis for Serviceability Limit State of Bridges Concerning Deflection Criteria," Structural Engineering International, 26(2), 168-175.

Govindasamy, A. V., Briaud, J. L., Kim, D., Olivera, F., Gardoni, P. and Delphia, J. (2010). "Observational Method for Estimating Future Scour Depth at Existing Bridges." In Scour and Erosion (pp. 41-65).

Karthigeyan, S., Ramakrishna, V. V. G. S. T., & Rajagopal, K. (2007). Numerical investigation of the effect of vertical load on the lateral response of piles. Journal of Geotechnical and Geoenvironmental Engineering, 133(5), 512-521.

Khandel, O., & Soliman, M. (2021). Integrated framework for assessment of time-variant flood fragility of bridges using deep learning neural networks. Journal of Infrastructure Systems, 27(1), 04020045.

Khodair, Y. and Abdel-Mohti, A. (2014). "Numerical Analysis of Pile–Soil Interaction Under Axial and Lateral Loads." International Journal of Concrete Structures and Materials, 8(3), 239-249.

Kim, Y., & Jeong, S. (2011). Analysis of soil resistance on laterally loaded piles based on 3D soil–pile interaction. *Computers and Geotechnics*, *38*(2), 248-257.

Kishore, Y. N., Rao, S. N. and Mani, J. S. (2009). "The Behavior of Laterally Loaded Piles Subjected to Scour in Marine Environment." KSCE Journal of Civil Engineering, 13(6), 403-408.

Klinga, J. V. and Alipour, A. (2015). "Assessment of Structural Integrity of Bridges Under Extreme Scour Conditions." Engineering Structures, 82, 55-71.

Lagasse, P. F., Clopper, P. E., Zevenbergen, L. W. and Girard, L. G. (2007). Countermeasures to Protect Bridge Piers from Scour (No. Project 24-07 (2)).

Li, F., Han, J., and Lin, C. (2013). "Effect of Scour on The Behavior of Laterally Loaded Single Piles in Marine Clay." Marine Georesources and Geotechnology, 31(3), 271-289.

Li, H., Ong, M. C., Leira, B. J. and Myrhaug, D. (2018). "Effects of Soil Profile Variation and Scour on Structural Response of An Offshore Monopile Wind Turbine." Journal of Offshore Mechanics and Arctic Engineering, 140(4), 10pages.

Liang, F., Zhang, H. and Huang, M. (2015). "Extreme Scour Effects on The Buckling of Bridge Piles Considering the Stress History of Soft Clay." Natural Hazards, 77(2), 1143-1159.

Lin, C. and Wu, R. (2019). "Evaluation of Vertical Effective Stress and Pile Lateral Capacities Considering Scour-Hole Dimensions." Canadian Geotechnical Journal, 56(1), 135-143.

Lin, C., Bennett, C., Han, J. and Parsons, R. L. (2012). "Integrated Analysis of The Performance Of Pile-Supported Bridges Under Scoured Conditions." Engineering Structures, 36, 27-38.

Lin, C., Han, J., Bennett, C. and Parsons, R. L. (2014). “Case History Analysis of Bridge Failures Due To Scour.” In Climatic Effects on Pavement and Geotechnical Infrastructure (pp. 204-216).

Liu, W., Chen, S. and Hauser, E. (2011). “LiDAR-Based Bridge Structure Defect Detection.” Experimental Techniques, 35(6), 27-34.

Liu, W., Chen, S. E. and Hasuer, E. (2012). “Bridge Clearance Evaluation Based on Terrestrial LIDAR Scan.” Journal of Performance of Constructed Facilities, 26(4), 469-477.

Liu, W., Chen, S. E., Boyajian, D. and Hauser, E. (2010). “Application of 3D LiDAR Scan of A Bridge Under Static Load Testing.” Materials Evaluation, 68(12), 1359-1367.

Majumder, M., & Chakraborty, D. (2021). Effects of scour-hole depth on the bearing and uplift capacities of under-reamed pile in clay. Ocean Engineering, 240, 109927.

Mardfekri, M., Gardoni, P. and Roesset, J. M. (2013). “Modeling Laterally Loaded Single Piles Accounting for Nonlinear Soil-Pile Interactions.” Journal of Engineering, 2013.

McConnell, J. R. and Cann, M. (2010). “Assessment of Bridge Strength and Stability Under Scour Conditions.” In Structures Congress 2010 (pp. 121-132).

Melville, B. W., and Coleman, S. E. (2000). Bridge Scour. Water Resources Publication.

Poulos, H. G. (1971). “Behavior of Laterally Loaded Piles: I-Single Piles.” Journal of the Soil Mechanics and Foundations Division, 97(5), 711-731.

Prendergast, L. J., Hester, D., Gavin, K. and O'Sullivan, J. J. (2013). "An Investigation of The Changes In The Natural Frequency Of A Pile Affected By Scour." Journal of Sound and Vibration, 332(25), 6685-6702.

Richardson, E. V. and Davis, S. R. (2001). Evaluating Scour at Bridges (No. FHWA-NHI-01-001). United States. Federal Highway Administration. Office of Bridge Technology.

Strömblad, N. (2014). Modeling of Soil and Structure Interaction Subsea, Master's Thesis, Department of Applied Mechanics, Chalmers University of Technology, Göteborg, Sweden.

Suro, T.P., Huizinga, R.J., Fosness, R.L. and Dudunake, T.J., (2019) Assessment of Bridge Scour Countermeasures at Selected Bridges in the United States, 2014-18, Scientific Report 2019-5080, US Geological Survey.

Warren, L. P. (2011). Scour at Bridges: Stream Stability and Scour Assessment at Bridges In Massachusetts. Open-File Report, US Geological Survey.

Xing, W.W., Song, C. and Tin-Loi, F. (2018) "A Scaled Boundary Finite Element Based Node-to-Node Scheme for 2D Frictional Contact Problems," Computer Methods in Applied Mechanics and Engineering, 333, 114-146.

Yang, T. H., Chen, P. W., Lin, T. K., & Chang, K. C. (2021). Scour stability evaluation of bridge pier considering fluid-solid interaction. In Bridge Maintenance, Safety, Management, Life-Cycle Sustainability and Innovations (pp. 1386-1392).

4 ANALYSIS OF LOCAL AND COMBINED (GLOBAL) SCOURS ON BRIDGE PIERS-ON-BANK

Abstract

This paper examines scour problems related to piers-on-bank bridges resulting from frequently flooded and/or constricted waterways. While local scour problems for bridge piers in riverine channels have been addressed extensively in the literature, there have been few studies addressing piers-on-bank scour scenarios. A comprehensive three-dimensional finite element analysis using the element removal (ER) technique has been performed on a recently constructed bridge with an observable scour problem on multiple piers. The analysis is further extended to study the effect of 'combined scour' or extensive erosion of soil between adjacent piles. Three different loading cases were considered in the study and the results demonstrated that the effects of local and combined scours on bridge drilled shaft foundations can be significant under the combined actions of axial, lateral loads and bending moments. Results of this study show that interaction of soil displacement fields between adjacent piles should be investigated for bridge crossings with piers-on-bank with a high risk of flooding during moderate to low probability of occurrence precipitation events, as they can increase the pile head displacements and the bending moments in the soil and result in early failure of bridges.

Keywords: local scour; combined scour; finite element method, combined loads, piers-on-bank

Introduction

Flood and other hydraulic causes of bridge failure are of prime concern all over the world. The AASHTO LRFD Bridge Design Specifications (2010) states that "A majority of bridge failures in the United States and elsewhere are the result of scour" (C2.6.4.4.2) [[1,2]. Scour caused by the erosion of streambed material due to flowing water was responsible for more than 53% of bridge failures in the United States [3]. Cook et al. [2,4] have estimated an annual hydraulic collapse frequency of approximately 1/5,000, and there are about 504,000 bridges over waterways in the United States [5]. As per the Federal Highway Administration (FHWA) national bridge scour evaluation program, each state needs to evaluate its bridges for potential flood damage for a 100 to 500-year return period floods [6] and, scour susceptible bridges need to be retrofitted or replaced based upon the existing condition of the bridge. Researchers all over the world have recognized the importance of reliable scour monitoring methods, and frequent bridge scour vulnerability assessments of the existing bridges.

Scour resulting from hydrostatic and hydrodynamic forces at the streambed and channel margins that remove soil and alluvial sediments surrounding bridge piers exposes the bridge foundation and subject bridge structures to preemptive structural interventions or earlier than anticipated infrastructure replacement results. The properties of the soil and alluvial sediments surrounding the bridge foundation can determine the degree of scouring. However, conventional analysis of bridge scour treats scour depth as the prime or major parameter of scour analysis [2].

Several studies have been conducted to study the effect of scour on the performance of bridge sub-structure and superstructures: Avent and Alawady [7] and Lin et al. [8] studied the effects of scour on the buckling capacity of a bridge pier; McConnell and Cann [9] investigated scour effects on the pushover behavior of a bridge; Klinga et al. [10] conducted buckling, longitudinal and transverse pushover analyses, and modal analyses of a scoured bridge; and, Alipour et al. [11] considered earthquake and scour scenario to determine the probability of bridge failure under extreme conditions.

In the literature, most researchers would differentiate the impacts of scour on the lateral behavior of piles into either cohesive or non-cohesive soil cases. This is because scour hole formation (mass losses surrounding a bridge pier) in cohesionless soil can attain maximum depth within a few days, whereas in cohesive soils, this process may take months or even years. Lin et al. [8] demonstrated the importance of considering the stress history of cohesionless soil to determine the lateral behavior of piles accurately. Liang et al. [12] studied the effects of extreme scour on the buckling of bridge piles considering the stress history of soft clay. Finally, Ben et al. [13] demonstrated the impact of stress history in evaluating scour effects on lateral behavior of monopiles in soft clay.

Most of the research conducted were primarily focused on local scour surrounding single piles. In the majority of cases, these piles were analyzed for vertical load or lateral loads, separately. Where combined loading is considered in the literature, there is a conflict in opinions on the predicted behavior of drilled shafts: Jain et al. [14] and Phillips and Lehane [15] reported a reduction in lateral displacement due to the

presence of vertical load, whereas other studies suggested an increase in lateral deflection under vertical load [16],[17]. Achmus et al. and Hung et al. [18,19] observed that there is an interaction between axial and lateral loads in cohesive soils, which may indicate that the axial and lateral load interactions are soil type dependent. Unfortunately, there are insufficient case studies to definitively differentiate the combined load effects on piles installed by different soil types.

It is important to point out that scour is a complex, multi-physics problem involving several factors including river hydraulics, the geometry and stiffness of the embedded structure (pier) and geological conditions of the sites. Figure 4-1 shows the schematic of a scour hole formation surrounding a single pier, where rapidly moving water flowing against the pier forms vortices and scour generally occurs in an area at the base of the piers affected by the vortices. For example, a horseshoe-shaped vortex resulting from pileup of water on the upstream side and acceleration of flow at the nose of a pier removes bed material around the pier base and scoops a hole around the pier (scour hole). The local scour around the bridge pier from the horseshoe vortex is due to the high bed shear stresses created by the acceleration of the flow near the pier. With increasing flooding events, this scour hole gets deeper and further washes out the soil around the adjacent piles. As a result, the scour hole extends around the pile, and the scour depth grows over time.

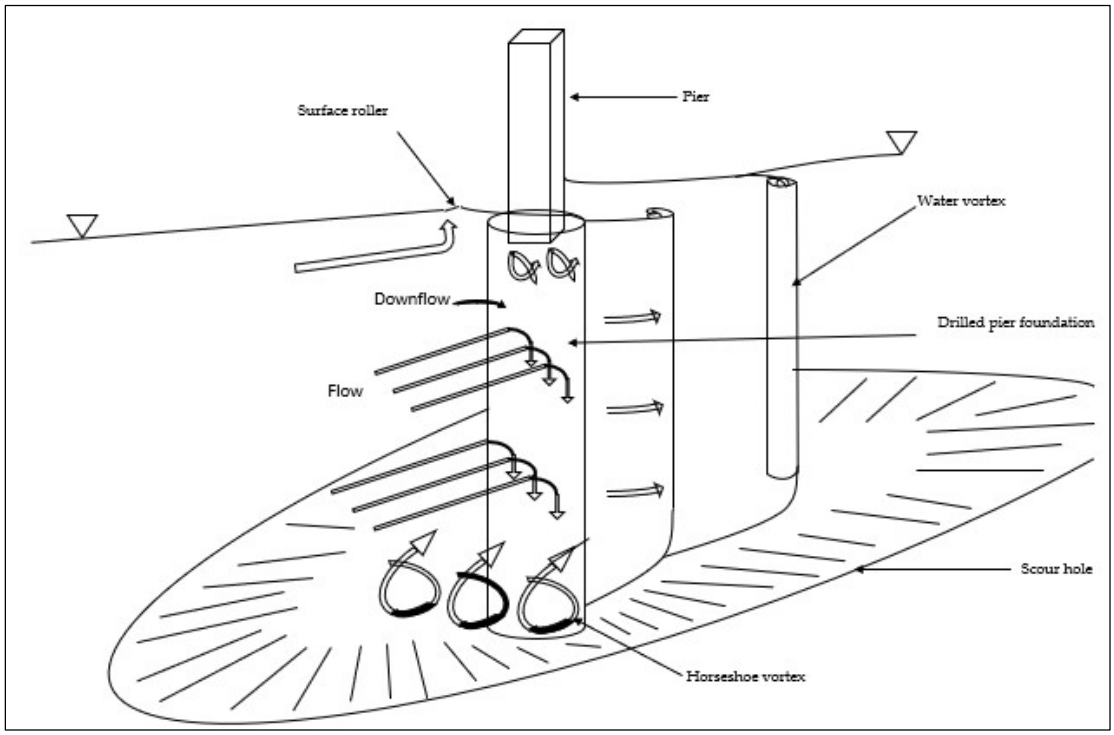

Figure 4-1.Scour mechanism around single pier

If the local scour problem is not corrected, the flow pattern around a pier may become further altered, resulting in the expansion of local scour holes forming a global or combined scour that can cause loss of supporting soil between piers. Unfortunately, only limited studies have been published on the subject of combined or global scour effects on bridge piers: notably, Zulhilmi [20] conducted laboratory experiments to compare the scour depths and patterns around a single pier and two piers in a side-by-side arrangement. They concluded that the local scour process is mainly governed by pier spacing, the horseshoe vortex, and reinforcement elements around the piers. Several laboratory studies have been carried out to investigate the relationship between pier spacing and maximum scour depth around two piers in a side-by-side arrangement [21-23]. To the best of the authors' knowledge, there is no literature on the effect of scouring between two side-by-side piers with consideration of the loading on piles.

In this paper, numerical analysis using the Finite Element (FE) modeling technique is used to study the combined scour effects between two bridge piers-on-bank for the Phillips Road bridge in Charlotte, North Carolina. The scour problem for piers-on-bank is usually not considered because it is always assumed that the waterway basin is sufficiently deep to accommodate the design flow of the stream water. Piers-on-bank bridges are common for auto crossings over small streams with sites not suitable for culverts. Figure 4-2 shows the Phillips Road bridge and the scoured piers. The bridge spans across Toby Creek on the UNC Charlotte campus and accommodates a four-lane traffic pattern. In the case of Phillips Road bridge, frequent high flows resulting from low to moderate return rainfall events immersed most of the active channel and channel

margins underneath the bridge resulting in significant scour around multiple bridge piers. The numerical modeling simulated the local and combined scours between two adjacent piers-on-bank for three different loading scenarios and the results are presented within. The objective of the study is to investigate the potential effects of the premature scours on the bridge piers.

Local and Combined Scour of the Phillips Road Bridge

Local scour is commonly seen around bridge piers located in the riverbed. However, local scour holes are also frequently visible near the piers located on the riverbank (piers-on-bank). At the Phillips Road bridge site, repetitive cycles of heavy floods cause overtopping of the floodplains and the rapid flood water scooped out scour holes around the piers on the embankments (Figure 4-2a). Phillips Road bridge sits above Toby Creek, which is a headwater tributary that rises in the Newell community of Charlotte, North Carolina. The creek drains approximately 13.3 km2, and discharges into the Mallard Creek, which is a tributary of the Yadkin-PeeDee River system. Toby Creek has an estimated average discharge of 0.17 m3/s and a mean flow velocity of 0.274 m/s [24]. The total stream length is 6.68 km. The width of the creek at the bridge at low flow stage is approximately 3.0 m and has a maximum bank full depth of 2.14 m. The constricted river cross section underneath the bridge, combined with high flow velocities during episodic runoff events, has resulted in significant bank erosion and has induced localized scour and combined scour at the piers on both streambanks.

(a) (b)

Figure 4-2.Scour Problem at the Phillips road bridge (a) bridge piers-on-bank with scours; (b) bridge site with flow and traffic scenarios

As the flooding recedes, unlike for the piers-in-the-river case, these scour holes at the Phillips Road bridge piers and like structures do not get filled in with sediments. As a result, large areas of soil between the adjacent piers were exposed to further erosion. Eventually, the erosion of soil over a widened area between the adjacent piers resulted in a groove formation between the piers, which is termed as "combined scour". Figure 4-3 shows close-ups of the scours at the Phillips Road bridge. Specifically, the scours occurred at the west side of the north-flowing creek. Figure 4-3a shows the marked local scour and Figure 4-3b shows the connection of the local scours to form the combined scour. We employ a square shaped local scour assumption to facilitate the numerical modeling. The actual scour is more rounded and complicated by loose sand and coarse gravels. Subsequent numerical models are built based on these two pier scenarios.

Current scour evaluation methods are based on observations and predictive evaluations and have relied on a single parameter: "scour depth". Most of the studies on scour depth estimates are based on empirical equations and various equations have been proposed to determine the scour depth based on historical data [25,26]. The depth equation proposed in Hydraulic Engineering Circular No.18 (HEC18) [26] is the most commonly used, which is expressed as:

$$d_s = 2yK_1K_2K_3(b/y)^{0.65}F^{0.43} \quad (1)$$

where, ds is scour depth, b is the pier width and y is flow depth upstream of the pier. K1, K2, and K3 are the correction factors for the pier nose shape, angle of attack flow and bed condition, respectively and, F = Froude number.

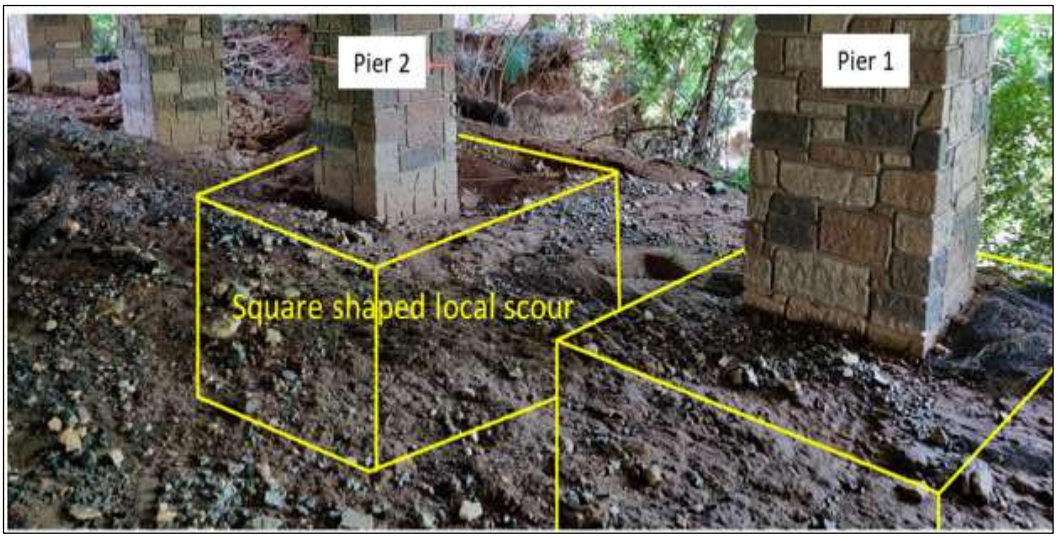

(a)

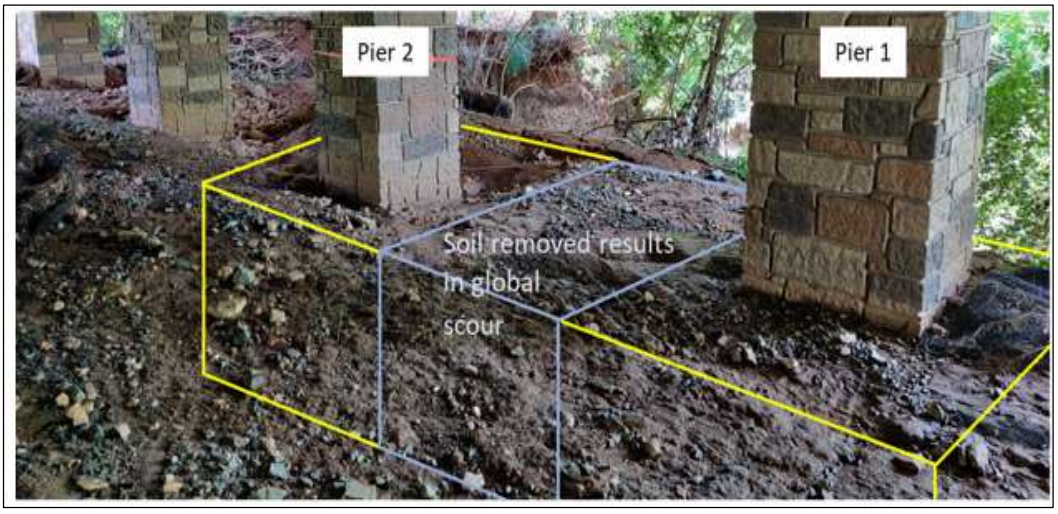

(b)

Figure 4-3.Image of the Phillips Road bridge pier scours (a) with indication of square shaped local scour and (b) include indication of combined scour between the two piers

Phillips Road bridge (Figure 4-2) is a three-span continuous bridge that spans Toby Creek (south to north flowing). The bridge has a total length of 50.6 m with two end bents and two intermediate bents. Bent 1 consists of 6 bridge piers connected through a pier cap and supported by drilled shaft foundations. Bent 2 is made up of 5 piers connected through a pier cap. Two end bents are founded on steel pile-supported strip footing. Phillips Road bridge has a clear roadway width of 9.8 m and supports two traffic lanes of 4.9 m width each. The overall width of the bridge deck is 15.5 m.

Numerical modeling of scour around bridge piers – a brief review

Numerical analysis methods such as the finite difference (FD) and the finite element (FE) methods have been used extensively in the study of soil-pile interactions [28,29]. A review on the different techniques for bridge scour analysis, which include p-y method, beam-on-Winkler method and soil spring method, etc., shows that the most widely used technique is the p-y method of analysis of laterally loaded piles. Klinga and Alipour and Lin et al. [10,30] developed p-y curves from full-scale test results. However, the p-y method and the more classical beam-on-Winkler foundation methods do not consider the three-dimensional nature of the pile-soil behavior and its effect on the performance of the pile. As a result, the more robust FE methods have been used: Mardfekri et al. [31], Strömblad [32], Salim [33] and Youssouf et al. [34], are some of the studies that employed three-dimensional FE methods to study the effect of soil-pile interaction on laterally loaded piles. Senturk and Pul [29] performed three-dimensional finite element push-over analyses of bridge piers considering the nonlinear behavior of reinforced concrete and soil under quasi-static loading. Khodair et al. [28] compared the

results obtained from the Finite Difference (FD) method and FE method to study the effect of pile-soil interaction under axial and lateral loads.

Development of Finite Element Model

The problem to be investigated can be best described as the effect of local and combined scours on two in-line drilled shafts. A comprehensive finite element model of the case study bridge pier was prepared using FEA software, ABAQUS [35] where one individual drilled shaft was first modelled using 3D, solid deformable elements and then a two-drilled shaft model was developed. These drilled shafts were protruded 15.24 cm above the ground level and are embedded through a multilayered alluvial and residual soil deposits that were identified at the Toby Creek site. The distance between these two piers is 4.2 m. To minimize boundary effects, the soil domain was modeled up to 10 times the diameter of the pile from the center. As suggested in previous studies [36], modeling of the soil for a more considerable distance would help avoid boundary effect on simulation results. Soil is extended to 2.13 m below the actual length of the shaft. The size of the FE model domain is therefore 38.4 m X 33.5 m X 15.1 m. The bottom of the pile was fixed to simulate the embedment of pile in weathered rock at its tip. The lateral and bottom sides of the model domain were fixed and restrained against translation in all directions. Figure 4-4 shows the full FE model defining the problematic piers and surrounding soils. Also shown in Figure 4-4 are the modeling of the local and combined scour scenarios.

The finite element model was built using two different element types: the piles and soil were modelled using continuum, 3D, eight-node, reduced integration elements,

while the longitudinal and transverse reinforcement of the pier was modeled using one-dimensional rebar elements. These solid and rebar elements were defined by first-order linear interpolation. FE model comprised of a total 79,866 linear continuum brick elements (C3D8R) defined for the piles and soil. To minimize the computational time, a finer mesh was selected for the soil region near the pile and relatively coarser mesh was created towards the boundary of the soil block.

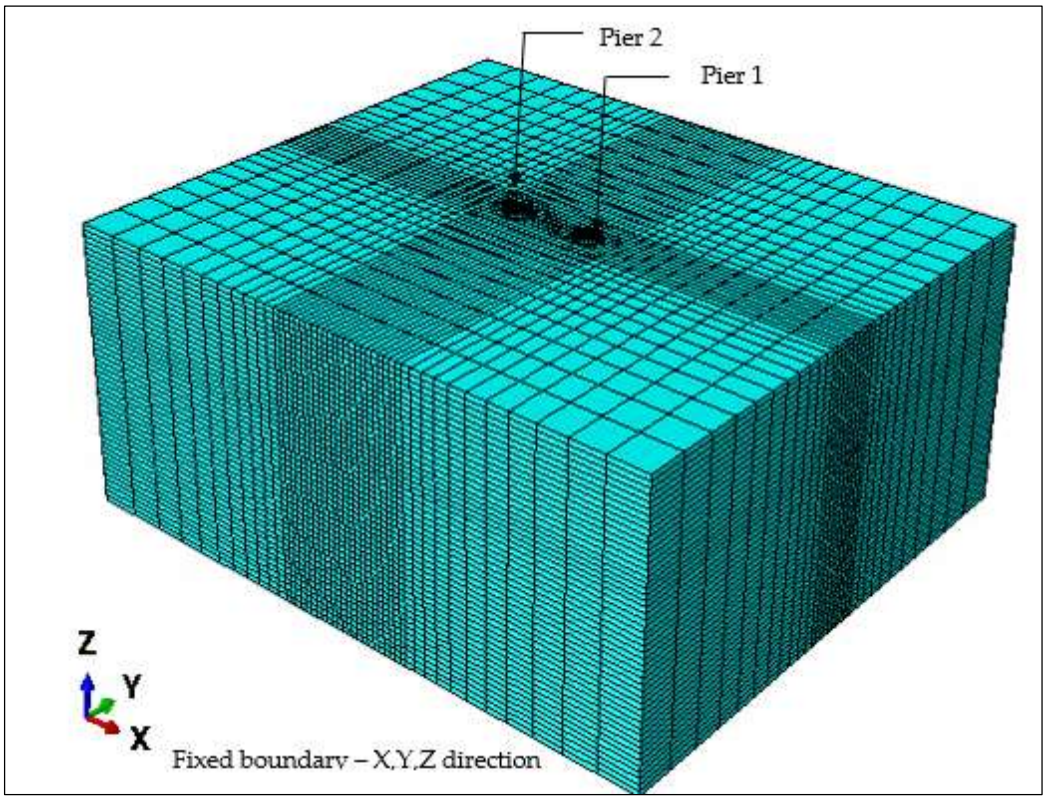

Figure 4-4.The full FE model for the two pier problem and the modeling of the Local and Combined scours

Geometry and Material Properties

Drilled shaft properties

The reinforced concrete drilled shafts are 1.68 m in diameter and 12.95 m in length. The cross section of the pier is shown in Figure 4-5. The 'Embedded region' constraint in ABAQUS was used to model the longitudinal and transverse reinforcements of the piles. The pile reinforcements are composed of 27 #10 longitudinal rebars with a clear cover of 127 mm. The shaft's transverse reinforcement or lateral ties are #4 deformed bars spaced at 127 mm c/c. A bridge pile is typically assumed to behave non-elastically up to significant deflection level, and thus for this study, the pile material is considered elastic. Hence, the nonlinear behavior is dominated by soil deformation behaviors. This consideration can reduce the computational time during the analysis. Material properties of the reinforced concrete and steel are depicted in Table 4-1.

Table 4-1. Material properties of pile concrete and pile reinforcement

Property	Concrete	Steel
Density (kN/m^3)	22.8	77
Youngs Modulus (E_c) kPa	$2.7x10^7$	$2x10^8$
Poisson's Ratio	0.2	0.2
Characteristic Strength (f'_c) kPa	31026.40	-
Yield Strength (f_y)	-	Grade 60

Soil material model

Typical behavior of laterally loaded shafts includes nonlinearities in the soil and pile resistance. Soil nonlinear behavior is modeled using the Mohr-Coulomb plasticity model in ABAQUS. As described earlier, the soil domain is assumed as multi-layered geo-materials comprised of five layers of alluvial soil, residual soil, and with the bottom

layer of weathered rock, as shown in Figure.4-6. Table 4-2 shows the material properties used in the models.

Table 4-2. Properties of different soil layers at the study site (Phillips Road bridge, UNC Charlotte)

			Elastic Properties		Mohr-Coulomb Plasticity Parameters		
Soil	**Unit weight (γs) (kN/m^3)**	**Young's modulus (E) (kPa)**	**Poisson's ratio (υ)**	**Cohesion intercept (c) (kPa)**	**Friction angle (Ø°)**	**Dilation angle (ψ°)**	**Absolute Plastic Strain(ε 50)**
Layer 1- (c-phi)	8.258	47880	0.25	1000	26	0.01	0.1
Layer 2- (c-phi)	9.043	28728	0.3	800	26	0.01	0.01
Layer 3- (c-phi)	9.828	76608	0.32	4000	36	0.01	0.005
Layer 4- (c-phi)	12.183	95760	0.35	72000	40	0.01	0.00005
Layer 5- (c-phi)	12.183	95760	0.35	72000	40	0.01	0.00005

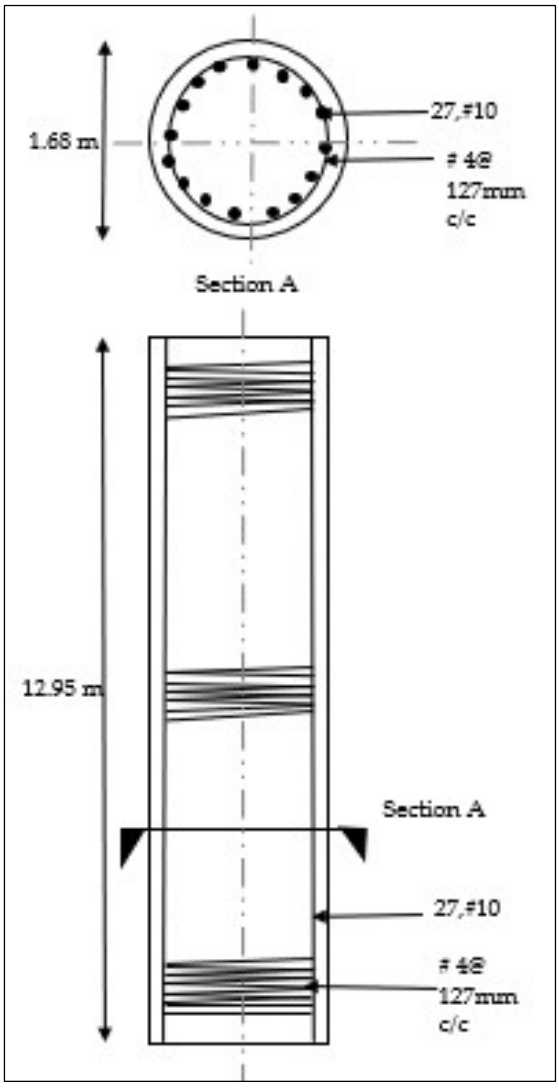

Figure 4-5.Cross section of the reinforced concrete pile foundation

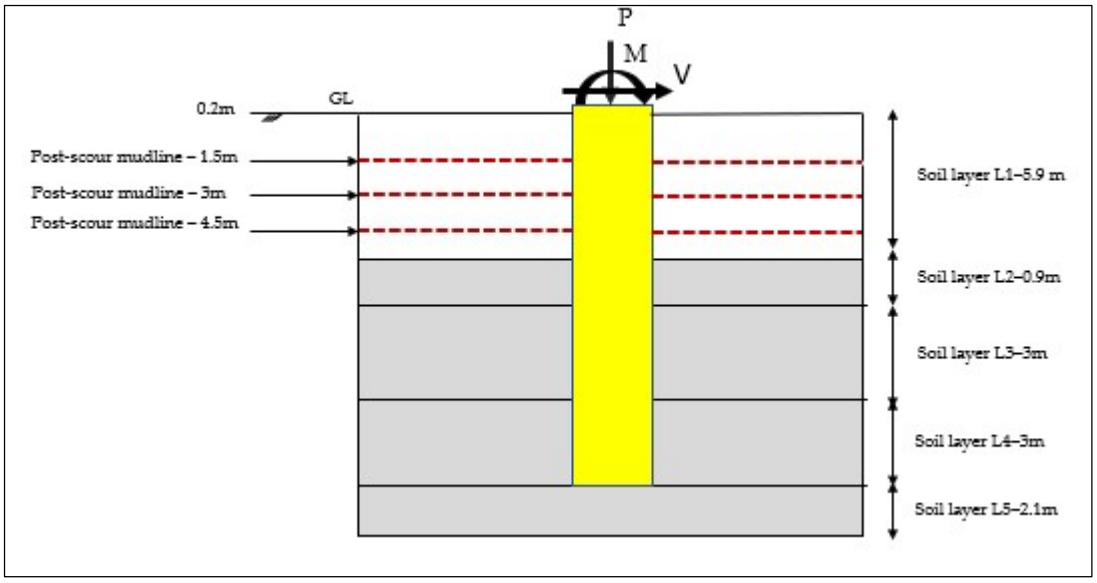

Figure 4-6.Schematics of soil layers and pier scouring at the Phillips Road bridge

Pile-soil interaction

The pile-soil interface was modeled using ABAQUS contact features with identified Master (pile) and Slave (soil) sides, which allows soil pile separation and models the frictional behavior at the interface. The Master-Slave contact pair formulation allows simulation of the load transfer between the pile and soil as show in Figure 4-7. As shown, the piles being stiffer was selected as the Master surface, while the soil domain was the Slave surface. The separation between the soil and pile contact interface is a critical feature of the modeling technique that models the actual scenario of the bridge piers.

In ABAQUS, surface-to-surface contact discretization can be applied between two material types and in the current modeling, a penalty enforcement method was selected to assure proper load transfer between the pile and the soil. The penalty method enforces the load transfer in the normal direction by constraining the contact interface. In this study a default stiffness value (defined as a ratio to the element material stiffness) was selected for the linear contact stiffness. Shear behavior between pile and soil was described using a Coulomb friction coefficient of 0.3. No limit penalty friction formulation was used to depict the tangential behavior between contact surfaces. The FE analysis of the scour simulation was performed using multiple steps as shown in Figure 4-8. In order to ensure equilibrium, the 'Geostatic' option is applied prior to and after the scour condition simulation. This step ensures that the geostatic stresses are in equilibrium.

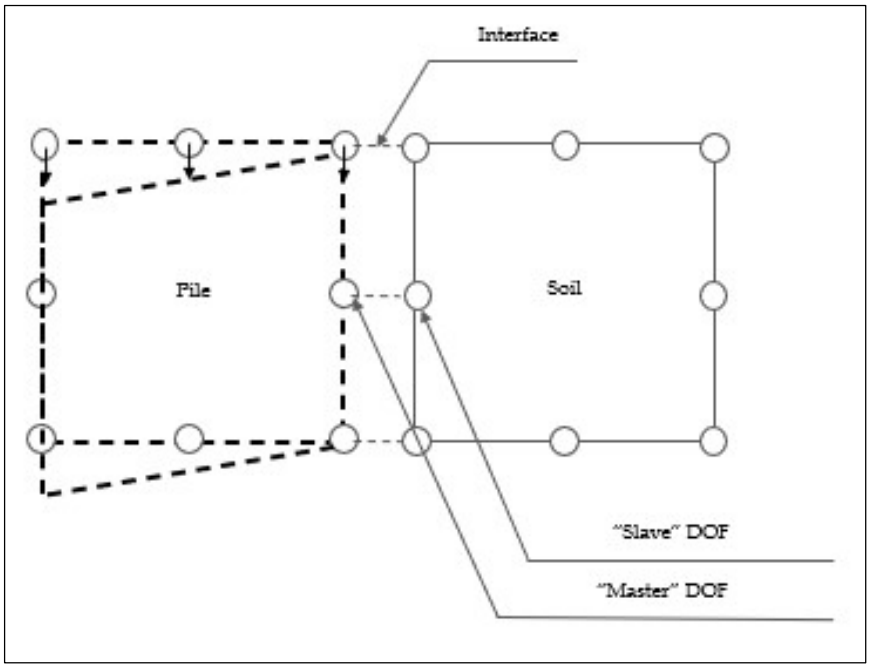

Figure 4-7.Contact pair formulation of pile-soil in ABAQUS

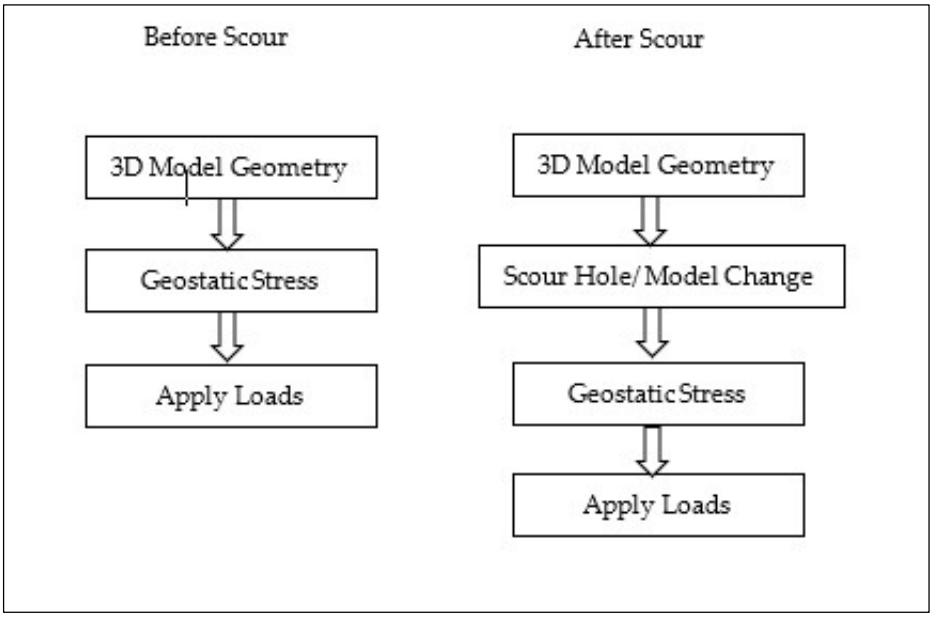

Figure 4-8.ABAQUS FE Steps for geo-mechanics modeling

Scour simulation

Scour holes of rectangular shape were created in ABAQUS using an element removal 'ER' technique, where elements were removed surrounding each pile. This approach ignored the hydrodynamic effects in scouring and represent an instantaneous loss of soil around the piers. The general static step uses the 'Model Change' option so that the initial model can be further analyzed after ER. Before the defined ER step, ABAQUS stored the forces exerted by the scour hole region on the remaining part of the soil domain at the boundary nodes. The nodal variables of the removed elements were not changed directly when the elements were removed [35]. The element removal method used to simulate scouring represents a permanent soil mass loss and these elements were not reactivated again for the remaining analysis. Hence, the corresponding master-slave contact pair was removed to avoid any convergence issue. Figure 4-9 shows the results of ER in the numerical models: Figure 4-9a shows the surrounding soil sans the piles and Figures 4-9b and 4-9c show the local scour holes and the combined scour hole with the two piles in place.

Initial stresses in the soil were simulated by applying geostatic stress in ABAQUS. The user-specified predefined stress field was created by defining the effective vertical stress between any two points within each soil layer with lateral earth pressure coefficient and vertical effective stresses calculated using the following equations, respectively:

$$k0 = 1 - \ sin\phi \tag{2}$$

$$\sigma' = \gamma sat.h \tag{3}$$

where, γ_{sat} = saturated unit weight of the soil, h = depth to the soil layer of interest, ϕ = coefficient of friction for i^{th} soil layer and, k_0 = the lateral earth pressure coefficient, which is determined and used as data input in the calculation of the lateral effective stresses in the soil.

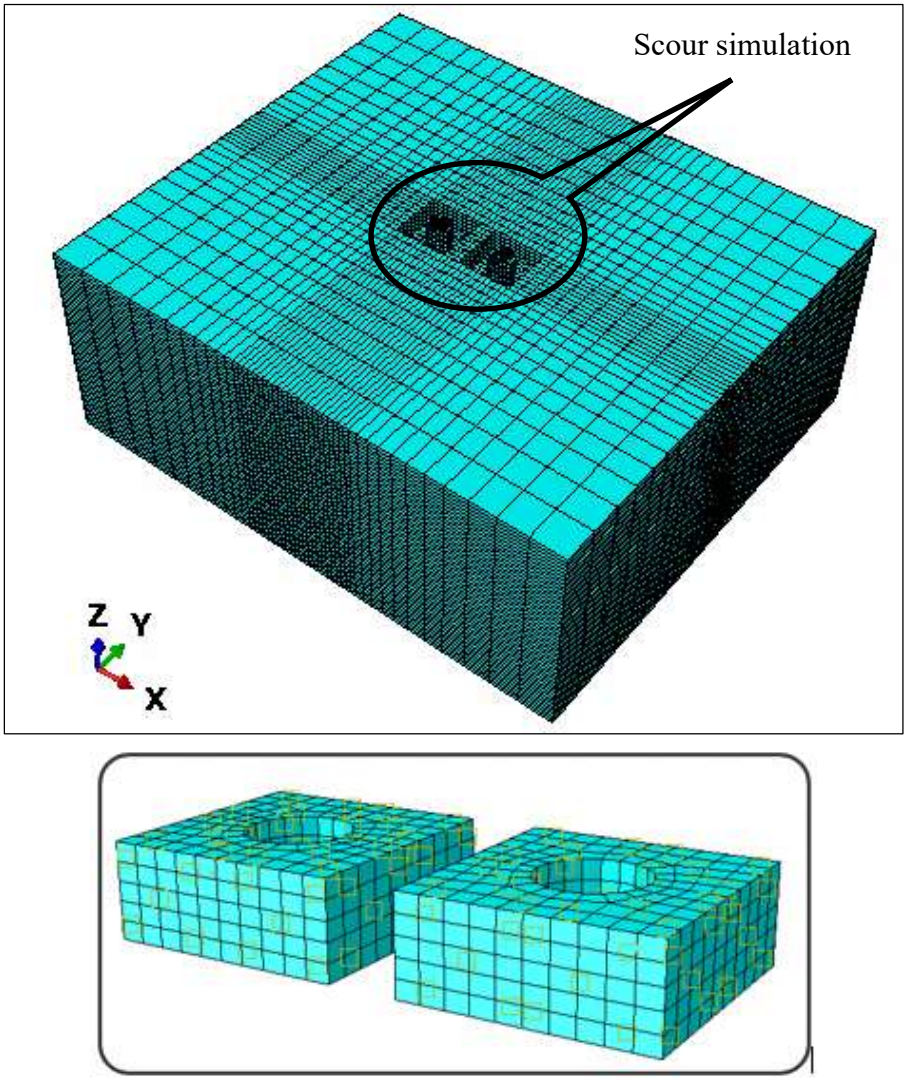

(a) Element Removal – 'Model Change'

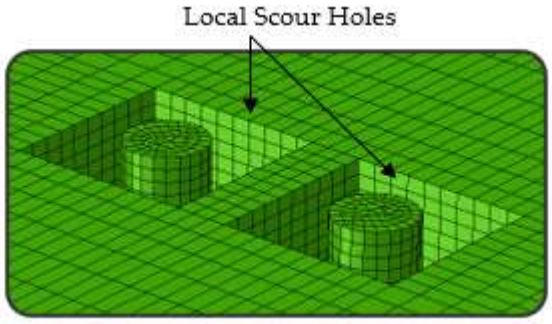

(b**)** Local scour holes

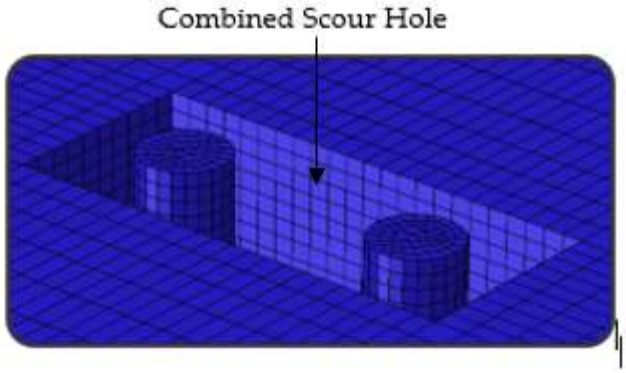

(c**)** Combined scour hole

Figure 4-9.Element removal for (a) Local scour hole region, (b) View of local scour holes and (c) View of combined scour hole

Loading scenarios

In contrast to conventional design practices of considering separately the axial and lateral loads on the pile top, this study considered the combined effects of loading applied to the bridge piers, which is a better representation of the actual condition of existing bridges. In the actual working conditions, ongoing traffic would subject the bridge piers to different combinations of axial loads, lateral loads, and moments as a result of traffic coming from both (west bound and east bound) directions. Different load combinations pertaining to maximum axial, maximum lateral and maximum moment cases considered in the original design of the bridge shafts were analyzed for evaluating scour effects in this study. The static loadings shown in Table 4-3 were applied to each pier through a reference point identified at the top of the pier's cross-section.

Table 4-3. Load cases considered in Phillips Road bridge scour study

Type	Fx (kN)	Fy (kN)	Fz (kN)	Mx (kN-m)	My (kN-m)
Load case 1 – Maximum Axial	-67	-71	2750	-324	-149
Load case 2 – Maximum Lateral	-67	-169	2029	-1001	-75
Load case 3 – Maximum Moment	-40	-71	1900	-1433	-5

A total of three load cases are considered in order to generate the maximum axial stress and deformation (load case 1), the maximum lateral pressures (load case 2) and the maximum bending moment in the piers (load case 3).

To investigate the combined scour effect, two piers were considered in the current study. A parametric study has been performed considering different scour depths including existing scour depths at the Phillips Road bridge. The degrees of freedom of the elements at the top of the pier were constrained using a kinematic coupling to limit the motion of the coupling nodes to the reference node.

Results and Discussion

Initial Soil Displacement Field Analysis

An initial simulation of the pier behavior was first performed without considering any soil scour. Figure 4-10 shows the soil displacement fields of the three analysis load cases depicted in Table 4-3. In the case of the multi-pier interactions, Figure 4-10 shows that the two piers considered are close enough that the soil displacement fields of the adjacent piles overlapped and visibly interacted in the space between the two piers. This observation indicated that the combined scouring (soil mass loss between the piers) may be critical to the stability of the bridge.

Parametric Studies

To investigate the effect of local and combined scour holes, parametric studies were conducted for different scour depths ranging from 0.9D (1.5 m), 1.8D (3 m) and 2.7D (4.5 m), respectively. The initial 0.9D (1.5 m) scour depth is the existing scour conditions at the Phillips Road bridge estimated from field observations. Figures 4-11 through 13 show the profiles of lateral pile head displacements in the X-direction (along the pile length). Negative sign of the displacement indicates displacement of pile in the

negative X-direction. Table 4-4 summarizes the pile deflections for the different load cases.

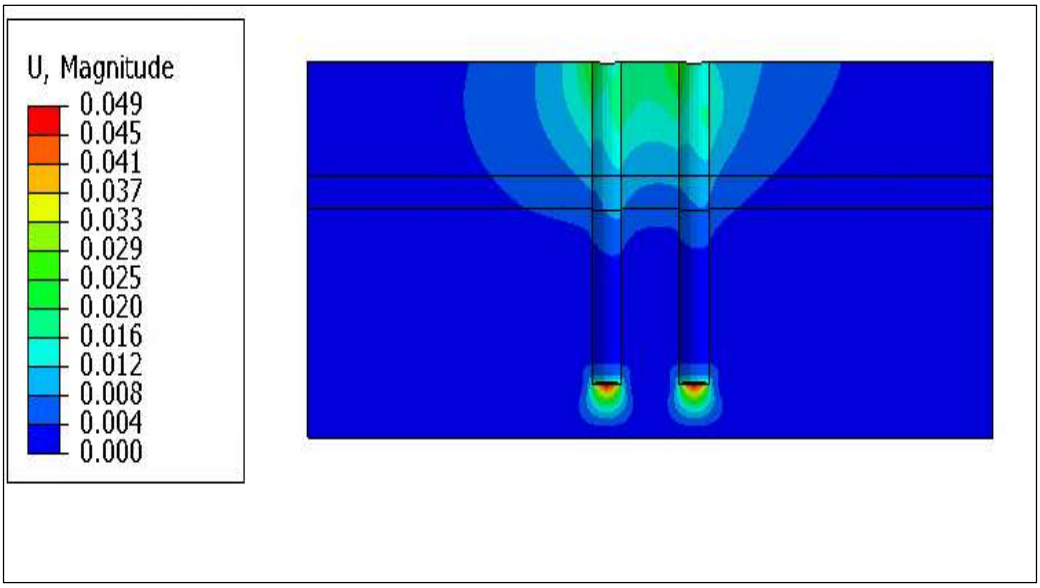

(a) Load Case 1

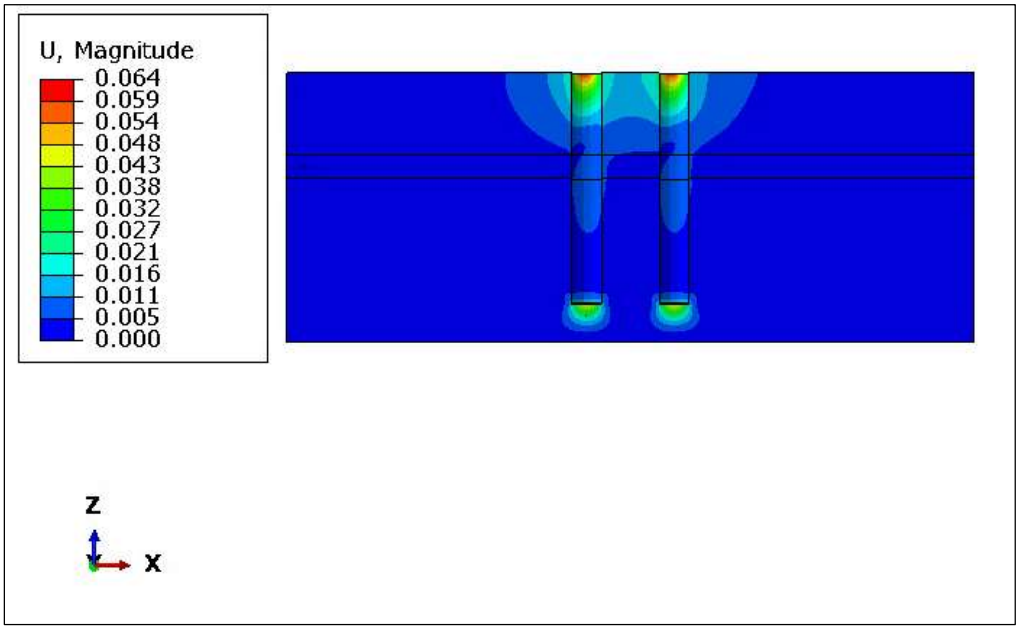

(b) Load Case 2

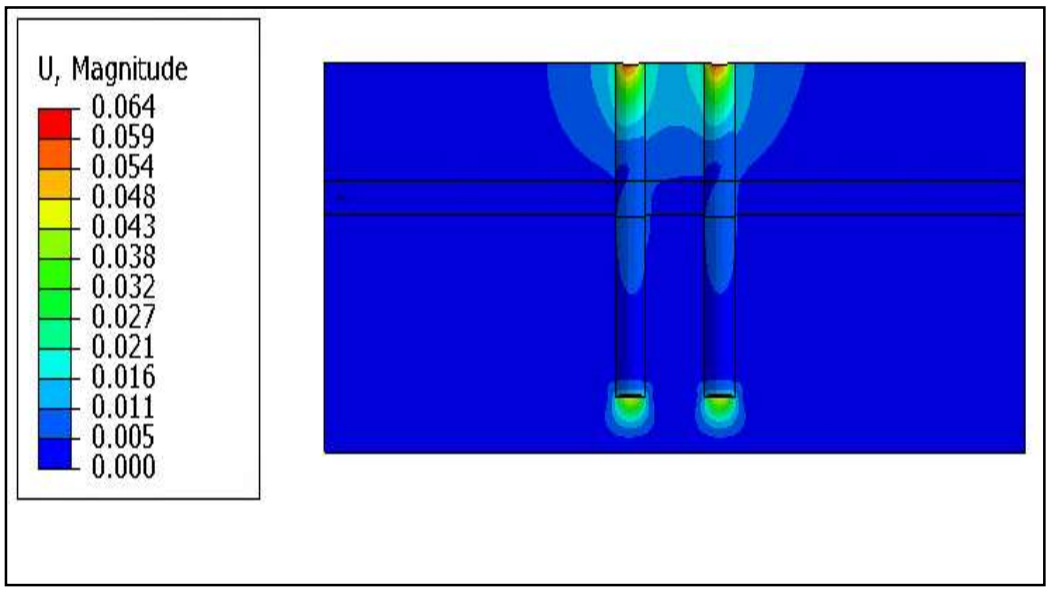

(c) Load Case 3

Figure 4-10.Soil displacement fields for (a) load case 1, (b) load case 2, and (c) load case 3

Pile displacement profiles

In all simulated cases, the pile displacements have increased due to scouring. In the case of load case 1, maximum pile head displacement for 1.5m scour depth due to local scour condition increases by around 55% when compared to no scour condition. There was no visible increase in the lateral displacement when comparing the local and combined scour conditions at the same depth. With an increase in scour depth from 1.5 m to 3m and 4.5m, pile displacement increased by 144% and 278%, respectively, when compared to the no scour condition. For load cases 2 and 3, a nearly similar increase in lateral displacement was observed as shown in Figure 4-11 and Figure 4-12, respectively.

Also shown in Table 4-4 are the percentage changes between different scour depths indicating potential projected effects due to unmanaged scouring.

Table 4-4. Summary of pile head deflection in mm

Scour Depth(m)	Scour Type	Load case 1	Load case 2	Load case 3	% Change[1] (LC1)	% Change[2] (LC2)	% Change[3] (LC3)
Sd = 0	-	0.67	0.58	0.31	-	-	-
Sd = 1.5	Local scour	1.03	0.80	0.41	55.0	37.5	24.9
	Combined scour	0.98	0.95	0.53	47.4	61.8	63.4
Sd = 3	Local scour	1.62	1.33	0.69	144.1	127.9	113.2
	Combined scour	1.59	1.52	0.86	139.6	159.6	165.8
Sd = 4.5	Local scour	2.51	2.14	1.13	278.1	265.6	246.5
	Combined scour	2.51	2.38	1.376	277.6	306.9	320.3
Validation							
The geotechnical design report for the Phillips Road bridge used L-Pile for a single pile analysis and the pile head displacement obtained for extreme loading is 2.57 mm, respectively. The maximum bending moment obtained at 6.1 m depth below pile head is 557.1 kN-m.							

[1,2,3] % changes with respect to no scour conditions of load case 1,2 and 3, respectively.

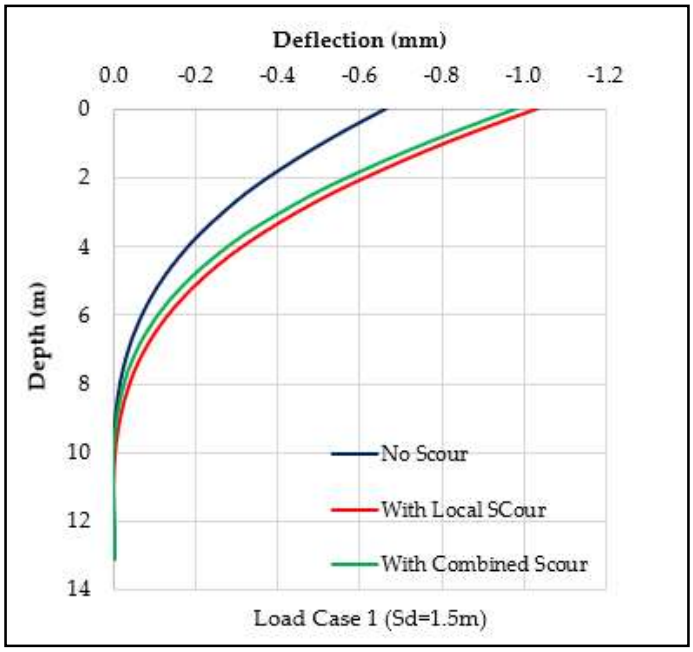
Deflection (mm)
0.0 -0.2 -0.4 -0.6 -0.8 -1.0 -1.2
Depth (m)
0 2 4 6 8 10 12 14
No Scour
With Local SCour
With Combined Scour
Load Case 1 (Sd=1.5m)

(a)

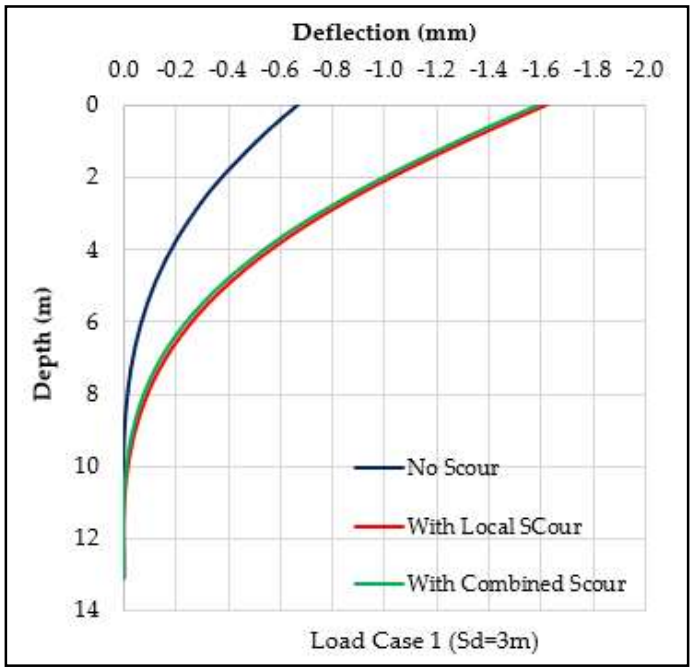
Deflection (mm)
0.0 -0.2 -0.4 -0.6 -0.8 -1.0 -1.2 -1.4 -1.6 -1.8 -2.0
Depth (m)
0 2 4 6 8 10 12 14
No Scour
With Local SCour
With Combined Scour
Load Case 1 (Sd=3m)

(b)

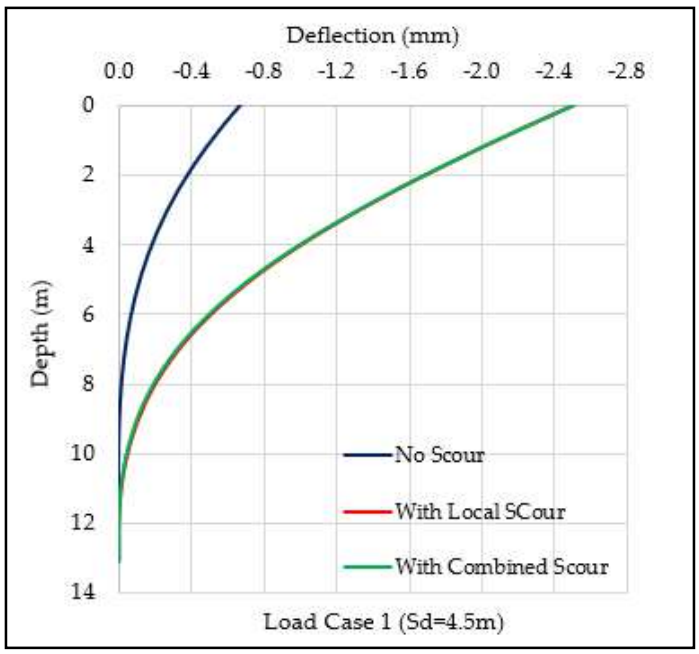

(c)

Figure 4-11.Pile head displacement Vs Depth profiles of load case 1 for (a)1.5 m scour, (b)3 m scour, and (c)4.5 m scour

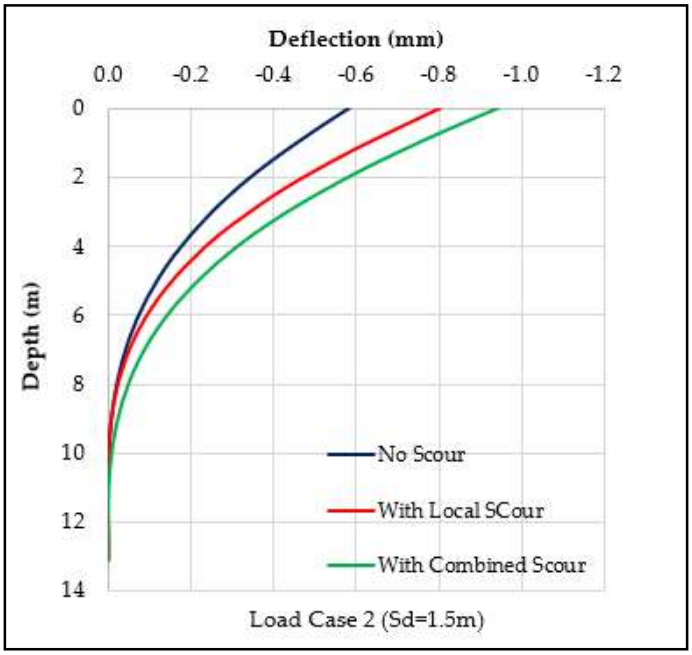
Deflection (mm)
0.0 -0.2 -0.4 -0.6 -0.8 -1.0 -1.2
0
2
4
6
8
10
12
14
Depth (m)
No Scour
With Local SCour
With Combined Scour
Load Case 2 (Sd=1.5m)

(a)

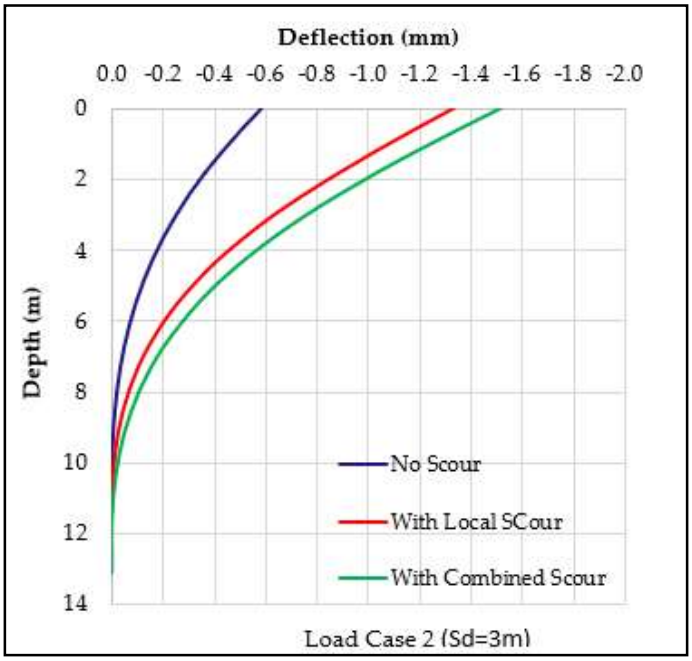
Deflection (mm)
0.0 -0.2 -0.4 -0.6 -0.8 -1.0 -1.2 -1.4 -1.6 -1.8 -2.0
0
2
4
6
8
10
12
14
Depth (m)
No Scour
With Local SCour
With Combined Scour
Load Case 2 (Sd=3m)

(b)

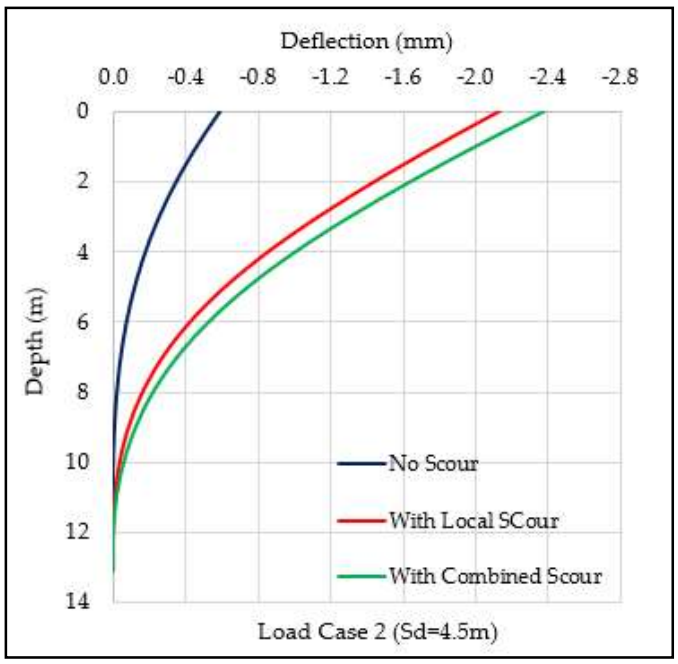

(c)

Figure 4-12. Pile head displacement Vs Depth profiles of load case 2 for (a)1.5 m scour, (b)3 m scour, and (c)4.5 m scour

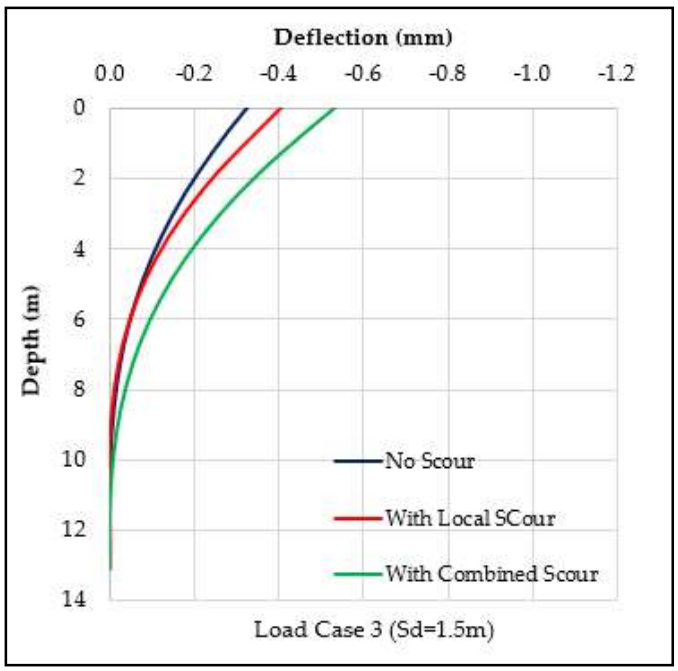
Deflection (mm)
0.0
-0.2
-0.4
-0.6
-0.8
-1.0
-1.2
0
2
4
6
8
10
12
14
Depth (m)
No Scour
With Local SCour
With Combined Scour
Load Case 3 (Sd=1.5m)

(a)

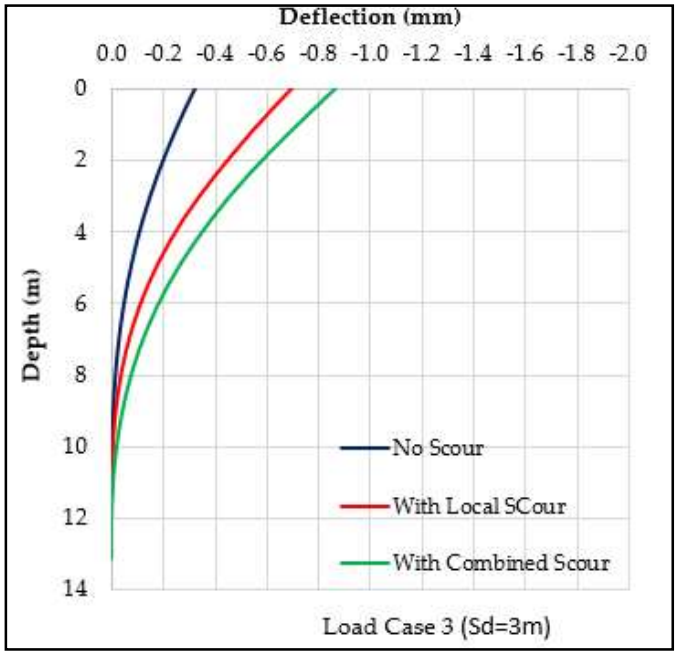
Deflection (mm)
0.0
-0.2
-0.4
-0.6
-0.8
-1.0
-1.2
-1.4
-1.6
-1.8
-2.0
0
2
4
6
8
10
12
14
Depth (m)
No Scour
With Local SCour
With Combined Scour
Load Case 3 (Sd=3m)

(b)

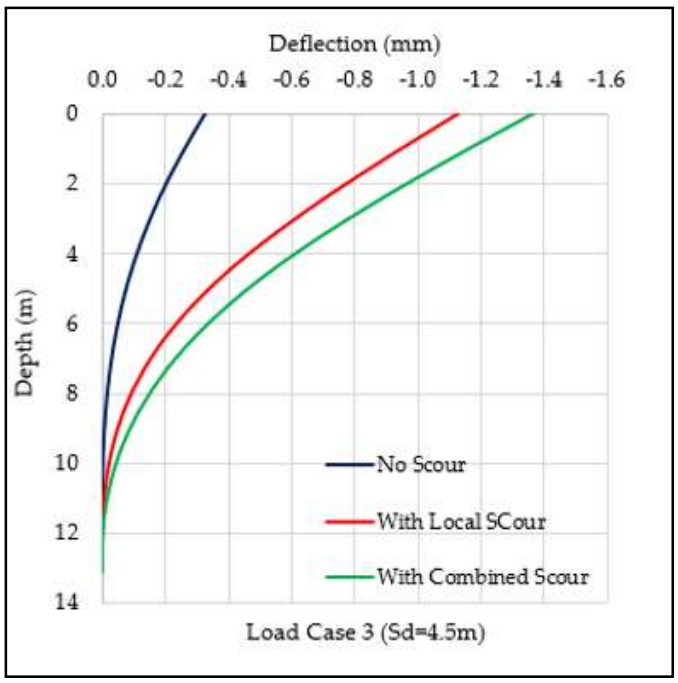

(c)

Figure 4-13. Pile head displacement Vs Depth profiles of load case 3 for (a)1.5 m scour, (b)3 m scour, and (c)4.5 m scour

Bending Moment Profiles

Figures 4-14 through 4-16 present bending moment profiles along the pile for load cases 1 to 3, respectively. The analysis results show no visible effect of scour on the structural responses of the drilled shafts in terms of bending moments for the top 0.6 m of pile length. However, the effect of scour on the bending moments are clearly noticeable on the pile sections below this level: for load case 1, the local scour holes of 1.5 m depth resulted in an average increase of about 23.9% in bending moments, whereas these values increased only by an additional 4.5% for the combined scour case. With an increase in the depth of the local scour hole to 3 and 4.5 m, the average bending moment along the pile length increased by 46 and 65%, respectively. Furthermore, the combined scour resulted in an additional increase of 6%. For load case 2, there is no significant increase in bending moments for the scour depths of 1.5 m and 3 m. However, the effect of scour was observed for a depth of 4.5 m below the ground level for load case 2 – especially after 4 m depth.

As expected, the results of load case 3 showed significant increase in the average bending moments for both the local and combined scour cases. A scour hole of 1.5 m depth resulted in 40% increase in the average bending moment up to 9.1 m length of pile. With further deepening of the scour hole, the average bending moment increases exponentially by 80-82%. There is little difference between the bending moments for local and combined scour cases, however, there is a clear deviation between the two curves at 6-8 m depth for load case 2 and 8-10 m depth for load case 3. Since there is no

clear explanation for this deviation, the results indicate that there was little difference between the local and combined scour cases for load case 3.

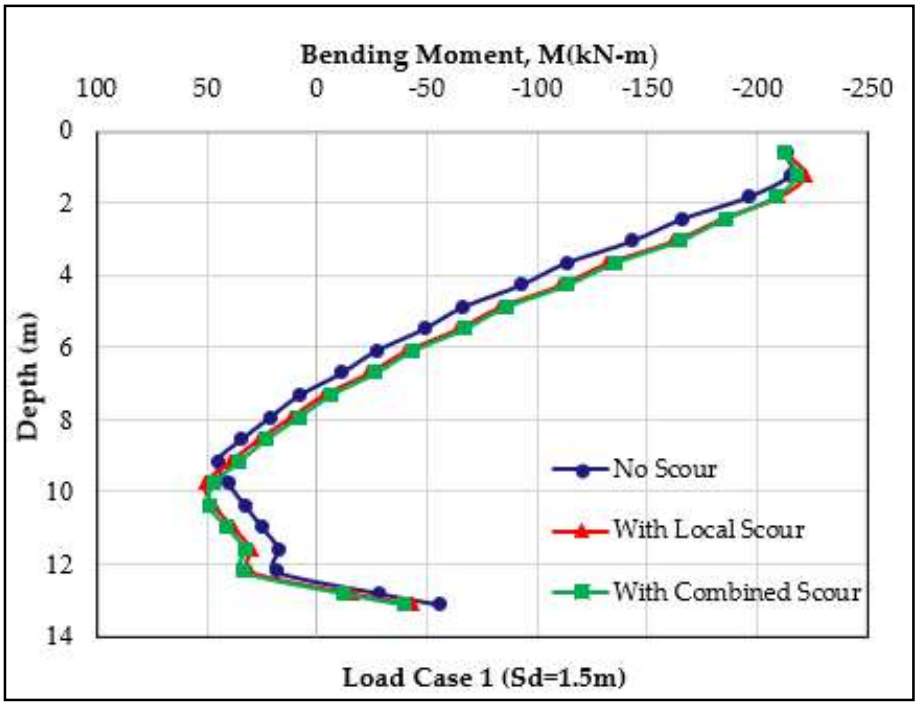
Bending Moment, M(kN-m)
100
50
0
-50
-100
-150
-200
-250
0
2
4
6
8
10
12
14
Depth (m)
No Scour
With Local Scour
With Combined Scour
Load Case 1 (Sd=1.5m)

(a)

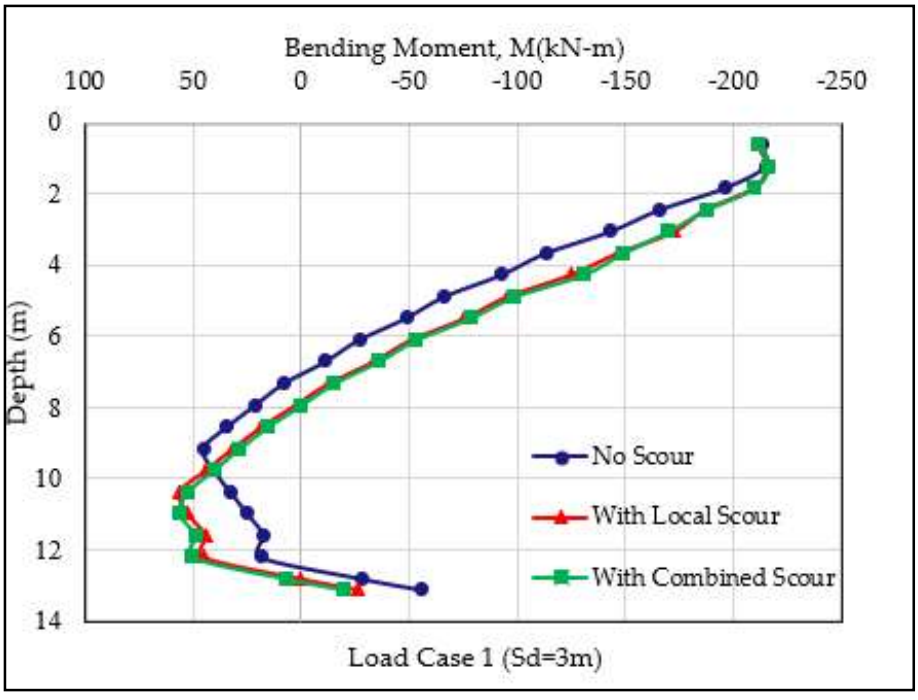
Bending Moment, M(kN-m)
100
50
0
-50
-100
-150
-200
-250
0
2
4
6
8
10
12
14
Depth (m)
No Scour
With Local Scour
With Combined Scour
Load Case 1 (Sd=3m)

(b)

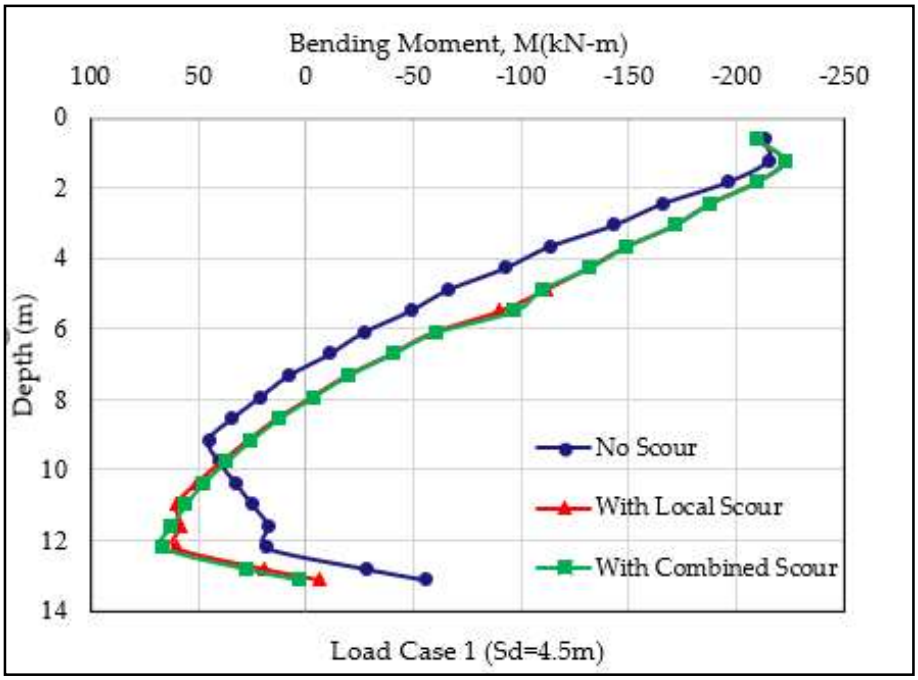

(c)

Figure 4-14.Bending Moment Vs Depth profiles of load case 1 for (a)1.5 m scour, (b)3 m scour, and (c)4.5 m scour


Bending Moment, M(kN-m)
50
-50
-150
-250
-350
-450
-550
-650
-750
0
2
4
6
8
10
12
14
Depth (m)
No Scour
With Local Scour
With Combined Scour
Load Case 2 (Sd=1.5m)

(a)

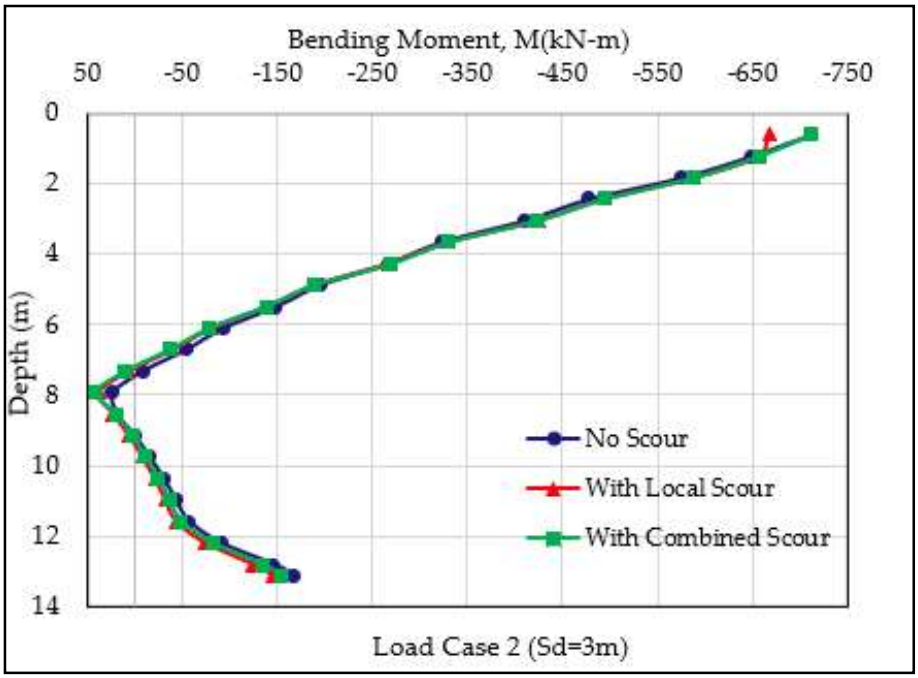
Bending Moment, M(kN-m)
50
-50
-150
-250
-350
-450
-550
-650
-750
0
2
4
6
8
10
12
14
Depth (m)
No Scour
With Local Scour
With Combined Scour
Load Case 2 (Sd=3m)

(b)

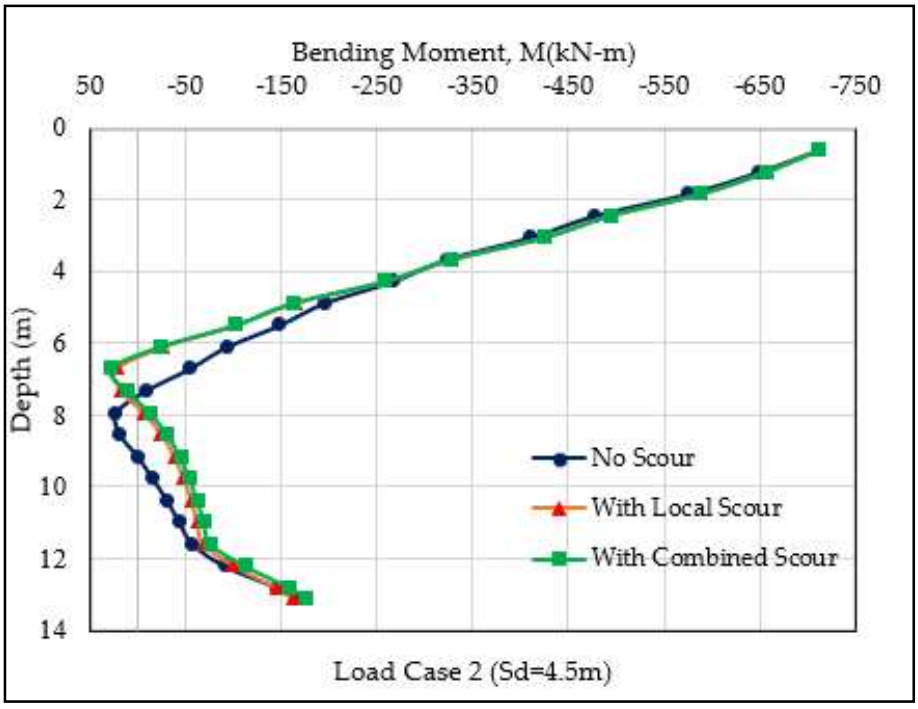

(c)

Figure 4-15. Bending Moment Vs Depth profiles of load case 2 for (a)1.5 m scour, (b)3 m scour, and (c) 4.5 m scour

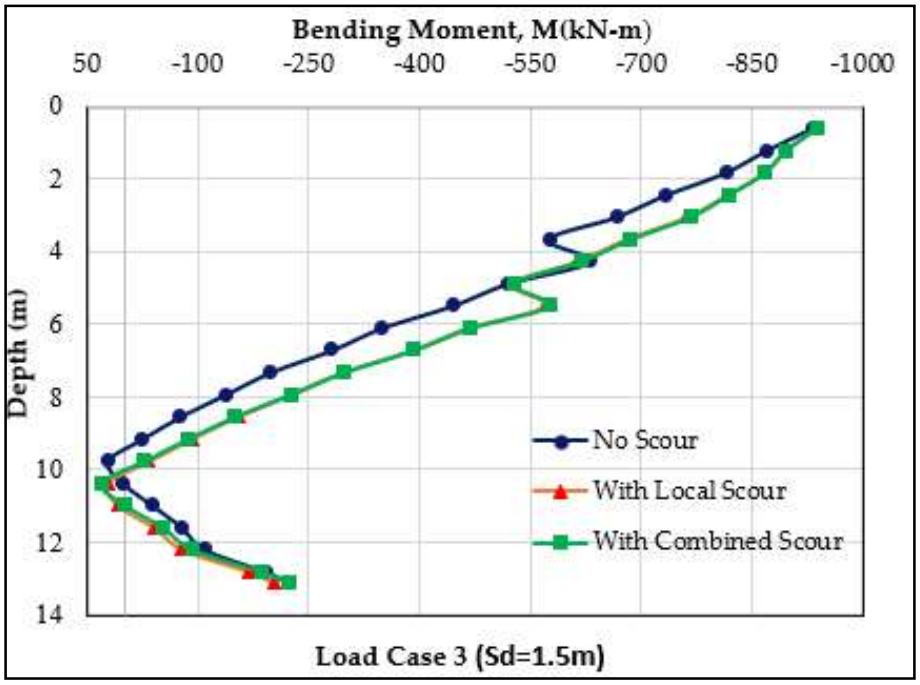
Bending Moment, M(kN-m)
50
-100
-250
-400
-550
-700
-850
-1000
0
2
4
6
8
10
12
14
Depth (m)
No Scour
With Local Scour
With Combined Scour
Load Case 3 (Sd=1.5m)

(a)

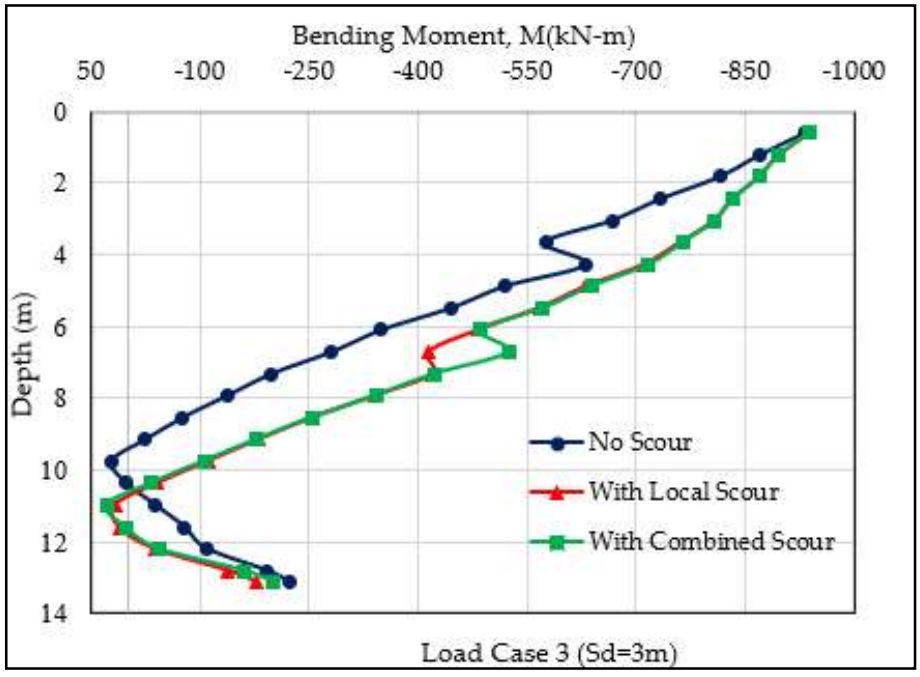
Bending Moment, M(kN-m)
50
-100
-250
-400
-550
-700
-850
-1000
0
2
4
6
8
10
12
14
Depth (m)
No Scour
With Local Scour
With Combined Scour
Load Case 3 (Sd=3m)

(b)

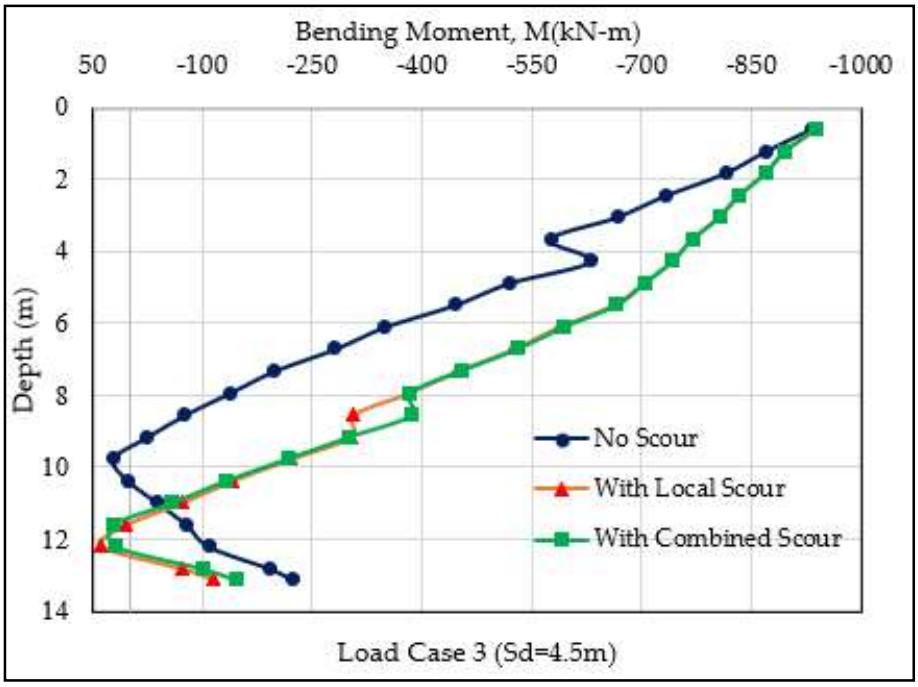

(c)

Figure 4-16.Bending Moment Vs Depth profiles of load case 3 for (a)1.5 m scour, (b)3 m scour, and (c)4.5 m scour

Conclusions

In this paper, three-dimensional nonlinear FE models with scours were used to analyze the effects of scouring on a pier-on-bank bridge with congested channel and frequent over bank flooding. Spanning Toby Creek, Phillips Road Bridge has experienced scouring problems despite its piers-on-bank design. Specifically, this paper investigated the impact of local and combined scours on two adjacent drilled piles under combined actions of axial load, lateral load, and bending moments. Scour was modeled using the element removal (ER) method in ABAQUS and nonlinear behaviors of the soil element was modeled as elastic-plastic. Both pile displacements and bending moments from the numerical modeling have been compared and the results showed clear impacts

of scour on the bridge piers. It is concluded that investigation of scour potentials for piers-on-bank should be considered in bridge design as it may result in early failure of similar bridges.

Based on the numerical simulation results discussed above, the following conclusions can be drawn:

1. Scours have been observed to result in an increase in the bending moments in the piles and can significantly impact the bending moment capacity of the bridge foundations. For example, with an increase in scour depth from 3 to 4.5m, an average bending moment increases along with the pile increases by about 45-60%. While this increase in bending moment does not exceed the maximum design capacity of the bridge pier, the long-term implication of early failures is of concern, should the problem not be rectified.
2. For the load case scenarios assessed in this study, pile head (ground level) deflection increases exponentially from 55% to 278% for local scour depths ranging from 1.5m to 5m depth. This again was deemed critical to the long-term performance of the bridge. When comparing local and combined scours, the combined scour only increased the average bending moments from the local scour cases by an additional 5-6% (worst case scenario), and hence, is deemed not significant for contributing to the increase in bending moments.

Conventional design of bridges with piers-on-bank foundations usually ignore the potential for significant scouring problems. Using the Phillips Road bridge as a case

study, we demonstrate that an unmanaged scour problem can result in significant increase in lateral displacement of the pier head and bending moments, even for piers-on-bank bridges. Hence, timely preventive measures are needed to rectify the scour problem at the initial stage of local scour development in order to avoid further widening of scour holes resulting in the weakening of the bridge support.

While the last observation showed limited effects from the combined scour case to the Phillips Road bridge foundation, this may be due to the close spacing between the bridge piers. Further studies should be conducted to determine if the effects of combined scour may be worsened with wider bridge pier spacings.

References

1. AASHTO, "AASHTO LRFD Bridge Design Specifications." American Association of State Highway and Transportation Officials, Washington, DC, 2012.
2. Cook, W. "Bridge Failure Rates, Consequences, and Predictive Trends." Utah State University, 2004.
3. Wardhana, K., and Hadipriono, F. C. "Analysis of Recent Bridge Failures in the United States." Journal of Performance of Constructed Facilities, 17(3), 144-150, 2003.
4. Flint, M. M., Fringer, O., Billington, S. L., Freyberg, D. and Diffenbaugh, N. S. "Historical Analysis of Hydraulic Bridge Collapses in the Continental United States." Journal of Infrastructure Systems, 23(3), 04017005, 2017.

5. FHWA (Federal Highway Administration). “National Bridge Inventory.” ⟨https://www.fhwa.dot.gov/bridge/nbi.cfm⟩ (Apr. 14, 2014).
6. Richardson, E. V. and Davis, S. R. “Evaluating Scour At Bridges.” No. FHWA-NHI-01-001 United States. Federal Highway Administration. Office of Bridge Technology, 2001.
7. Avent, R. R. and Alawady, M. “Bridge Scour and Substructure Deterioration: Case Study.” Journal of Bridge Engineering, 10(3), 247-254, 2005.
8. Lin, C., Bennett, C., Han, J. and Parsons, R. L. “Scour Effects on The Response of Laterally Loaded Piles Considering Stress History of Sand.” Computers and Geotechnics, 37(7-8), 1008-1014, 2010.
9. McConnell, J. R., and Cann, M. “Assessment of Bridge Strength and Stability under Scour Conditions.” Proceedings, Structures Congress, 121-132, 2010.
10. Klinga, J. V. and Alipour, A. “Assessment of Structural Integrity of Bridges Under Extreme Scour Conditions.” Engineering Structures, 82, 55-71, 2015.
11. Alipour, A., Shafei, B. and Shinozuka, M. “Reliability-Based Calibration of Load and Resistance Factors for Design of RC Bridges Under Multiple Extreme Events: Scour and Earthquake.” Journal of Bridge Engineering, 18(5), 362-371, 2013.
12. Liang, F., Zhang, H. and Huang, M. “Extreme Scour Effects on The Buckling of Bridge Piles Considering the Stress History of Soft Clay.” Natural Hazards, 77(2), 1143-1159, 2015.

13. Ben H., Lai, Y., Wang, L., Hong, Y. and Zhu, R. “Scour Effects on The Lateral Behavior of a Large-Diameter Monopile in Soft Clay: Role of Stress History.” Journal of Marine Science and Engineering, 7(6), 170, 2019.
14. Jain, N. K., Ranjan, G. and Ramasamy, G. “Effect of Vertical Load on Flexural Behavior of Piles.” Geotechnical Engineering, 18: 185-204, 1987.
15. Phillips, D. T. P., & Lehane, B. M. “The Response of Driven Single Piles Subjected to Combined Loads.” Proceedings, International Conference on Case Histories in Geotechnical Engineering, New York, NY, 2004.
16. Davisson MT, Robinson KE (1965) “Bending and Buckling of Partially Embedded Piles.” Proceedings, 6th International Conference on Soil Mechanics and Foundation Engineering, 2, 243–246, 1965.
17. Goryunov, B. F. “Discussion on Analysis of Piles Subjected to the Combined Action of Vertical and Horizontal Loads.” J. Soil Mech. Found. Eng., 10(1), 10, 1975.
18. Achmus, M. and Thieken, K. “Behavior of Piles under Combined Lateral and Axial Loading, 2nd International Symposium on Frontiers in Offshore Geotechnics (ISFOG) II, Perth, Western Australia, 2010. 465-470.
19. Huang, J., & Bin-Shafique, S. “Performance of Drilled Shaft under Combination of Complicated Loads under Hurricane Event.” Technical Report: 18GTTSA02, Transportation Consortium of South Central States, 2019.

20. Ismail, Z., Jumain, M., Sidek, F., Wahab, A. K., Ibrahim, Z., & Jamal, M. “Scour Investigation Around Single and Two Piers Side by Side Arrangement,” Int. J. of Research in Engineering and Technology, 2(10), 459-465, 2013.
21. Movahedi, N., Dehghani, A. A., Aarabi, M. J., & Zahiri, A. R. “Temporal Evolution Of Local Scour Depth Around Side-By-Side Piers.” Journal homepage: http://www. ojceu. ir/main, 82, 86, 2011.
22. Malik, R., & Setia, B. “Interference Between Pier Models and Its Effects On Scour Depth.” SN Applied Sciences, 2(1), 1-12, 2020.
23. Wang, H., Tang, H., Liu, Q., and Wang, Y. “Local Scouring Around Twin Bridge Piers in Open-Channel Flows.” Journal of Hydraulic Engineering, 142(9), 06016008, 2016.
24. EPA (2021), Toby Creek Watershed Report, US EPA Geoviewer. US EPA. Retrieved 7 July 2021, Watershed Report | Office of Water | US EPA.
25. Melville, B. W., & Sutherland, A. J. (1988). Design method for local scour at bridge piers. Journal of Hydraulic Engineering, 114(10), 1210-1226.
26. Heza, Y. B. M., Soliman, A. M., & Saleh, S. A. (2007). Prediction of the scour hole geometry around exposed bridge circular-pile foundation. JOURNAL OF ENGINEERING AND APPLIED SCIENCE-CAIRO-, 54(4), 375.
27. Arneson, L., Zevenbergen, L., Lagasse, P., and Clopper, P. (2012). “Evaluating scour at bridges. Fifth edition.” HEC-18: FHWA-HIF-12-003,FHWA, Washington, DC.

28. Khodair, Y. and Abdel-Mohti, A. (2014). “Numerical Analysis of Pile–Soil Interaction Under Axial and Lateral Loads.” International Journal of Concrete Structures and Materials, 8(3), 239-249.
29. Senturk, M., & Pul, S. (2017). Finite element analysis for obtaining structural performance of bridge pier interacting with soil. In Proceeding Conference SMAR 2017-Fourth Conference on Smart Monitoring, Assessment and Rehabilitation of Civil Structures, Zürich, Switzerland.
30. Lin, C., Han, J., Bennett, C. and Parsons, R. L. (2014). “Case History Analysis of Bridge Failures Due To Scour.” In Climatic Effects on Pavement and Geotechnical Infrastructure (pp. 204-216).
31. Mardfekri, M., Gardoni, P. and Roesset J. M. (2013). “Modeling Laterally Loaded Single Piles Accounting For Nonlinear Soil-Pile Interactions.” Journal of Engineering, 2013.
32. Strömblad, N. (2014). Modeling of soil and structure interaction subsea (Master's thesis).
33. Salim, R. R., & Abdulrazzaq, O. A. (2017). Analysis of Cast in Place Piles Using Finite Elements Method. International Journal of Applied Engineering Research, 12(16), 6029-6036.
34. Youssouf, T., Yu, T., Abdramane, D., Cyriaque, A. O., & Youssouf, D. (2019). Force Performance Analysis of Pile Behavior of the Lateral Load. Infrastructures, 4(2), 13.
35. Abaqus. (2013). Abaqus version 6.13 documentation.

36. Chen, L., and Poulos, H. G. (1993). “Analysis of Pile-Soil Interaction under Lateral Loading Using Infinite and Finite Elements.” Computers and Geotechnics, 15(4), 189-220.

5 CONCLUSION

This dissertation addressed the investigation of the scour problem of bridges with piers-on-bank. The investigative approach used terrestrial LiDAR scanning to quantify local scour area around bridge piers and nonlinear Finite element (FE) modeling technique to simulate the scouring effect on the bridge pier. The Phillips Road bridge at the University of North Carolina at Charlotte campus spans the Toby Creek and is used as a case study bridge. The bridge has multiple piers on either banks of the creek and the piers have experienced scour. To study the performance of bridge pile under critical scour conditions, different scour depths were analyzed.

To evaluate pier performance, original bridge design loading has been applied to the models. Loadings on bridge pier are functions of the bridge superstructure weight, external environmental loading such as earthquake and wind and, design traffic loads. It should be noted that hydraulic loading due to river flow was not considered in current study for piers-on-bank. The general idea is that when inspection of scour is conducted, there is no flooding. Hence, scour formation is ignored in the analytical process.

Based on the numerical investigation of the case study bridge pier/piers subjected to various scour levels, the following conclusions can be drawn:

1. Scour around the piers-on-bank is as important as piers located in the riverbed and the terrestrial LiDAR is an effective monitoring technique for frequent and periodic investigations of scour extent, before, during and after a scour event. Moreover, the collected site-specific data can be used to establish the bridge damage/bridge failure scenario.

2. Local scour has significant impacts on the pile head deflection when compared to the no scour condition. Pile head deflection increased exponentially with an increase in scour depth. Specifically, for the simulated scour depths of 1.5 m to 3 m, the pile head deflection increased by about 76%. This significant increase in pile head deflection would be detrimental to the bridge superstructure performance resulting in early damage or failure of bridges.
3. Scour noticeably alters the structural load carrying capacity of bridge pier foundations. For the current study, scour resulted in a significant increase in bending moments in the pile. For 1.5 m scour depth, the bending moment values increased by about 212% when compared to the no scour condition. With a further increase in scour depth, there is a steep increase in bending moments under the same loading conditions.
4. Unmanaged local scour problems could potentially result in widened scour holes – combined scour, between the adjacent piers. Further investigation of the effect of combined scour on the lateral performance of bridge piles is crucial, especially when the bridge piers are closely spaced.
5. For the Phillips Road bridge, analysis of bridge piles subjected to combined loading actions, it was observed that the piles behaved significantly differently under different loading scenarios. This is of particular importance in the case of combined scour with overlapping stress fields between the piles.

6. Combined scour considerably increases the pile head deflection as compared to the local scour case. For example, in the case of maximum moment load case, for the top 1.5m of scour depth, pile deflection increased by 154.6%. However, with further increase in scour depth to 3m and 4.5m, combined scour resulted in 46.5% and 29.9% increase in deflection. Thus, the rate of increase in deflection is comparatively slow below 1.5m scour depth.
7. Combined scour has a limited effect on bending moment capacity as compared to local scour cases. However, this effect would become significant under the increased loads resulting from debris accumulation in and around the scoured region.

This study suggested the use of LiDAR scan for bridge scour monitoring. However, we are also mindful that, LiDAR scan does not penetrate water, hence, is limited to dry scour hole monitoring. Other techniques such as ultrasonic sounding techniques are better suited for piers located in the river. If the scour is deeper than the riverbed and can potentially be flooded due to ground water seepage, then the use of LiDAR scanning can be problematic. These are obvious limitations of the terrestrial LiDAR scanning technique.

The contribution of current study is the introduction of modern investigative tools (LiDAR scan and non-linear FE analysis with ER for scour hole simulation) for scour analysis of piers-on-bank. While both techniques have been applied to piers-in-river bridges, they have not been applied to piers-

on-banks which represents a unique scenario for scour problems. Our preliminary assessment indicated that bridges with piers-on-bank are more common than one would expect. Introduction of these two techniques is particularly suited for piers-on-bank scour problems.

Our contributions to the domain knowledge are the confirmation of scour problem for piers-on-bank bridges and the application of modern investigative tool to address such problems. Evidences of potential scour induced increases in pier displacement and bending moment on the Philipps Road bridge have been demonstrated. Researchers can further our study by applying both techniques for periodic monitoring of scour problem for the specific bridge type. The data collected can be used to quantify the long-term effects of uncorrected scour problem which can shorten the life cycle of the bridge.

6 RECOMMENDED FUTURE RESEARCH

This study introduced the scour problem of pier-on-bank bridges and demonstrated the use of non-linear finite element method to analyze the specific scour problem. However, there are several issues that have not been addressed - One issue being the effect of soil types to the scour problem due to high flood. For the Phillips Road bridge, both residual and alluvial soil were involved, and the scour analysis should include an investigation of the unique behaviors of soil type to flood water scour. A detailed hydro-geologic investigation of the Toby creek would be helpful in expanding the scour potential of the Phillips Road bridge.

Furthermore, the shape of scour modelling can be detrimental to the evaluation of load effects on the modelled piers. Additional study should be performed. This is especially critical considering the stress concentration due to assumption of square shape scour vs circular shape scour which may result in different interpretation of stress in soil. Additional studies should be performed in different geometric modelling of scour. The following are the recommendations for future study.

1. For the accurate/exact simulation of scour hole dimensions in the FE model, an integrated LiDAR-based FE model needs to be developed. The possibility of importing the point clouds into the ABAQUS model needs to be investigated further.
2. This study was primarily focused on the effect of local and combined scour on a bridge pier foundation. Further investigation of the scour effects on an integrated model - including bridge substructure and superstructure, would help document the effect of increased pile-head displacements on bridge superstructure performance.

3. The results of this study can be further compared with other numerical investigation methods such as finite difference methods or conventional p-y methods. For the more accurate comparison of ER based finite element method and p-y method, the vertical (t-z curves) and torsional (t-θ curves) soil springs can be included.
4. A comprehensive review of all pier-on-bank bridges should be conducted to help assess the extent of such problems, which when investigated over a multiple year period can help establish a correlation to climate change induced damage effects to bridge infrastructures.

REFERENCES

AASHTO, L. (2012). AASHTO LRFD Bridge Design Specifications. American Association of State Highway and Transportation Officials, Washington, DC.

Abaqus. (2013). Abaqus version 6.13 documentation.

Achmus, M. and Thieken, K. "Behavior of Piles under Combined Lateral and Axial Loading, 2nd International Symposium on Frontiers in Offshore Geotechnics (ISFOG) II, Perth, Western Australia, 2010. 465-470.

Alipour, A., Shafei, B. and Shinozuka, M. (2013). "Reliability-Based Calibration of Load and Resistance Factors for Design of RC Bridges Under Multiple Extreme Events: Scour and Earthquake." Journal of Bridge Engineering, 18(5), 362-371.

Apsilidis, N., Diplas, P., Dancey, C. L., Vlachos, P. P. and Raben, S. G. (2010). "Local Scour at Bridge Piers: The Role of Reynolds Number on Horseshoe Vortex Dynamics." In Scour and Erosion (pp. 86-94).

Arneson, L., Zevenbergen, L., Lagasse, P., and Clopper, P. (2012). "Evaluating scour at bridges. Fifth edition." HEC-18: FHWA-HIF-12-003,FHWA, Washington, DC.

Avent, R. R. and Alawady, M. (2005). "Bridge Scour and Substructure Deterioration: Case Study." Journal of Bridge Engineering, 10(3), 247-254.

Beg, M. (2010). "Characteristics of Developing Scour Holes Around Two Piers Placed in Transverse Arrangement." In Scour and Erosion (pp. 76-85).

Ben H., Lai, Y., Wang, L., Hong, Y. and Zhu, R. (2019). "Scour Effects on The Lateral Behavior of A Large-Diameter Monopile in Soft Clay: Role of Stress History." Journal of Marine Science and Engineering, 7(6), 170.

Breusers, H.N.C., Nicollet, G. and Shen, H.W. (1977) “Local Scour around Cylindrical Piers,” Journal of Hydraulic Research, 15(3), 211-252.

Chen, L., and Poulos, H. G. (1993). “Analysis of Pile-Soil Interaction under Lateral Loading Using Infinite and Finite Elements.” Computers and Geotechnics, 15(4), 189-220.

Cook, W. “Bridge Failure Rates, Consequences, and Predictive Trends.” Utah State University, 2004.

Davisson MT, Robinson KE (1965) “Bending and Buckling of Partially Embedded Piles.” Proceedings, 6th International Conference on Soil Mechanics and Foundation Engineering, 2, 243–246, 1965.

EPA (2021), Toby Creek Watershed Report, US EPA Geoviewer. US EPA. Retrieved 7 July 2021, Watershed Report | Office of Water | US EPA.

FHWA (1995), Recording and Coding Guide for the Structure Inventory and Appraisal of the Nation’s Bridges, Report No. FHWA-PD-96-001, Federal Highway Administration, US Department of Transportation, Washington, DC.

Flint, M. M., Fringer, O., Billington, S. L., Freyberg, D. and Diffenbaugh, N. S. "Historical Analysis of Hydraulic Bridge Collapses in the Continental United States.” Journal of Infrastructure Systems, 23(3), 04017005, 2017.

Ghasemi, S.H. and Nowak, A.S. (2016) “Reliability Analysis for Serviceability Limit State of Bridges Concerning Deflection Criteria,” Structural Engineering International, 26(2), 168-175.

Goryunov, B. F. “Discussion on Analysis of Piles Subjected to the Combined Action of Vertical and Horizontal Loads.” J. Soil Mech. Found. Eng., 10(1), 10, 1975.

Govindasamy, A. V., Briaud, J. L., Kim, D., Olivera, F., Gardoni, P. and Delphia, J. (2010). “Observational Method for Estimating Future Scour Depth at Existing Bridges.” In Scour and Erosion (pp. 41-65).

Heza, Y. B. M., Soliman, A. M., & Saleh, S. A. (2007). Prediction of the scour hole geometry around exposed bridge circular-pile foundation. JOURNAL OF ENGINEERING AND APPLIED SCIENCE-CAIRO-, 54(4), 375.

https://www.ayresassociates.com/

Huang, J., & Bin-Shafique, S. “Performance of Drilled Shaft under Combination of Complicated Loads under Hurricane Event.” Technical Report: 18GTTSA02, Transportation Consortium of South Central States, 2019.

Ismail, Z., Jumain, M., Sidek, F., Wahab, A. K., Ibrahim, Z., & Jamal, M. “Scour Investigation Around Single and Two Piers Side by Side Arrangement,” Int. J. of Research in Engineering and Technology, 2(10), 459-465, 2013.

Jain, N. K., Ranjan, G. and Ramasamy, G. “Effect of Vertical Load on Flexural Behavior of Piles.” Geotechnical Engineering, 18: 185-204, 1987.

Karthigeyan, S., Ramakrishna, V. V. G. S. T., & Rajagopal, K. (2007). Numerical investigation of the effect of vertical load on the lateral response of piles. Journal of Geotechnical and Geoenvironmental Engineering, 133(5), 512-521.

Khandel, O., & Soliman, M. (2021). Integrated framework for assessment of time-variant flood fragility of bridges using deep learning neural networks. Journal of Infrastructure Systems, 27(1), 04020045.

Khodair, Y. and Abdel-Mohti, A. (2014). “Numerical Analysis of Pile–Soil Interaction Under Axial and Lateral Loads.” International Journal of Concrete Structures and Materials, 8(3), 239-249.

Kim, Y., & Jeong, S. (2011). Analysis of soil resistance on laterally loaded piles based on 3D soil–pile interaction. *Computers and Geotechnics*, *38*(2), 248-257.

Kishore, Y. N., Rao, S. N. and Mani, J. S. (2009). “The Behavior of Laterally Loaded Piles Subjected to Scour in Marine Environment.” KSCE Journal of Civil Engineering, 13(6), 403-408.

Klinga, J. V. and Alipour, A. (2015). “Assessment of Structural Integrity of Bridges Under Extreme Scour Conditions.” Engineering Structures, 82, 55-71.

Lagasse, P. F., Clopper, P. E., Zevenbergen, L. W. and Girard, L. G. (2007). Countermeasures to Protect Bridge Piers from Scour (No. Project 24-07 (2)).

Li, F., Han, J., and Lin, C. (2013). “Effect of Scour on The Behavior of Laterally Loaded Single Piles in Marine Clay.” Marine Georesources and Geotechnology, 31(3), 271-289.

Li, H., Ong, M. C., Leira, B. J. and Myrhaug, D. (2018). “Effects of Soil Profile Variation and Scour on Structural Response of An Offshore Monopile Wind Turbine.” Journal of Offshore Mechanics and Arctic Engineering, 140(4), 10pages.

Liang, F., Zhang, H. and Huang, M. (2015). “Extreme Scour Effects on The Buckling of Bridge Piles Considering the Stress History of Soft Clay.” Natural Hazards, 77(2), 1143-1159.

Lin, C. and Wu, R. (2019). “Evaluation of Vertical Effective Stress and Pile Lateral Capacities Considering Scour-Hole Dimensions.” Canadian Geotechnical Journal, 56(1), 135-143.

Lin, C., Bennett, C., Han, J. and Parsons, R. L. (2012). “Integrated Analysis of The Performance Of Pile-Supported Bridges Under Scoured Conditions.” Engineering Structures, 36, 27-38.

Lin, C., Bennett, C., Han, J. and Parsons, R. L. “Scour Effects on The Response of Laterally Loaded Piles Considering Stress History of Sand.” Computers and Geotechnics, 37(7-8), 1008-1014, 2010.

Lin, C., Han, J., Bennett, C. and Parsons, R. L. (2014). “Case History Analysis of Bridge Failures Due To Scour.” In Climatic Effects on Pavement and Geotechnical Infrastructure (pp. 204-216).

Lin, C., Han, J., Bennett, C. and Parsons, R. L. (2014). “Case History Analysis of Bridge Failures Due To Scour.” In Climatic Effects on Pavement and Geotechnical Infrastructure (pp. 204-216).

Liu, W., Chen, S. and Hauser, E. (2011). “LiDAR-Based Bridge Structure Defect Detection.” Experimental Techniques, 35(6), 27-34.

Liu, W., Chen, S. E. and Hasuer, E. (2012). “Bridge Clearance Evaluation Based on Terrestrial LIDAR Scan.” Journal of Performance of Constructed Facilities, 26(4), 469-477.

Liu, W., Chen, S. E., Boyajian, D. and Hauser, E. (2010). “Application of 3D LiDAR Scan of A Bridge Under Static Load Testing.” Materials Evaluation, 68(12), 1359-1367.

Majumder, M., & Chakraborty, D. (2021). Effects of scour-hole depth on the bearing and uplift capacities of under-reamed pile in clay. Ocean Engineering, 240, 109927.

Malik, R., & Setia, B. "Interference Between Pier Models and Its Effects On Scour Depth." SN Applied Sciences, 2(1), 1-12, 2020.

Mardfekri, M., Gardoni, P. and Roesset, J. M. (2013). "Modeling Laterally Loaded Single Piles Accounting for Nonlinear Soil-Pile Interactions." Journal of Engineering, 2013.

McConnell, J. R. and Cann, M. (2010). "Assessment of Bridge Strength and Stability Under Scour Conditions." In Structures Congress 2010 (pp. 121-132).

Melville, B. W., & Sutherland, A. J. (1988). Design method for local scour at bridge piers. Journal of Hydraulic Engineering, 114(10), 1210-1226.

Melville, B. W., and Coleman, S. E. (2000). Bridge Scour. Water Resources Publication.

Movahedi, N., Dehghani, A. A., Aarabi, M. J., & Zahiri, A. R. "Temporal Evolution Of Local Scour Depth Around Side-By-Side Piers." Journal homepage: http://www. ojceu. ir/main, 82, 86, 2011.

Phillips, D. T. P., & Lehane, B. M. "The Response of Driven Single Piles Subjected to Combined Loads." Proceedings, International Conference on Case Histories in Geotechnical Engineering, New York, NY, 2004.

Poulos, H. G. (1971). "Behavior of Laterally Loaded Piles: I-Single Piles." Journal of the Soil Mechanics and Foundations Division, 97(5), 711-731.

Prendergast, L. J., Hester, D., Gavin, K. and O'Sullivan, J. J. (2013). "An Investigation of The Changes In The Natural Frequency Of A Pile Affected By Scour." Journal of Sound and Vibration, 332(25), 6685-6702.

Richardson, E. V. and Davis, S. R. (2001). Evaluating Scour at Bridges (No. FHWA-NHI-01-001). United States. Federal Highway Administration. Office of Bridge Technology.

Salim, R. R., & Abdulrazzaq, O. A. (2017). Analysis of Cast in Place Piles Using Finite Elements Method. International Journal of Applied Engineering Research, 12(16), 6029-6036.

Senturk, M., & Pul, S. (2017). Finite element analysis for obtaining structural performance of bridge pier interacting with soil. In Proceeding Conference SMAR 2017-Fourth Conference on Smart Monitoring, Assessment and Rehabilitation of Civil Structures, Zürich, Switzerland.

Strömblad, N. (2014). Modeling of Soil and Structure Interaction Subsea, Master's Thesis, Department of Applied Mechanics, Chalmers University of Technology, Göteborg, Sweden.

Suro, T.P., Huizinga, R.J., Fosness, R.L. and Dudunake, T.J., (2019) Assessment of Bridge Scour Countermeasures at Selected Bridges in the United States, 2014-18, Scientific Report 2019-5080, US Geological Survey.

Wang, H., Tang, H., Liu, Q., and Wang, Y. "Local Scouring Around Twin Bridge Piers in Open-Channel Flows." Journal of Hydraulic Engineering, 142(9), 06016008, 2016.

Wardhana, K., and Hadipriono, F. C. “Analysis of Recent Bridge Failures in the United States.” Journal of Performance of Constructed Facilities, 17(3), 144-150, 2003.

Warren, L. P. (2011). Scour at Bridges: Stream Stability and Scour Assessment at Bridges In Massachusetts. Open-File Report, US Geological Survey.

Xing, W.W., Song, C. and Tin-Loi, F. (2018) “A Scaled Boundary Finite Element Based Node-to-Node Scheme for 2D Frictional Contact Problems,” Computer Methods in Applied Mechanics and Engineering, 333, 114-146.

Yang, T. H., Chen, P. W., Lin, T. K., & Chang, K. C. (2021). Scour stability evaluation of bridge pier considering fluid-solid interaction. In Bridge Maintenance, Safety, Management, Life-Cycle Sustainability and Innovations (pp. 1386-1392).

Youssouf, T., Yu, T., Abdramane, D., Cyriaque, A. O., & Youssouf, D. (2019). Force Performance Analysis of Pile Behavior of the Lateral Load. Infrastructures, 4(2), 13.

APPENDIX A: PHILLIPS ROAD BRIDGE IMAGES

Figure A-1 Road bridge (End Bent 2- 5 piers)

Figure A-2 Phillips road bridge (End Bent 1- 6 piers)

(a)

(b)

Figure A-3 Sample images showing local scour around Phillips Road bridge piers

Figure A-4 LiDAR scan image of Phillips Road bridge

Figure A-5 LiDAR scan image of riverbank deep cut(embankment scour) of Phillips Road bridge

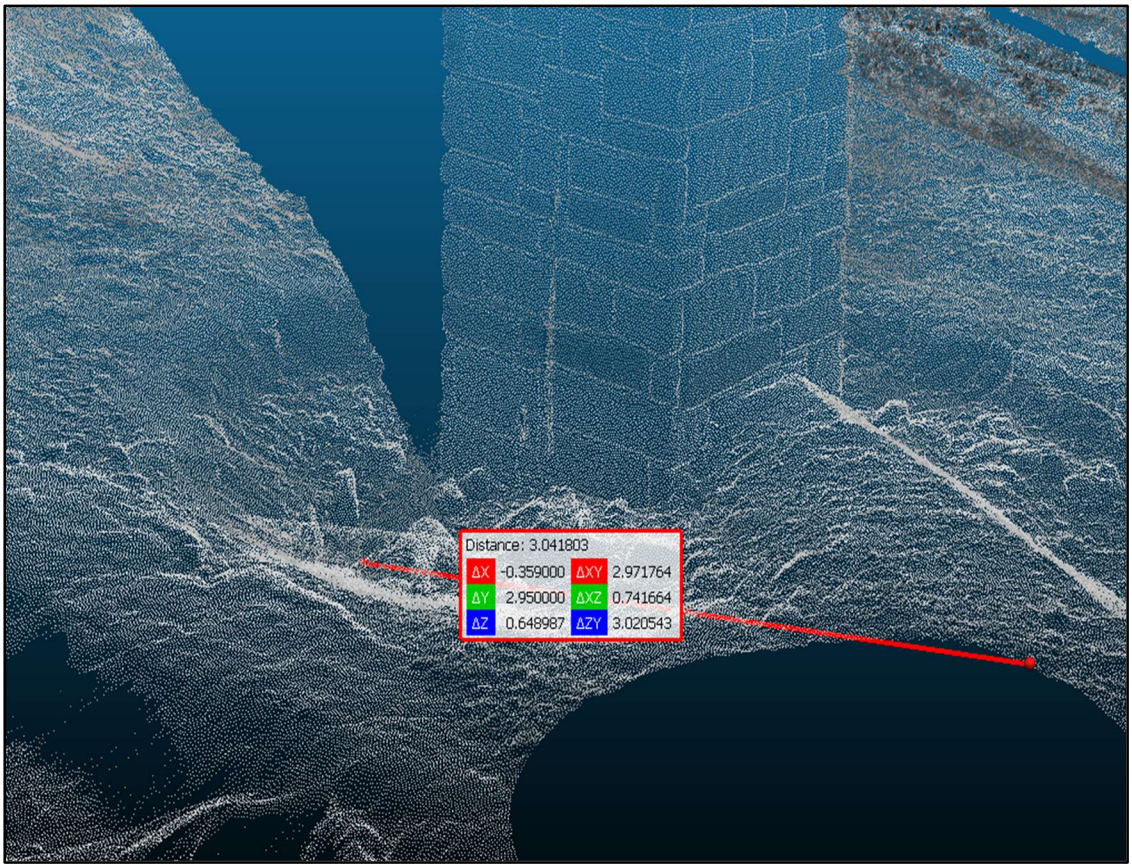

Figure A-6 Local scour hole image using Cloudcompare (August-2019)

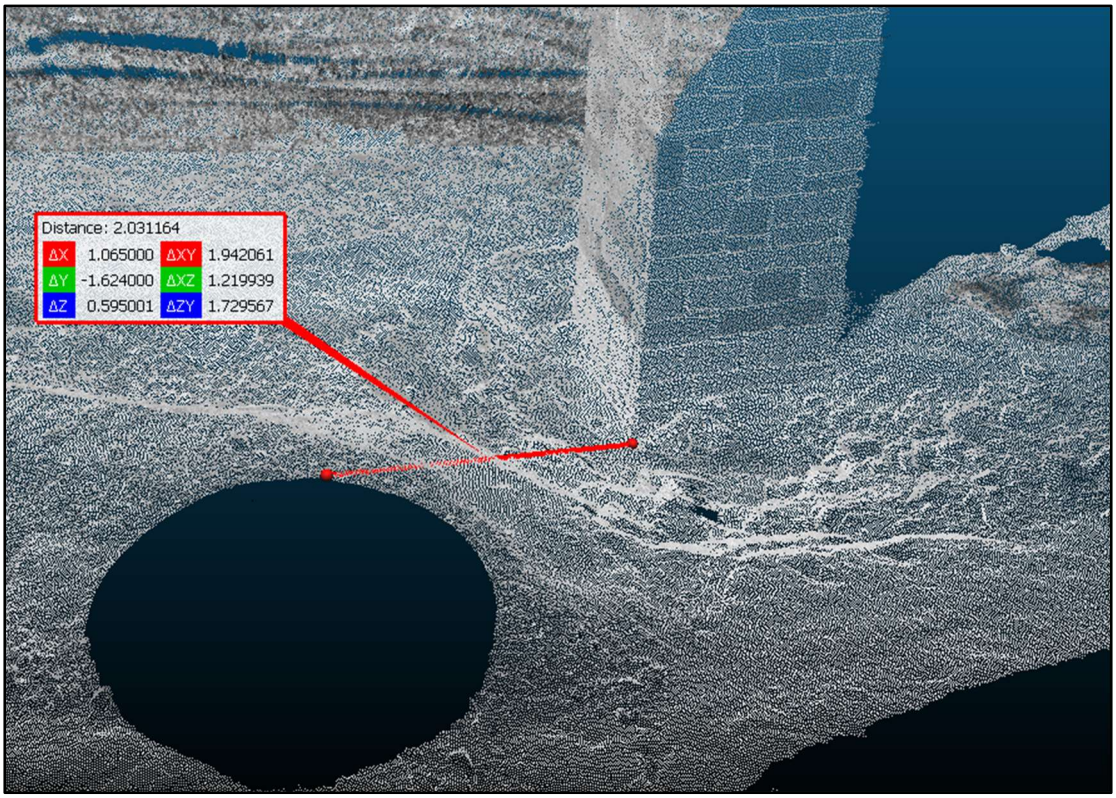

Figure A-7 Local scour hole image using Cloudcompare (November-2019)

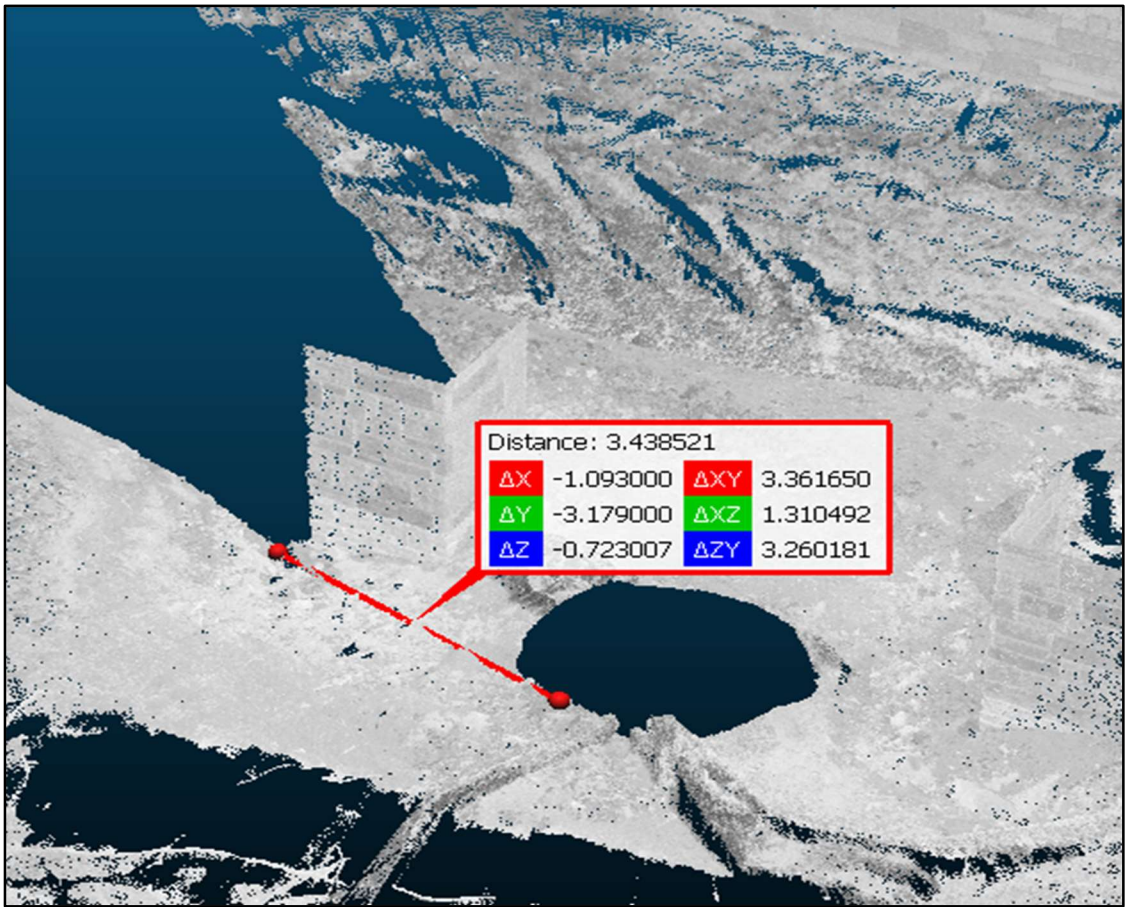

Figure A-8 Local scour hole image using Cloudcompare (June-2020)

APPENDIX B: MODEL III (ADDITIONAL RESULTS AND GRAPHS)

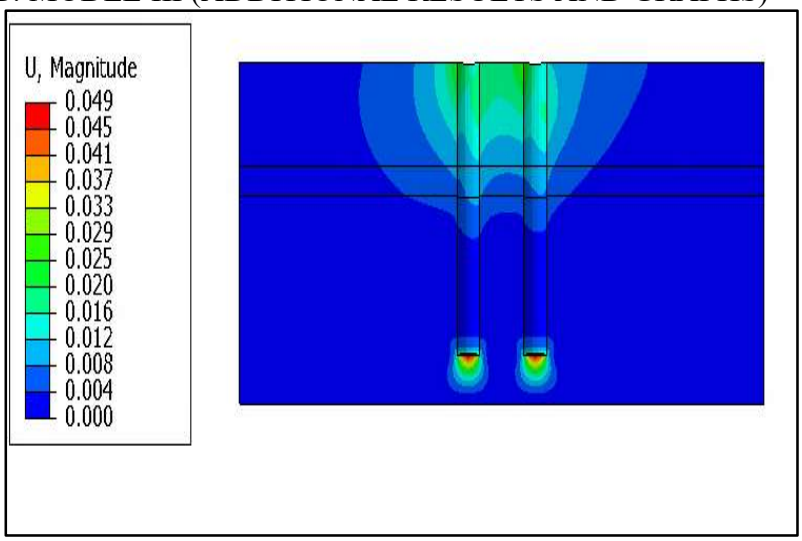

(a)

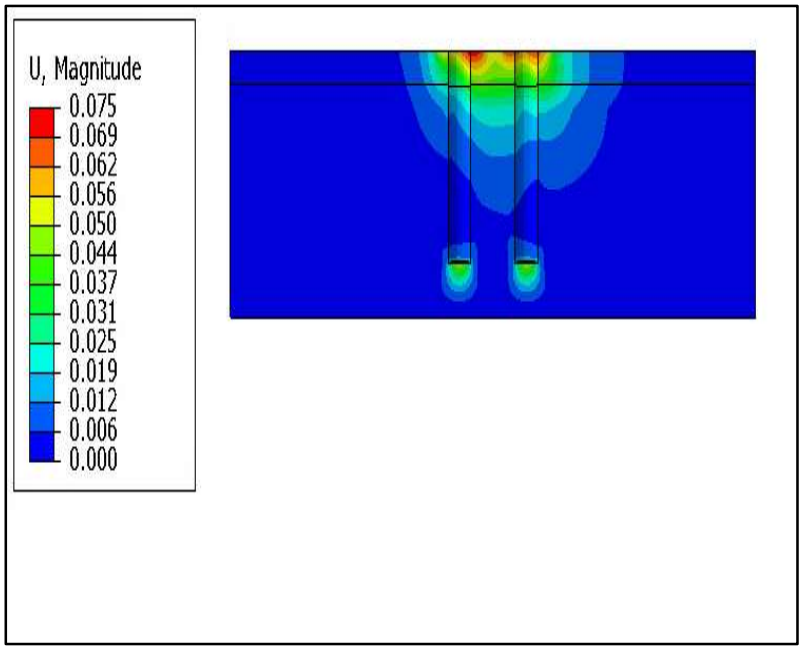

(b)

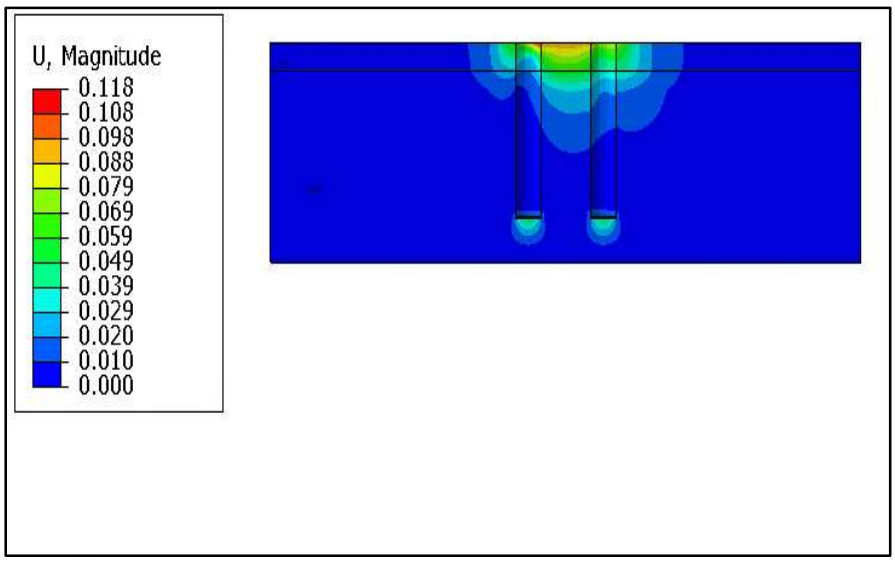

(c)

Figure B- 1 Soil displacement fields for load case 1 (a) no scour, (b) local scour, and (c) combined scour

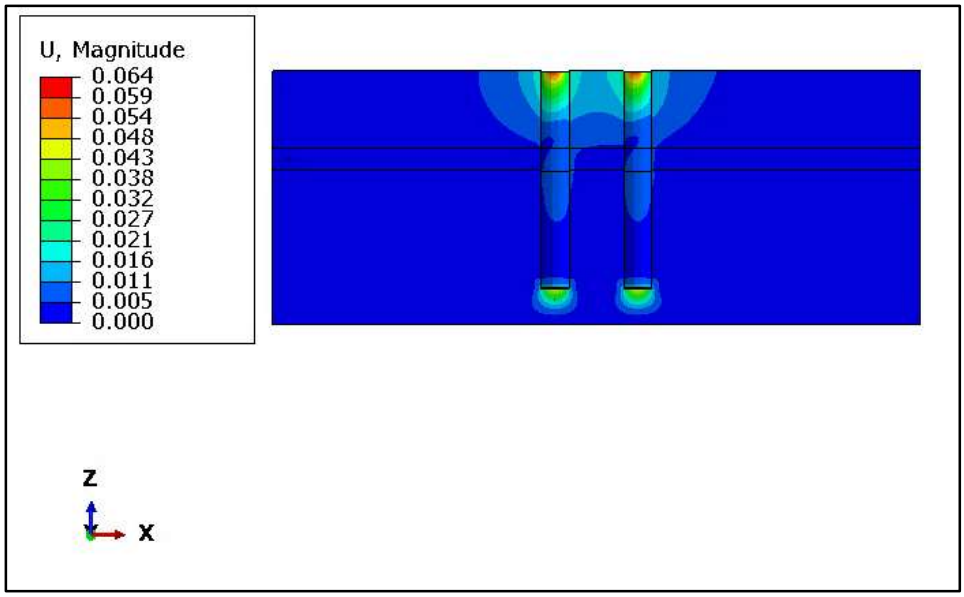
U, Magnitude
0.064
0.059
0.054
0.048
0.043
0.038
0.032
0.027
0.021
0.016
0.011
0.005
0.000
Z
X

(a)

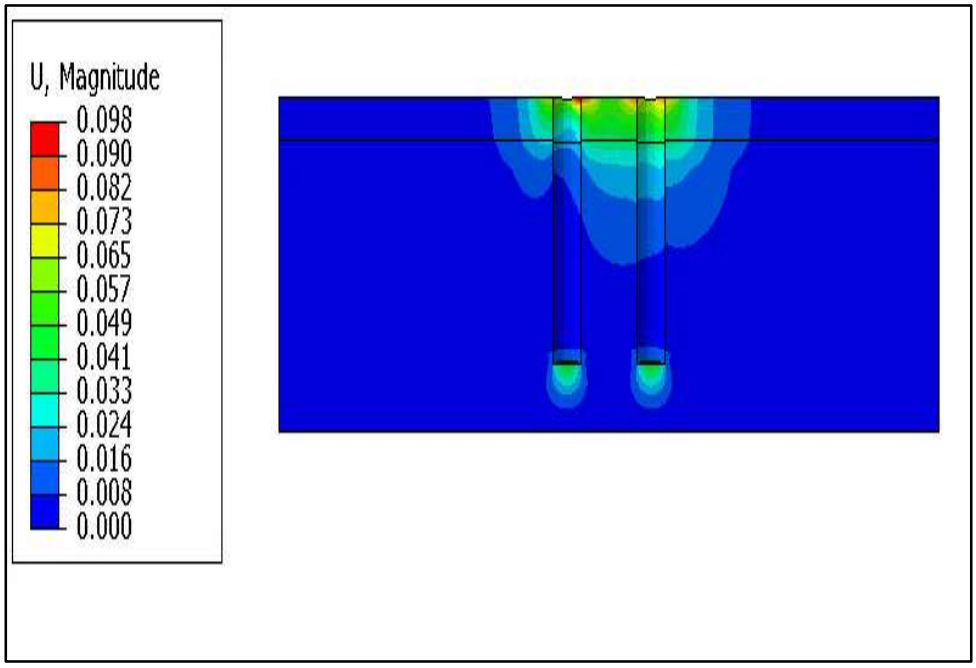
U, Magnitude
0.098
0.090
0.082
0.073
0.065
0.057
0.049
0.041
0.033
0.024
0.016
0.008
0.000

(b)

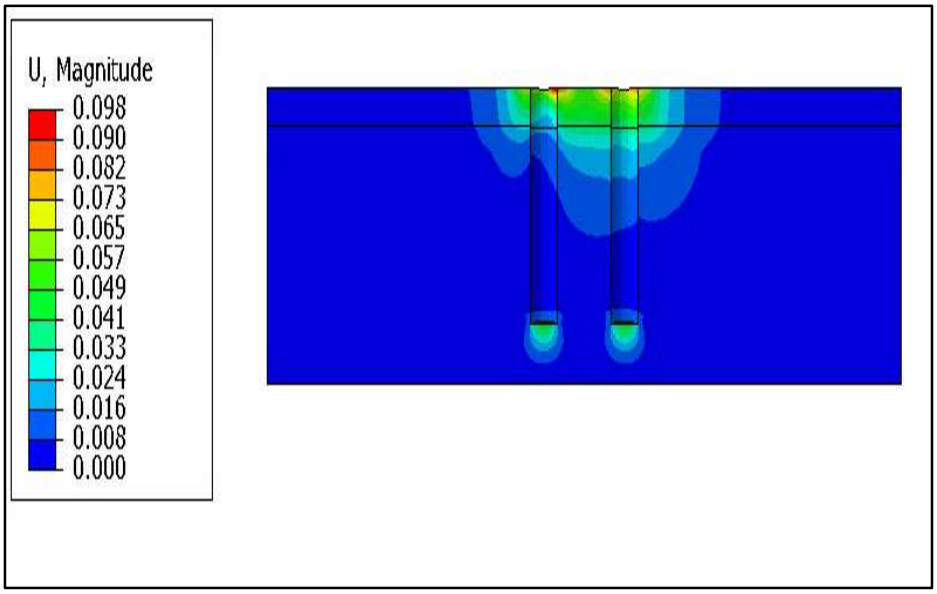

(c)

Figure B- 2 Soil displacement fields for load case 2 (a) no scour, (b) local scour, and (c) combined scour

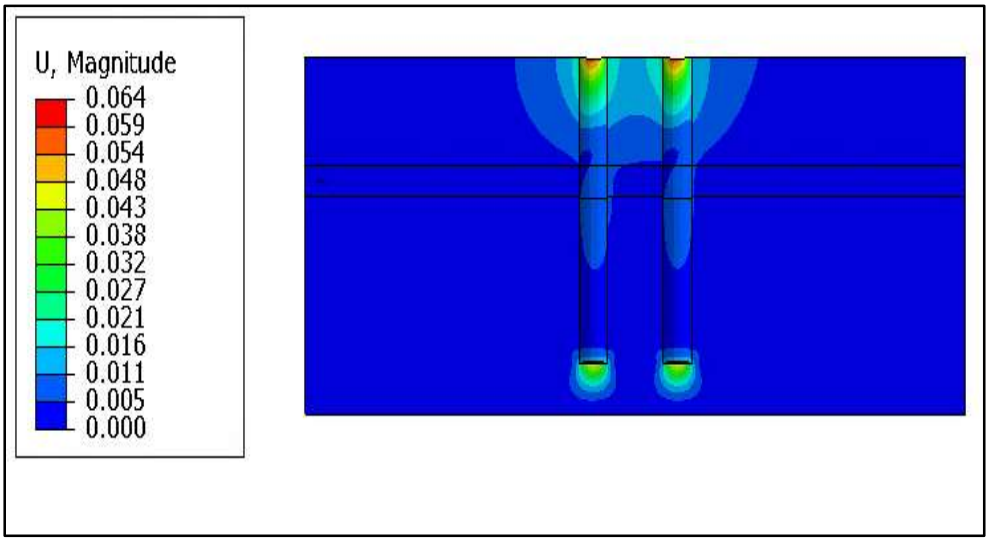
U, Magnitude
0.064
0.059
0.054
0.048
0.043
0.038
0.032
0.027
0.021
0.016
0.011
0.005
0.000

(a)

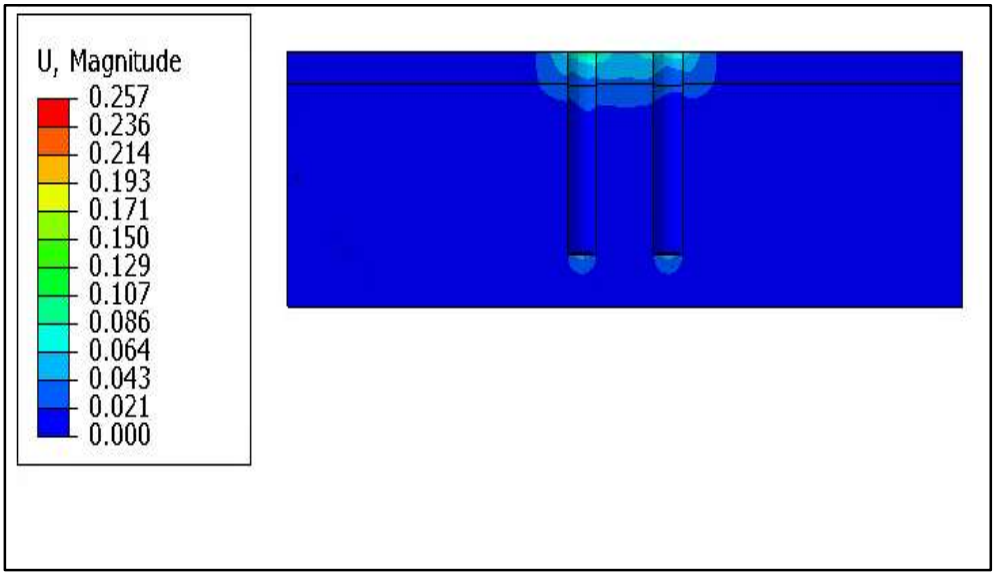
U, Magnitude
0.257
0.236
0.214
0.193
0.171
0.150
0.129
0.107
0.086
0.064
0.043
0.021
0.000

(b)

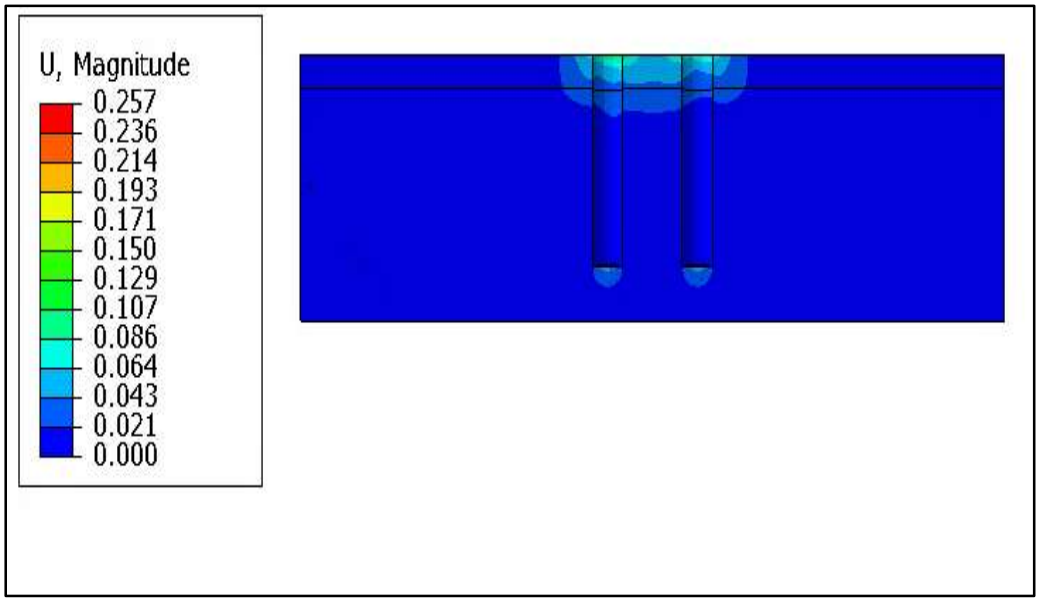

(c)

Figure B- 3 Soil displacement fields for load case 3 (a) no scour, (b) local scour, and (c) combined scour

APPENDIX C: SAMPLE MESH DEFORMATIONS (LOAD CASE 5)

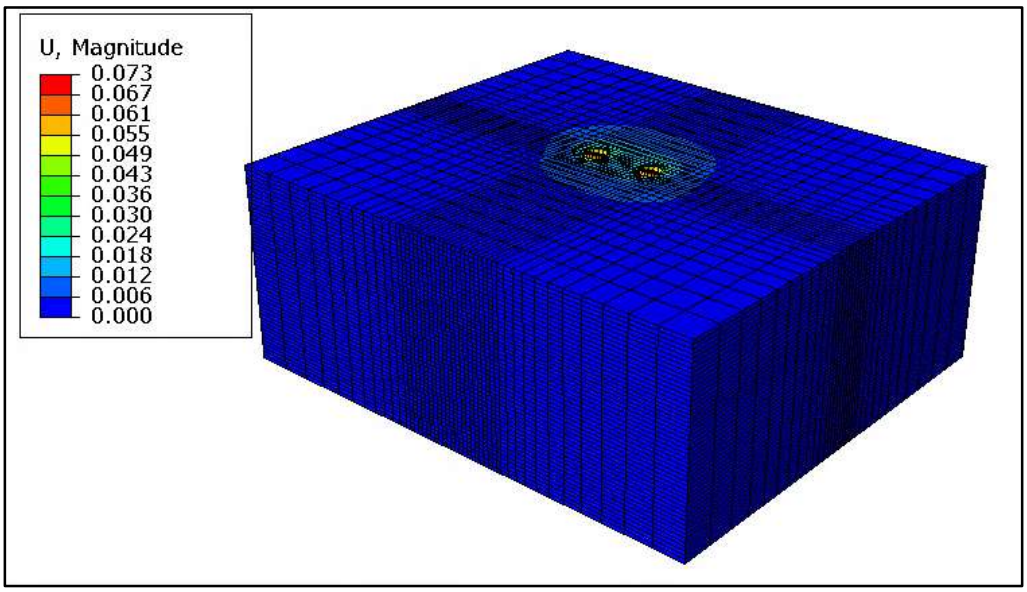

(a)

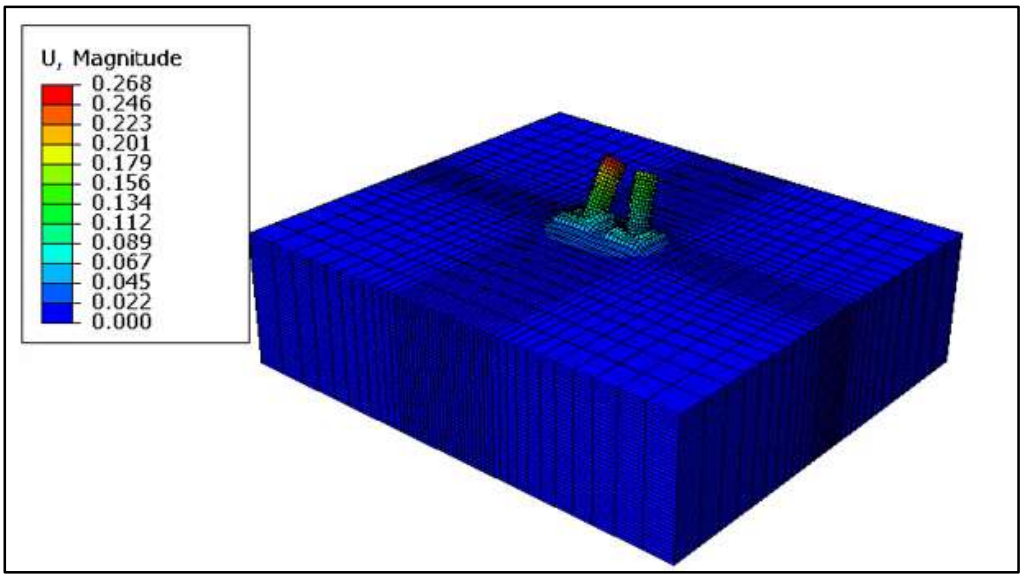

(b)

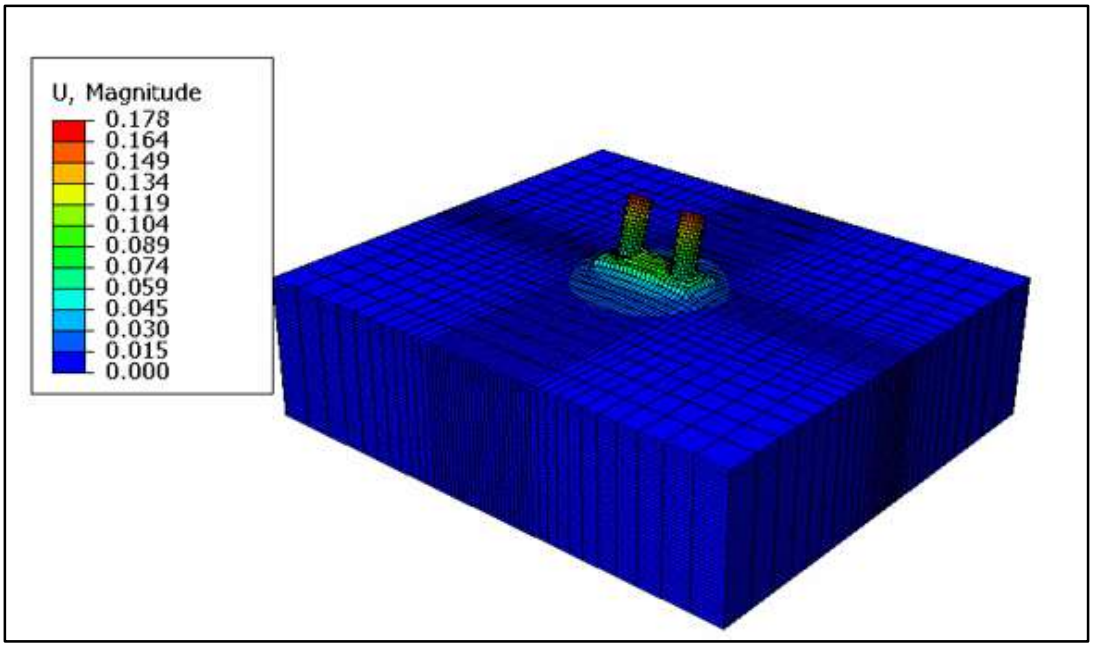

(c)

Figure C- 1 Mesh deformation for 15 ft scour depth for load case 3 (a) no scour-top soil layer, (b) local scour, and (c) combined scour

* Deformation scale is magnified to 500X.

APPENDIX D: STRESS CONTOURS

Shear Stress (S12)

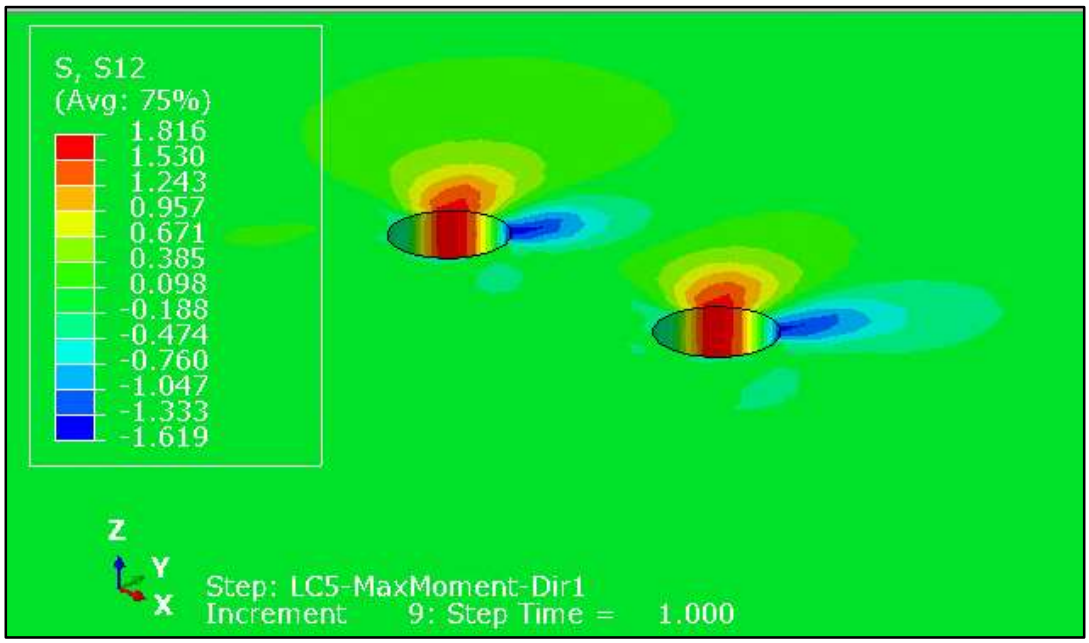

(a)

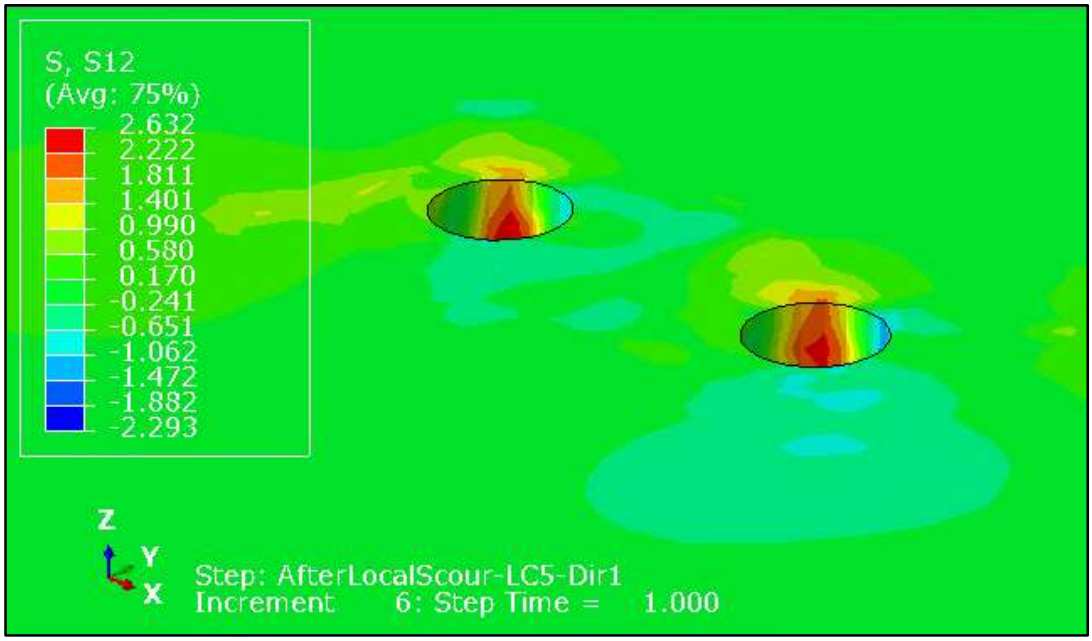

(b)

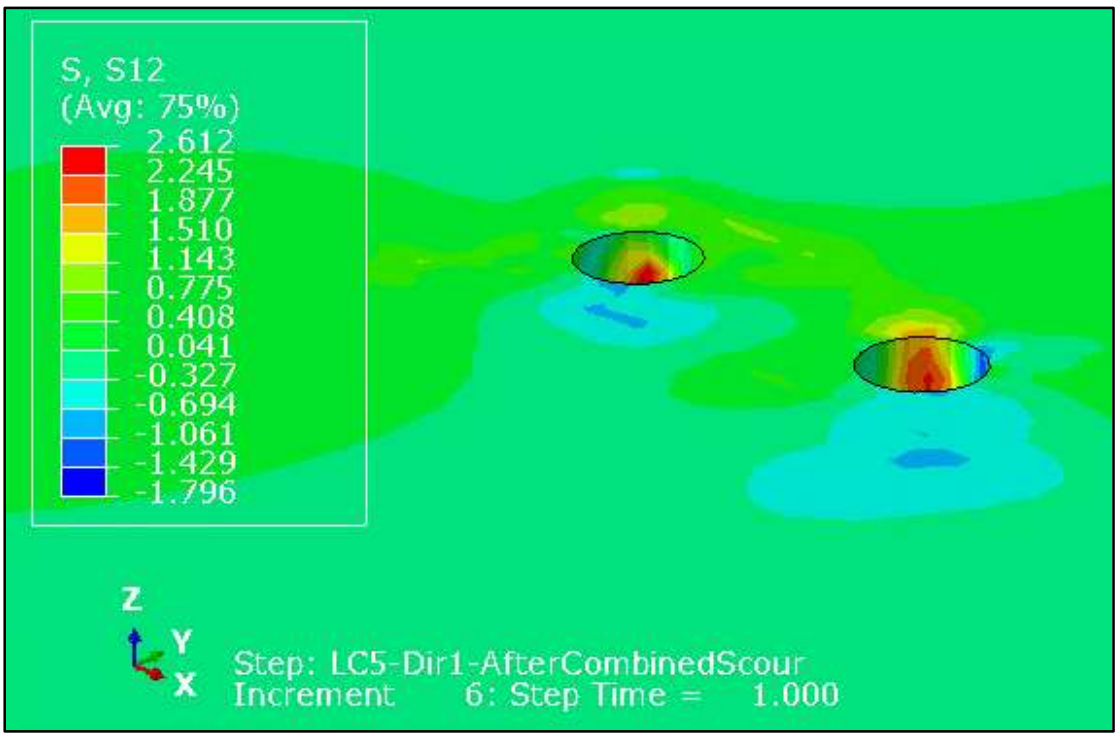

(c)

Figure D- 1 Contours of shear stresses (S12) for 15ft scour depth (load case 3) for (a) no scour (top soil layer), (b) local scour, and (c) combined scour

Stresses in X-direction (S11)

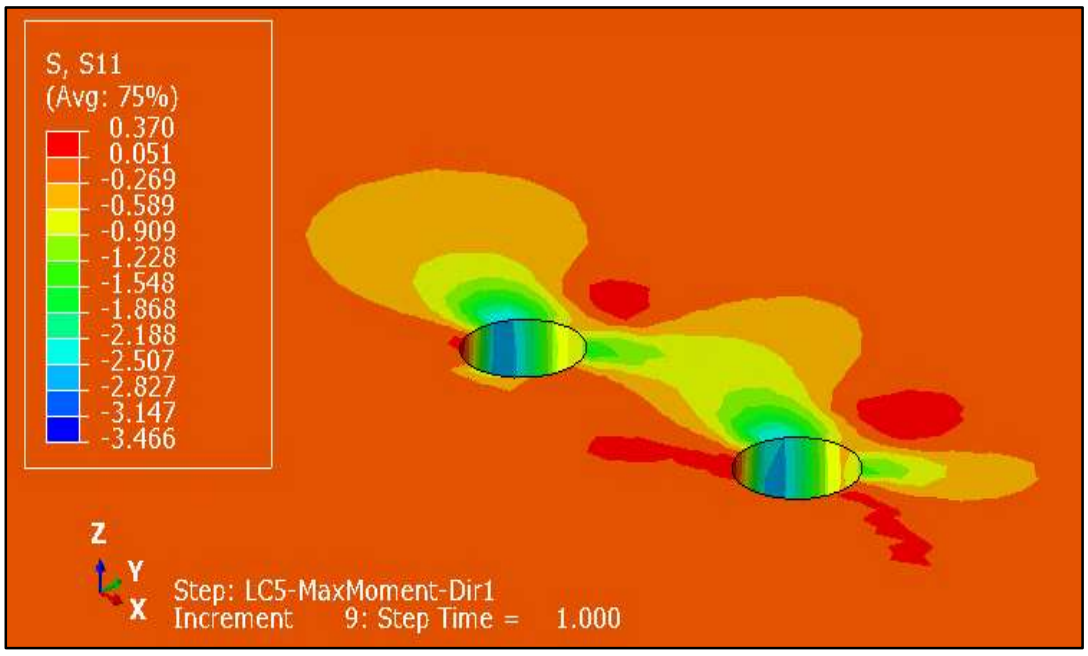

(a)

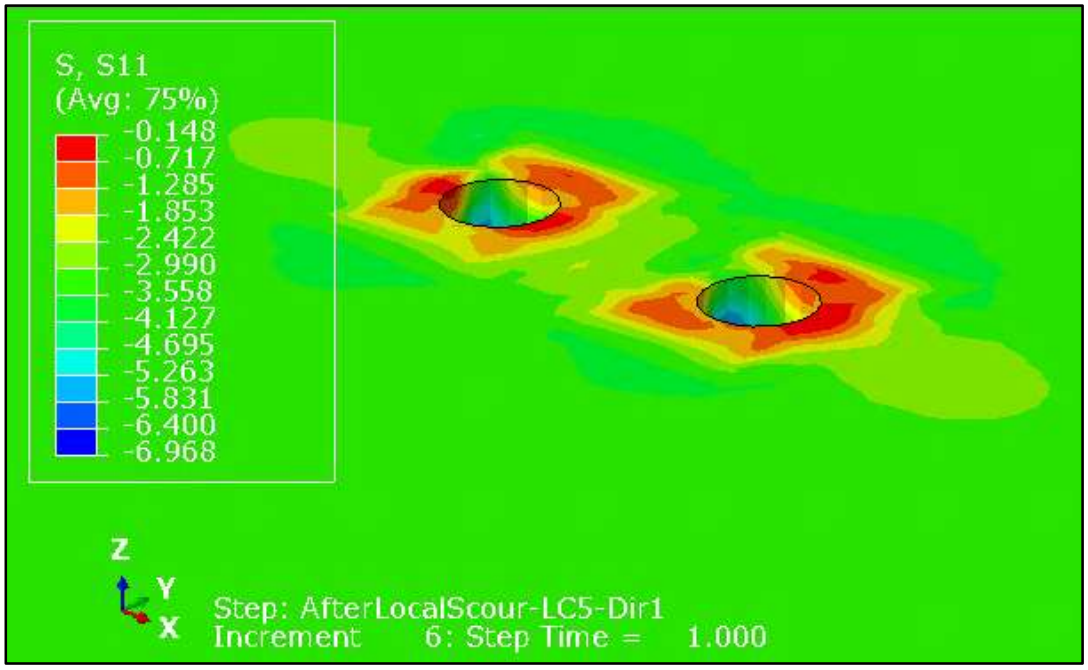

(b)

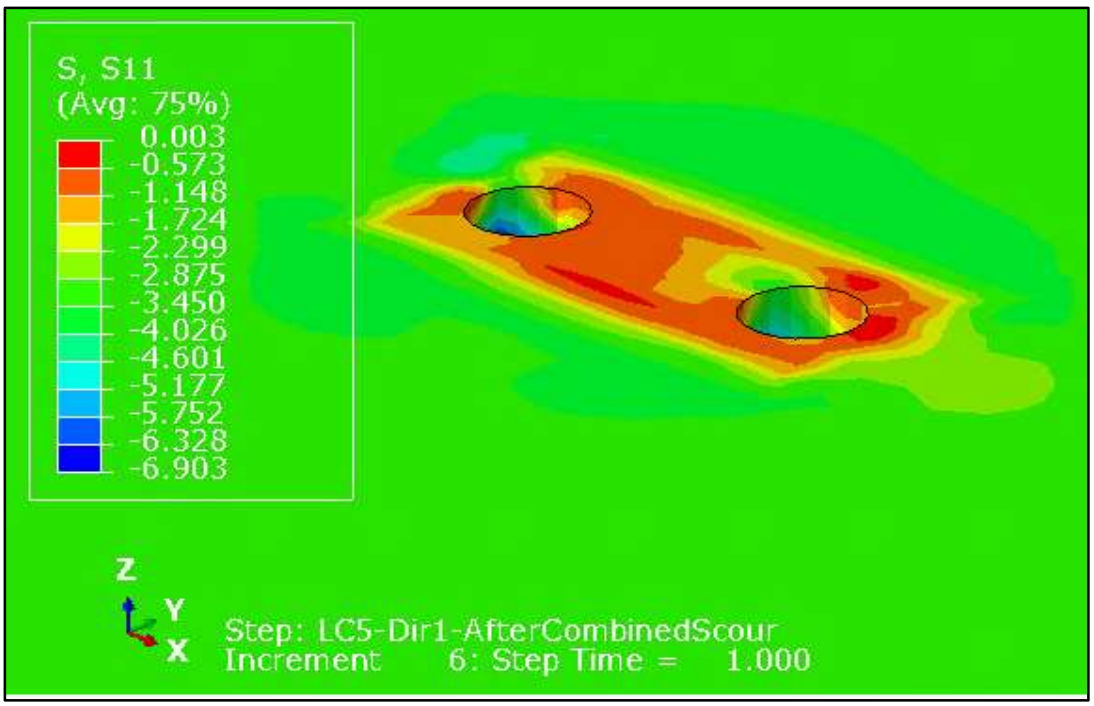

(c)

Figure D- 2 Contours of stresses (S11) for 15ft scour depth (load case 3) for (a) no scour (top soil layer), (b) local scour, and (c) combined scour

Stresses S22

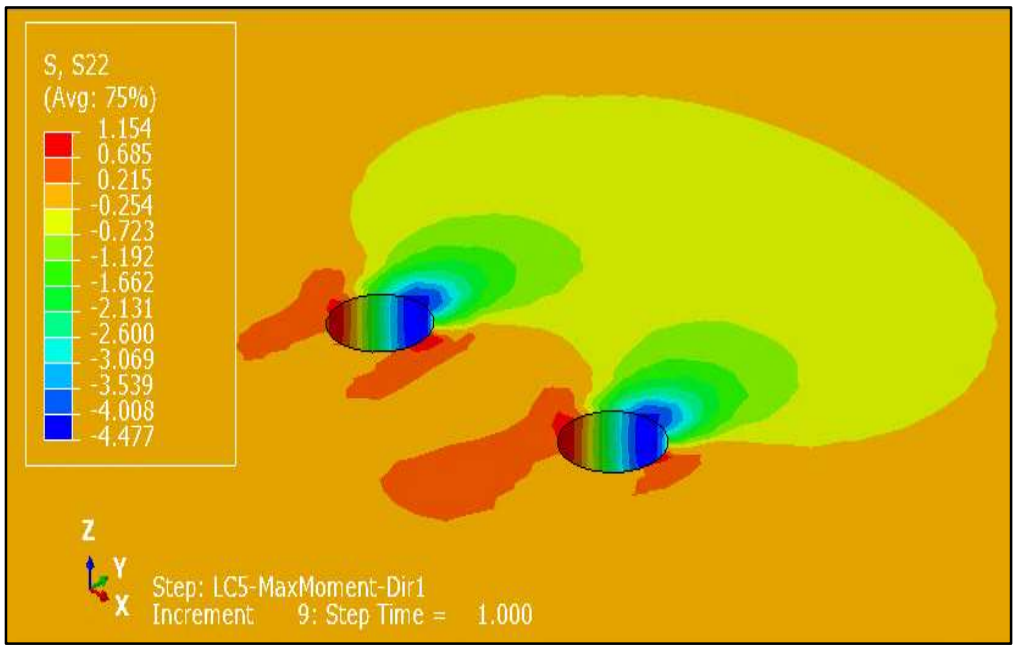

(a)

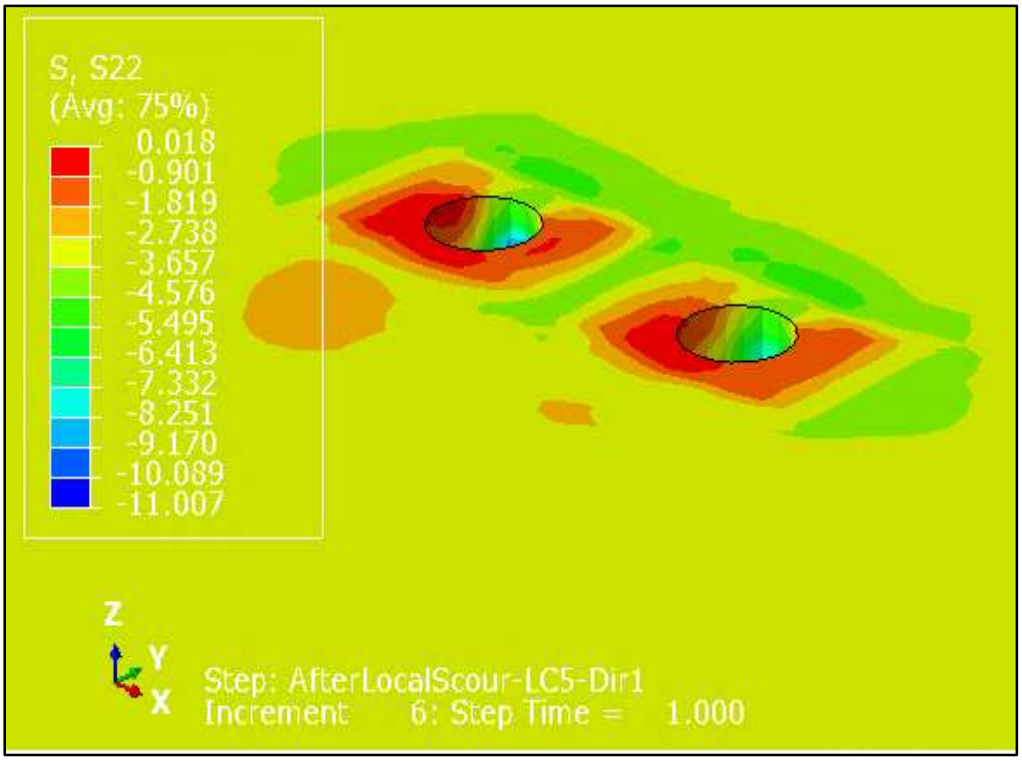

(b)

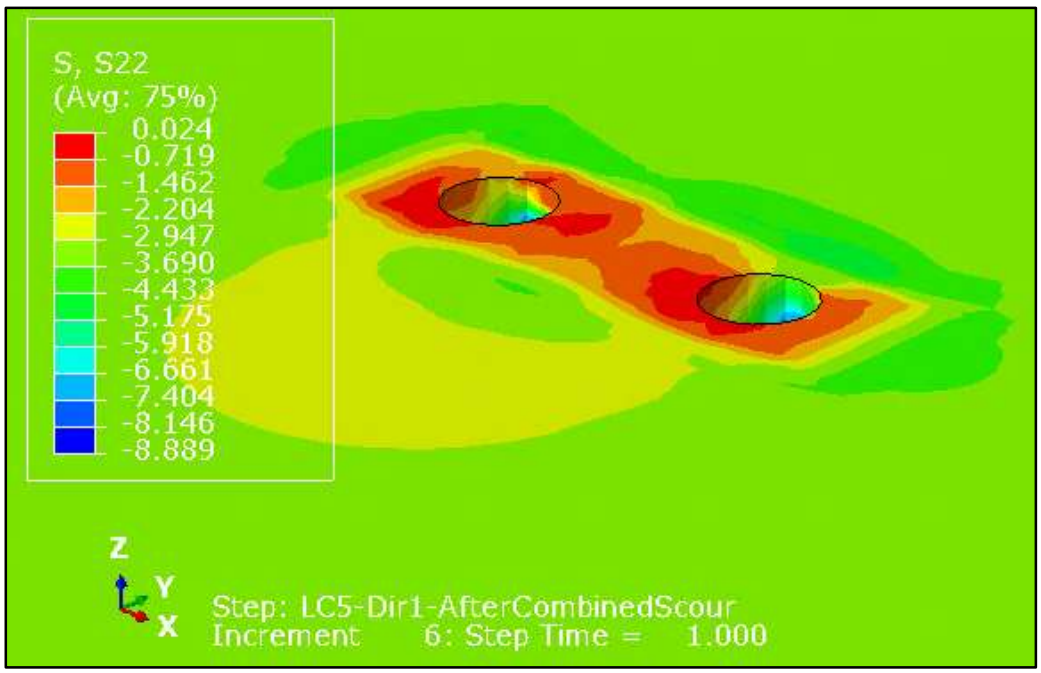

(c)

Figure D- 3 Contours of stresses (S22) for 15ft scour depth (load case 3) for (a) no scour (top soil layer), (b) local scour, and (c) combined scour

Soil Deformation(U)

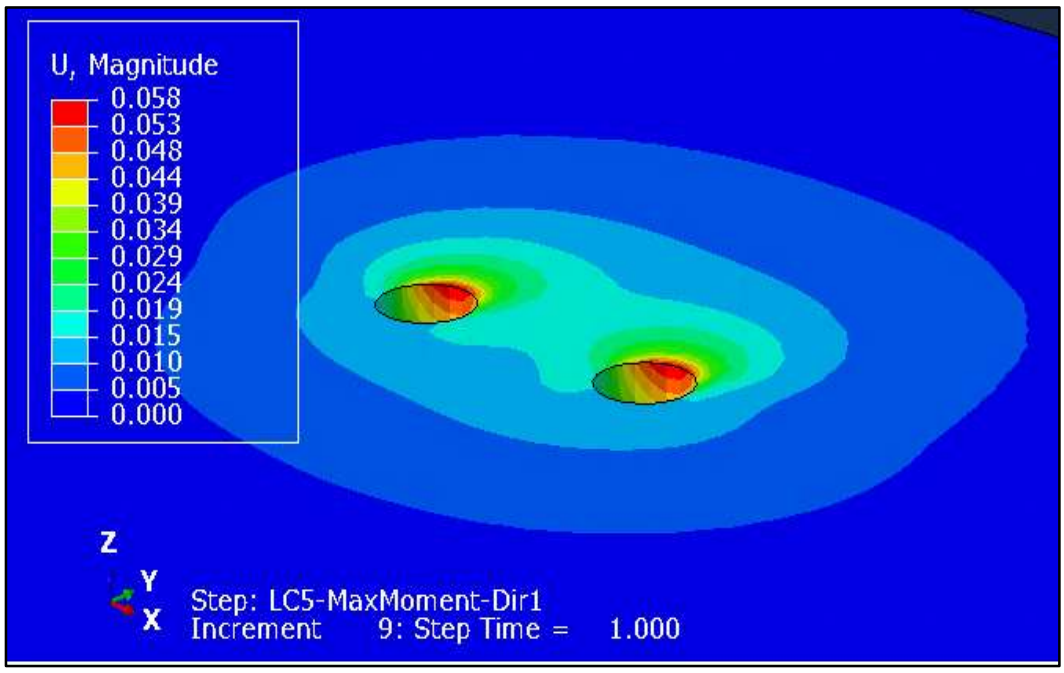

(a)

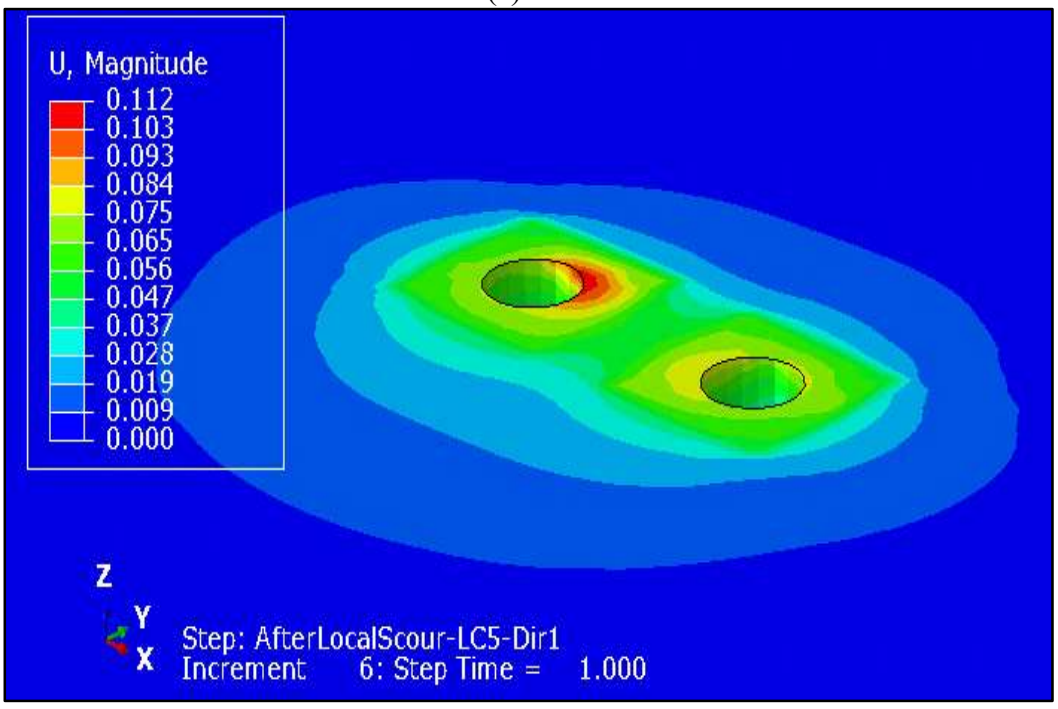

(b)

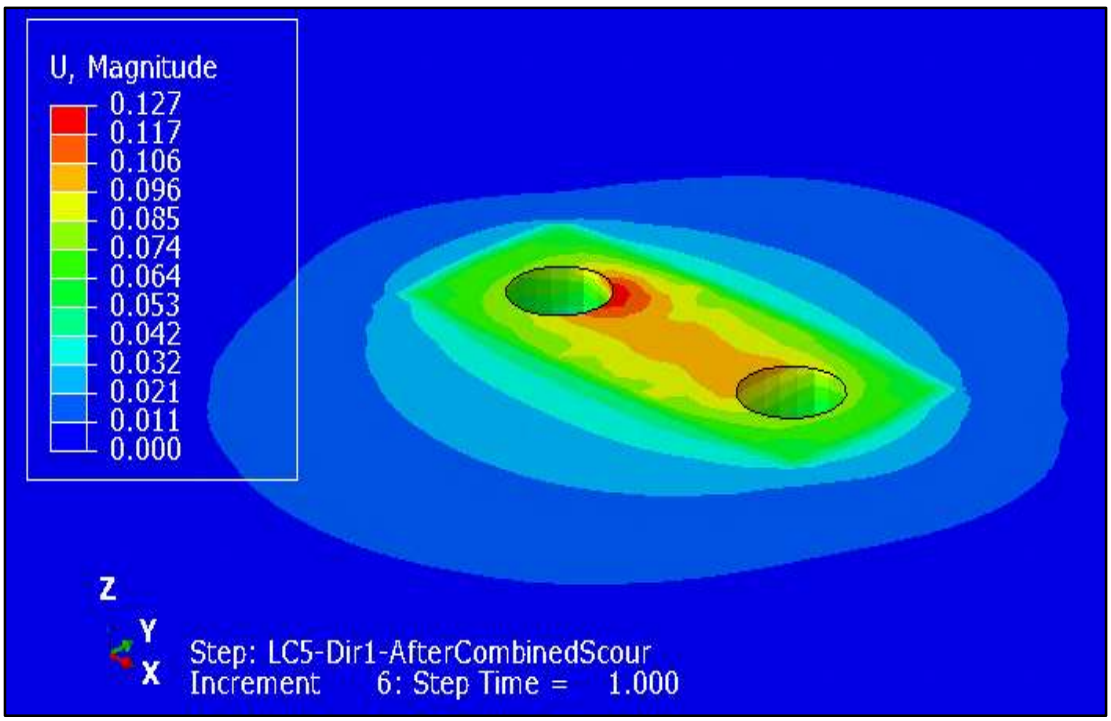

(c)

Figure D- 4 Contours of soil displacement (U) for 15ft scour depth (load case 3) for (a) no scour (top soil layer), (b) local scour, and (c) combined scour

APPENDIX E: MODEL III RESULTS SUMMARY

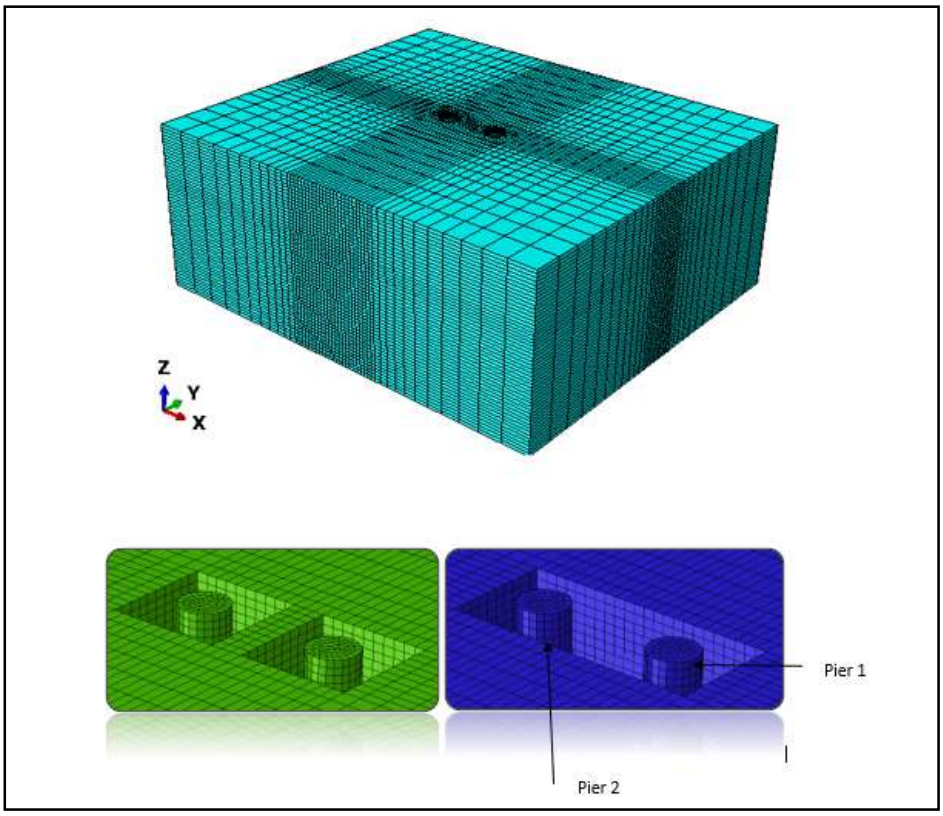

Figure E- 1 3D View FE Model III

Table E- 1 Load Cases (Model III)

	Pier 1					Pier 2				
Type	**Fx (kN)**	**Fy (kN)**	**Fz (kN)**	**Mx (kN-m)**	**My (kN-m)**	**Fx (kN)**	**Fy (kN)**	**Fz (kN)**	**Mx (kN-m)**	**My (kN-m)**
Load case 4 - Maximum Axial	-67	-71	2750	-324	-149	67	-71	2750	324	-149
Load case 5 - Maximum Lateral	-67	-169	2029	-1001	-75	67	-169	2029	1001	-75
Load case 6 - Maximum Moment	-40	-71	1900	-1433	-5	40	-71	1900	1433	-5

Table E- 2 Summary of pile head deflection (mm)

Scour Depth(m)	**Scour Type**	**Load case 4**	**Load case 5**	**Load case 6**
Sd = 0	-	0.533	1.092	1.473
Sd = 1.5	Local scour	3.683	5.131	6.121
	Combined scour	8.331	10.541	11.989
Sd = 3	Local scour	6.045	8.306	9.5
	Combined scour	12.827	16.002	17.729
Sd = 4.5	Local scour	9.246	12.471	14.173
	Combined scour	18.567	22.403	24.511